JOURNAL OF THE

Electrochemical Society

Vol. 105, No. 4 April 1958

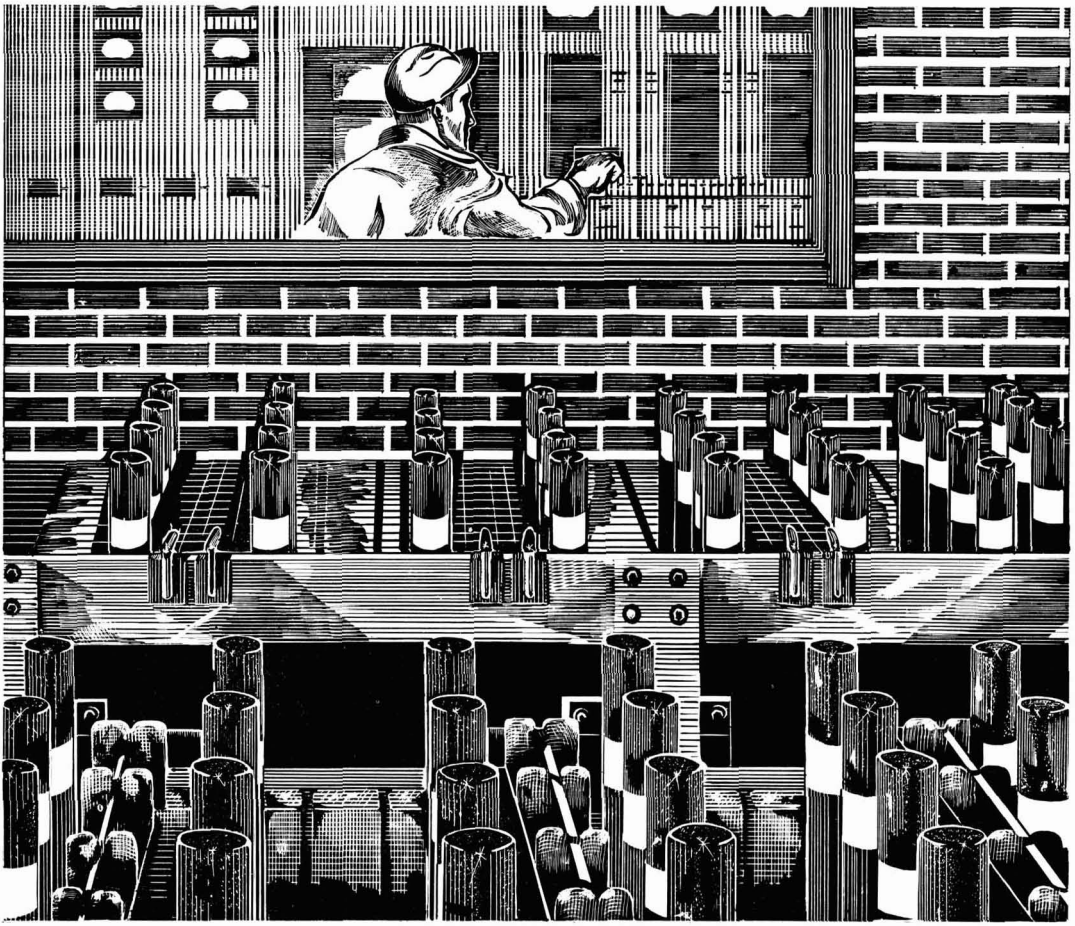

Better cell operations

The technical skills and experienced know-how of the men who operate mercury cells, are most important factors in low cost chlorine-caustic production.

Equally important is the superior performance of GLC anodes, which are "custom made" to individual cell requirements.

FREE—*The cell operation illustrated here has been handsomely reproduced with no advertising text. We will be pleased to send you one of these reproductions with our compliments. Simply write to Dept. W-4.*

ELECTRODE
GLC®
DIVISION

GREAT LAKES CARBON CORPORATION

18 EAST 48TH STREET, NEW YORK 17, N.Y. OFFICES IN PRINCIPAL CITIES

Journal of the Electrochemical Society

APRIL 1958 **VOL. 105 • NO. 4**

CONTENTS

Published monthly by The Electrochemical Society, Inc., from Manchester, N. H., **Executive Offices, Editorial Office** and **Circulation Dept.,** and **Advertising Office** at 1860 Broadway, New York 23, N. Y., combining the JOURNAL and TRANSACTIONS OF THE ELECTROCHEMICAL SOCIETY. Statements and opinions given in articles and papers in the JOURNAL OF THE ELECTROCHEMICAL SOCIETY are those of the contributors, and The Electrochemical Society assumes no responsibility for them. Nondeductible subscription to members $5.00; subscription to nonmembers $18.00. Single copies **$1.25 to members,** $1.75 to nonmembers.

Entered as second-class matter at the Post Office at Manchester, N. H., under the act of August 24, 1912.

SARGENT-MALMSTADT

Automatic Titrator

Using Second Derivative Method of H. V. Malmstadt

1. **Greater operational time saving than any former so-called automatic equipment.**
2. **No electrode problems. Most titrations can be carried out with plain platinum or platinum-rhodium wire electrodes.**
3. **Correct end point is automatically derived by the circuit — no statistical or theoretical studies needed. No pre-setting of voltages. Push-button start, automatic shutoff.**
4. **Inherent accuracy is superior to voltage measurement or color indication.**
5. **Precision better than limits of normal techniques and reading.**
6. **Directly applicable to all types of redox, acid-base, precipitation and complexation titration systems.**
7. **Low cost, minimum maintenance.**

Developed and manufactured by E. H. Sargent & Co.,
based on the original work of H. V. Malmstadt, (Anal. Chem., 26, 1348[1954]).

S-29690 ELECTROMETRIC TITRATION APPARATUS—Automatic, Potentiometer, Sargent-Malmstadt (Patents pending).

For use in all titrations usually classified as potentiometric. Consisting fundamentally of a mixing and delivery unit with associated supports and an electronic control circuit.

The control unit contains the detecting, amplifying, differentiating and relaying circuits with a simple operational panel. At the rear of the control unit are a stirring motor switch for manual use, a fuse, connecting outlets to the valve unit, connecting outlet to the power supply, and a recorder outlet permitting, for research purposes, the recording of the second derivative curve with automatic cutoff.

The delivery unit contains a valve mechanism with an adjustable rate controller, an open ended motor driven chuck for the stirrer, stirring motor and electrode holders. The valve mechanism, mounted on a support with swinging beaker platform and a clamp for the titrating burette, is designed to accommodate any form of burette with or without stopcocks, so that it may apply to any type of titrating installation.

Dimensions of control unit: height, 7¾ inches; width, 10 inches; depth, 9 inches; power consumption, 100 watts; total shipping weight, 35 lbs.

Complete, including: control unit; stirring valve unit; support stand with beaker platform and burette clamp; one S-30490 calomel electrode; one each S-30440 electrode, platinum and platinum rhodium; one S-29695 delivery tip with internal platinum electrode, one S-76667 stirring rod; one S-76668 large stirring rod; connecting cable for recorder; and connecting cord and plug for standard outlets. Without beakers or burettes. For operation from 115 vol, 60 cycle A.C. circuits..... **$450.00**

SARGENT

SCIENTIFIC LABORATORY INSTRUMENTS • APPARATUS • SUPPLIES • CHEMICALS

E. H. SARGENT & COMPANY, 4647 W. FOSTER AVE., CHICAGO 30, ILLINOIS
MICHIGAN DIVISION, 8560 WEST CHICAGO AVENUE, DETROIT 4, MICHIGAN
SOUTHWESTERN DIVISION 5915 PEELER STREET, DALLAS 35, TEXAS
SOUTHEASTERN DIVISION, 3125 SEVENTH AVE., N., BIRMINGHAM 4, ALA.

Editorial

April 27—May 1, 1958

THE approaching New York convention of the Society prompts some thoughts about conventions in general. The convention seems to be a peculiarly American institution. In the whole great city of London, for example, there is—at least so far as I know—not a single hotel capable of handling even so moderate-sized a gathering as a typical Electrochemical Society convention with its several simultaneous technical sessions and group meals. This is not to say that people do not hold meetings in foreign countries, but such meetings do not partake of the character of a typical American convention.

Well, what is a typical American convention? It ranges, in purpose and atmosphere, all the way from practically 100% high jinks and "whoop-de-doo" to practically 100% serious consideration of the problems in a particular field. It is to be expected that the meetings of our own Society will tend toward the latter; but, one hopes, they will not go all the way. The ancient saw about all work and no play still holds true; social, as well as business and technical, contacts with one's colleagues are not only enjoyable but valuable, and if they can be facilitated by judicious imbibition of appropriate beverages where is the harm?

It is taken for granted that when you come to the New York Meeting of the Society—and we of the New York Committee certainly hope you will come—your purpose is primarily a serious one, and that you will attend the symposia of your choice and learn much of value from both the formal sessions and the informal talks you will have with your colleagues. So much is obvious and hardly needs to be emphasized.

What does need to be said is that not enough registrants are taking advantage of the opportunities offered at Society conventions for social contacts. Proportionately fewer members and guests lately have been attending luncheons, dinners, and other functions. They are saying, in effect: "Why spend $X for a banquet when for half the price I can eat at a fine restaurant and get just as good a meal?" This is true, without argument. The economics of hotel operation appear to entail disproportionately high costs for group meals. Such functions often actually represent a financial loss to the local committee in spite of the prices charged.

But such a line of argument misses the point. The purpose of luncheons and banquets is not primarily to cater to the gourmet instinct. It is to provide an atmosphere, heightened by good food (and drink, if that is your taste), where people of good will and similar tastes can enjoy the benefits of contacts at the human, rather than technical, level, and by sharing experiences can become not only better scientists or engineers but better people.

"Highfalutin" doubletalk? Perhaps; but, until a prescription for human understanding better than sharing a meal and a glass comes along, it will have to do.

So when you visit us in New York, come to the Mixer—and the Banquet—and the Society Luncheon; and if the Division of your interest is having a special luncheon, come to that too. If you don't, you are only half-attending the convention.

—F. A. LOWENHEIM*

* General Chairman, New York Meeting, The Electrochemical Society.

SILICON RECTIFIERS are finding increasing use at elevated temperatures in aircraft and missile applications by providing more power per pound.

Now... design improvements made possible with components of Du Pont Hyperpure Silicon

Today silicon rectifiers make possible a vast improvement in jet-age aircraft generators—the use of engine oil as a coolant instead of less-efficient ram air. Silicon rectifiers take the place of oil-sensitive brushes, commutator and slip rings . . . are completely unaffected by 150°C. engine oil. Result: a *brushless* generator of less weight and size than ordinary generators.

Silicon devices can similarly help you miniaturize—improve design and performance. Silicon rectifiers have excellent stability . . . can operate continuously at −65 to 200°C. They're up to 99% efficient—reverse leakages are only a fraction of those of other semiconductors. Both transistors and rectifiers of silicon can pack *more* capacity into *less* of your equipment space.

Note to device manufacturers:
You can produce high-quality silicon transistors and rectifiers with Du Pont Hyperpure Silicon now available in three grades for maximum efficiency and ease of use... purity range of 3 to 11 atoms of boron per billion... available in 3 forms, needles, densified, cut-rod. Technical information is available on crystal growing from Du Pont... pioneer producer of semiconductor-grade silicon.

NEW BOOKLET ON DU PONT HYPERPURE SILICON

You'll find our new, illustrated booklet about Hyperpure Silicon helpful and interesting—it describes the manufacture, properties and uses of Du Pont Hyperpure Silicon. Just drop us a card for your copy. E. I. du Pont de Nemours & Co. (Inc.), Silicon N-2496-JE-4, Wilmington 98, Delaware.

PIGMENTS DEPARTMENT

DU PONT
REG. U. S. PAT. OFF.

BETTER THINGS FOR BETTER LIVING
...THROUGH CHEMISTRY

An Investigation of Some New Cathode Depolarizer Materials

A. B. Tripler, Jr., and L. D. McGraw

Electrochemical Engineering Division, Battelle Memorial Institute, Columbus, Ohio

ABSTRACT

A stable trivalent manganese compound, manganic phosphate, has been found to have good cathode depolarizer properties in strongly acid electrolytes. Manganic phosphate-carbon cathodes of the type used in this work delivered up to 8.5 amp-min/g of $MnPO_4$. This corresponds to over 80% utilization. When coupled with lead in excess HBF_4 electrolyte, the watt-minute capacity per gram of $MnPO_4$ was 8. The electrochemical behavior, and charge retention of the cathodes are described. Manganic phosphate and another less stable depolarizer, $BaFeO_4$, furnish cathodes which can be discharged at 200 ma/in.^{3} (16.4 cc) without severe polarization. The maximum nonpolarizing currents for the $MnPO_4$ are discussed in terms of the surface area of carbon admixed with it to form cathodes. The depolarizing properties of a strongly oxidizing, insoluble organic compound chloranil are reported.

Inorganic compounds containing metals in unusual valence states and organic compounds of high oxidizing power are of interest as potential cathode depolarizers. Tervalent manganese compounds and hexavalent iron compounds have not been investigated in this connection, although they are known to have excellent oxidizing power. A literature search disclosed that manganic orthophosphate might have desirable properties. The material is very slightly soluble in water, and is not attacked by 6*N* HCl. In the case of iron, the most promising choice for a reasonably stable and insoluble compound containing the element in the hexavalent state was barium ferrate. Among the organics, chloranil (tetrachloroquinone) is attractive because of its insolubility and its high oxidation potential (1). Accordingly, these three materials were investigated.

Materials

Manganic phosphate.—Manganic phosphate was successfully prepared chemically, and also by anodic oxidation of the metal. The electrochemical method was devised in the course of this work. The chemical method is a modification of a reported preparation (2). Electrolytic Mn was oxidized anodically in a solution of 7 parts by volume water to 6 parts by volume sirupy phosphoric acid (85 wt % H_3PO_4) at 82°-93°C. The temperature was maintained by the electrolytic current between the anode and a platinum cathode. At an apparent anode current density of about 6 amp/in.^{2} (0.93 amp/cm^2), 40 amp-min of current produced 1.06 g $MnPO_4$. This corresponds to about 28% current efficiency. Electrolysis was accompanied by rhythmic polarization of the anode and by current fluctuation. The first product of electrolysis was a pink solution. With the formation of powdery $MnPO_4$, the pink color disappeared and further $MnPO_4$ appeared to form directly at the anode without formation of the intermediate pink manganic solution.

For the chemical preparation, a mixture of 185 ml of sirupy phosphoric acid and 20 g MnO_2 was heated slowly to 250°C. The MnO_2 reacted to form a purple viscous solution. The temperature of the solution was held at 250°C for ½ hr after which it was lowered to 150°-200°C. Then 200 ml distilled water were added while the solution was stirred. The $MnPO_4$ precipitated as a gray-green powder.

Samples of $MnPO_4$, prepared by the above chemical method, had an equivalent weight of 165 (theor. 150), as determined by titrating the iodine liberated from acid iodide solutions. The apparent density of the material was 3.024 g/cc, as determined by the displacement of water.

The solubility of the salt was measured in various electrolytes by analysis for the total amount of Mn dissolved when 1.000 g of the salt was stirred with 100 ml of the electrolytes for 1 hr at room temperature (24°-27°C). There was no detectable amount of $MnPO_4$ dissolved by 30 wt % HBF_4 and only a trace dissolved by 60 wt % $HClO_4$. Water dissolved 0.9 mg Mn/100 ml, and 30 wt % H_2SO_4 dissolved 6.1 mg Mn/100 ml. It is possible that these results are not properly called solubilities. They may be only indicative of the rate of hydrolysis of the phosphate.

Because solubility tests had indicated the possibility of hydrolysis of $MnPO_4$, observations were made on the stability of the compound over a range of *p*H. The product retained its gray-green color when suspended in solutions of *p*H below 5.3, changed to tan at *p*H 5.3, and changed to dark brown at *p*H 8.8. At *p*H 10.6 the material was black, indicating a change to MnO_2. Possibly the trivalent Mn disproportionates to divalent and tetravalent Mn. In any event, erratic results were expected and were found when the material was used as a depolarizer in electrolytes of *p*H above 5.

Barium ferrate.—$BaFeO_4$ was prepared by a double decomposition reaction between sodium ferrate solution and crystalline $Ba(OH)_2 \cdot 8H_2O$. The sodium ferrate solution was prepared by oxidation of ferric nitrate solution with caustic hypochlorite solution (3). The assay of the precipitated $BaFeO_4$ was not high but was raised to 90% or better by washing

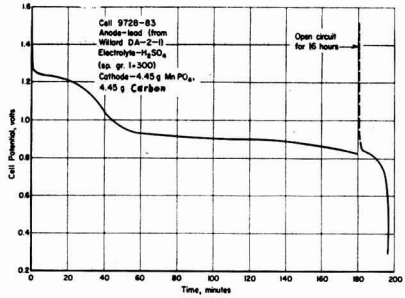

Fig. 1. Discharge characteristics for a cell of the type $Pb/H_2SO_4/MnPO_4$, C drained at 220 ma.

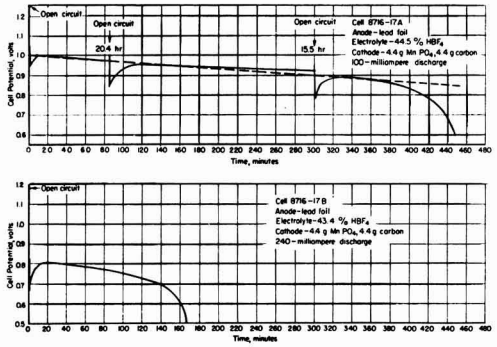

Fig. 2. Discharge characteristics for cells of the type $Pb/HBF_4/MnPO_4$, C.

with glacial acetic acid followed by drying with alcohol and ether.

The solubility of $BaFeO_4$ was measured in 0.18*M* $Ba(OH)_2$ at 27°C. The concentration of ferrate found, 0.0068 g/l, furnished a rough value for the solubility product of $BaFeO_4$, 4.75×10^{-6}.

Chloranil.—Chloranil was used as purchased from Eastman.

Apparatus

In most cases, the electrochemical behavior of the new materials was studied by discharge of cells containing a large excess of electrolyte, a large unpolarizable anode, and a cathode consisting of an Alundum thimble or a double Dacron bag into which a mixture of depolarizer and acetylene black[1] was packed. A pointed carbon rod was driven into the depolarizer mix to make electrical contact. The Alundum thimble was 19 mm (¾ in.) OD x 90 mm (3½ in.) long, and had a wall thickness of 1.6 mm (1/16 in.). The Dacron bags were made to approximately the same dimensions as the Alundum thimbles. When the cells had to be stored for a period of time, a thin layer of mineral oil was poured on top of the electrolyte. This was effective in preventing evaporation of water. The container for the cell was a Pyrex or polyethylene beaker. The cathodes had a volume of about 1 in.[3] (16.4 cc). All cells were discharged at constant current.

[1] Shawinigan Acetylene Black, 100% compressed, Shawinigan Chemicals, Ltd., Montreal, Quebec, Canada.

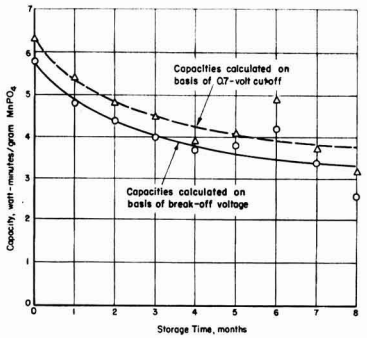

Fig. 3. Decrease in capacity with storage time for $MnPO_4$ cells calculated on basis of break-off voltage and on basis of a 0.7-v cutoff.

Electrochemical Characteristics of Chemically Prepared Manganic Phosphate

An anode from a commercial lead-acid storage battery (Willard DA-2-1) was coupled with a $MnPO_4$ cathode to determine the characteristics of the new cathode depolarizer in 1.300 sp gr H_2SO_4 (nominally 40% by weight). The cell had an open circuit potential of 1.61 v. It was discharged at 220 ma to an 0.8 v cutoff; its characteristics are illustrated in Fig. 1. The cell had a capacity of 37.8 watt-min, or 8.5 watt-min/g $MnPO_4$. The 8.9 amp-min/g capacity of the cathode was 83% of theoretical.

Sheet lead anodes were used in cells for evaluation of the $MnPO_4$-carbon cathodes in a HBF_4 electrolyte. Beaker-type cells having 45 wt % HBF_4 as electrolyte were assembled and tested. Figure 2 shows typical discharge characteristics at 100 and 240 ma for the 1 in.[3] (16.4 cc) cathodes containing 4.4 g $MnPO_4$. Cell 8716-17A had a capacity of 7.8 watt-min/g $MnPO_4$ and Cell 8716-17B had a capacity of 5.5 watt-min/g $MnPO_4$.

The $MnPO_4$ cathode was evaluated for shelf life in HBF_4. Figure 3 presents preliminary capacity-storage data. The lower curve of Fig. 3 is based on capacities calculated from end voltages corresponding to sharp breaks in the individual polarization curves. For some cells, sharp breaks were not apparent, so all capacities were recalculated for a 0.7 v cutoff (upper curve). The same conclusions regarding shelf life can be made from either curve. Approximately 50% of the capacity of the cathodes was lost in 8 months in the shelf-life test. At the end of the 8-month period, however, the rate of loss of capacity had been reduced to a low value. The bobbins were 1.9*M* in divalent Mn at the end of an 8-month storage by virtue of the fact that half of the Mn had been reduced. The following calculations illustrate that the cathode potential would be too low to oxidize water when the concentration of divalent Mn reached 1.9*M*, and explain the arrest in the rate of loss of capacity after 8 months.

The measured potential of the manganic-manganous couple is given by Latimer (4):

$$Mn^{+2} = Mn^{+3} + e, E^\circ = 1.51 \text{ v} \qquad (I)$$

From the approximate solubility of $MnPO_4$ (less

Table I. Effect of Divalent Mn on the Retention of Capacity of $MnPO_4$ Cathodes

Group	Electrolyte	Average open-circuit potential immediately after makeup, v	Average open-circuit potential after 1 month, v	Average capacity immediately after makeup, watt-min/g $MnPO_4$	Average capacity after 1 month, watt-min/g $MnPO_4$	Loss in capacity, %
1	50% HBF_4 solution	1.51	1.53	8.0	5.65	29
2	29% HBF_4 solution	1.48	1.45	6.5	4.75	27
3	29% HBF_4 plus 0.01*M* $Mn_3(PO_4)_2$	1.48	1.48	6.9	5.0	27.5
4	29% HBF_4 plus 0.10*M* $Mn_3(PO_4)_2$	1.46	1.46	6.65	5.9	11

than 7×10^{-5}M), the potential of the $MnPO_4$ electrode must be at least:

$$Mn^{+2} + PO_4^{-3} = MnPO_4 + e, E^\circ = 1.265 \text{ v} \quad \text{(II)}$$

In order to bring the potential of the $MnPO_4$ electrode to 1.229 so it can no longer decompose water, it is necessary to have a Mn^{+2} and PO_4^{-3} concentration of 2.02*M* according to the Nernst equation applied to (II). This corresponds to a 0.67*M* concentration of $Mn_3(PO_4)_2$. This is in good agreement with the fact that the $MnPO_4$ cathodes lost capacity very slowly after 50% was, presumably, reduced to form a 1.9*M* solution of divalent Mn.

Attempts were made to improve the shelf life of the electrode by incorporation of $Mn_3(PO_4)_2$ in the HBF_4 electrolyte. From the data of Table I, it appears that manganous phosphate of 0.10*M* concentration has effected a reduction in the rate of loss of capacity. The manganous salt did not appear to be more soluble than 0.1*M*, so no attempts were made to check the complete arrest of loss of capacity expected with 0.67*M* solution.

Fabrication of a Pb-$MnPO_4$ *Dry Cell*

All the experiments described thus far on $MnPO_4$ were performed with excess electrolyte. For practical application, a dry-type cell would have advantages. Therefore, the following experiments were performed.

By using materials immediately at hand, cells were fabricated which did not contain excess electrolyte and yet had fairly good characteristics. The cell construction was patterned after the common LeClanché cell. The anode consisted of a lead-alloy can supplied in the form of an unfilled collapsible tube made from an alloy containing 2¼% Sb, ¼% Sn, with the balance Pb. Whatman filter-paper extraction thimbles which fitted snugly into the lead tubes were used as separators. When wetted with 2 g 50 wt % HBF_4, they swelled to make intimate contact with the lead. Approximately 13 g of a mix of $MnPO_4$ and Shawinigan acetylene black was wetted with HBF_4 electrolyte and was placed into the lined can. A carbon rod was inserted into the center of the wet mix, and molten Pyseal[2] was poured into the vacant space at the top of the can, thus sealing the cell. The external dimensions of the cells were 1 in. in diameter by 3 in. long (2.5 cm x 7.5 cm).

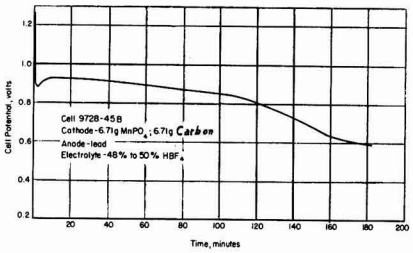

Fig. 4. Discharge characteristics for a $MnPO_4$ dry cell at 220-ma discharge.

A characteristic discharge curve is shown for such a cell in Fig. 4 (220-ma discharge). The initial dip and recovery were present in this dry cell as in the cells with excess electrolyte. The relatively flat discharge was also present. The sharp break-off was not observed, however, in the case of dry cells. For the cell of Fig. 4, the break-off was taken as 110 min. The capacity was 3.2 watt-min/g $MnPO_4$ or 3.6 amp-min/g $MnPO_4$.

The dry cells had virtually no shelf life because of the rapid attack of the electrolyte on the very thin walls of the lead cans (about 5 mils or 0.125 mm thick). It was because of this wall thinness that the discharge tests had to be run shortly after the cells were made. This was of no concern in evaluating the cathode material.

Discussion of the Electrochemical Characteristics of $MnPO_4$

Data on the manganic-manganous system (5) show that, on the basis of a measured exchange current on Pt of 10^{-5} amp/cm^2, activation polarization should not exceed 30 mv for 200 ma currents on 4 g of Shawinigan Acetylene Black having a true surface area of 2.8×10^6 cm^2. Polarization was much more severe than this in experimental cells. The actual polarization must be due either to concentration polarization owing to slow rate of dissolution of $MnPO_4$ or to the fact that carbon is a poor surface for the electrochemical reaction to take place. The latter alternative corresponds to different exchange currents on platinum and carbon electrodes.

It is concluded that slow dissolution of $MnPO_4$ is responsible for ultimate polarization because polarization is less severe in the electrolytes in which $MnPO_4$ dissolves more rapidly (30% H_2SO_4). The over-all effect of slow dissolution of $MnPO_4$ is a form of concentration polarization.

Electrochemical Characteristics of Barium Ferrate

Barium ferrate cathodes polarize strongly when drained in simple alkaline electrolytes. Polarization is probably due to a coating of insoluble ferric oxide on the ferrate particles. The reduction of hexavalent

[2] A proprietary sealing compound distributed by Fisher Scientific Company, Pittsburgh, Pennsylvania.

Table II. Preliminary Evaluation of $BaFeO_4$ Cathodes as Components of Alkaline Cells

	Cell I	Cell II	Cell III	Cell IV
Anode	Zinc	Zinc	Zinc	Zinc
Electrolyte	$K_4P_2O_7$, 40% KOH, 10%	$K_4P_2O_7$, 40% KOH, 10%	$K_4P_2O_7$, 40%	$K_4P_2O_7$, 40% KOH, 20%
Cathode				
Weight of $BaFeO_4$ (78%), g	4	4	4	4
Weight of Carbon Black, g	4	4	4	4
Theoretical capacity, amp-min	58.5	58.5	58.5	58.5
Open-circuit voltage, v	1.65	1.61	1.49	1.72
Discharge potential range, v	1.16-1.10	1.00-1.00	1.49-1.0	1.03-1.00
Discharge current, ma	100	220	220	220
Measured capacity				
amp-min	18.3	11.4	3.96	14.7
amp-min/g 78.0% $BaFeO_4$	4.6	2.9	1.0	3.7
Per Cent utilization of $BaFeO_4$	32	19.5	6.8	25

iron produces trivalent iron which is insoluble in alkaline media.

Far less polarization of the $BaFeO_4$ cathodes occurred when the alkaline electrolyte contained an agent such as potassium pyrophosphate which could complex and solubilize the reduction products.

Four electrolytes, each having a different ratio of $K_4P_2O_7$ to KOH, were tested in beaker cells having 3 x 3-in. (7.5 x 7.5-cm) zinc foil anodes. The make-up of the cells and their performances are given in Table II.

The importance of free alkali in the electrolyte may be seen from the poor discharge characteristics of Cell III, Table II, and the superior performance of Cell IV, Table II, and Fig. 5. The former cell had no free alkali and the latter had 20% free alkali. The flat discharge curve of the latter cell illustrates how effectively the pyrophosphate prevents cathodic polarization.

Stability of $BaFeO_4$

In lieu of shelf-life tests on cells with $BaFeO_4$ cathodes, quantitative chemical tests were made to determine the stability of $BaFeO_4$ in the alkaline electrolytes. These tests indicated an activated stand life of 24 hr and an unactivated stand of 6 weeks.

The stability of $BaFeO_4$ was not increased by the use of materials such as acetanilide which are used to stabilize other oxidizing agents. A more stable ferrate than $BaFeO_4$ is required for a storageable cell.

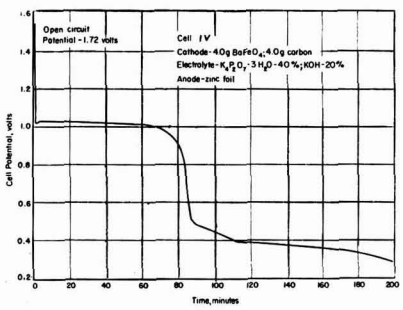

Fig. 5. Preliminary evaluation of $BaFeO_4$ cathode, as component of alkaline cell containing 20% KOH, by discharge at 220 ma (see Table II).

Electrochemical Characteristics of Chloranil (Tetrachloroquinone)

Chloranil (tetrachloroquinone) is a strong oxidizing agent used as an intermediate in the dye industry. Its oxidation potential is rather high, as indicated by Conant and Fieser (1). Chloranil is stable in oxidizing acids such as sulfuric and nitric acids, and has a low solubility. It has been suggested previously as a cathode depolarizer material (6).

Evaluation of chloranil as a cathode depolarizer.— Chloranil was evaluated in preliminary tests as a cathode depolarizer material in beaker-type cells.

The electrolytes in the preliminary tests were 5 wt % KOH, 48 to 50 wt % HBF_4, and dry cell electrolyte.[3] They were used with zinc, lead, and zinc anodes, respectively. The open circuit potential of the cells and their discharge capacities at a 100-ma drain rate were measured. The results are shown in Table III.

[3] Weight per cent composition: NH_4Cl-26, $ZnCl_2$-8.8, H_2O-65.2.

Table III. Evaluation of Cells with Chloranil Cathodes

	Cell I*	Cell II	Cell III*
Anode	Zinc	Lead	Zinc
Electrolyte	KOH, 5%	HBF_4, 50%	Dry cell
Cathode			
Weight of chloranil, g	3.86	3.90	3.50
Theoretical capacity, amp-min	50.4	50.9	45.7
Open-circuit potential, v	1.50	0.99	1.19
Discharge potential, v	1.2-1.15	0.85-0.80	1.04-0.99
Measured capacity (100-ma drain)			
amp-min	20	30	26
amp-min/g chloranil	5.1	7.8	7.4
watt-min/g chloranil	5.9	6.4	6.1

* The tabulated data on these cells are only approximations. Cell I was not discharged to its break-off point. The test was discontinued because the chloranil was obviously hydrolyzing and dissolving in the alkaline electrolyte. Cell III discharged erratically because the anode did not corrode uniformly.

This quinone was electrochemically active in alkaline solution (Cell I). However, it hydrolyzed in the alkali so it would not have good shelf-life. Chloranil was also electrochemically active in highly and moderately acid electrolytes (Cells II and III).

The cell containing dry cell electrolyte (III) did not discharge at a steady potential until the zinc anode was activated by treatment with 1 to 1 (Vol) HCl. Prior to such treatment, three zinc foil anodes failed by corrosion at the solution level, one prior to discharge of the cell and two during discharge of the cell. Also, when the fresh anodes were placed in the electrolyte, they corroded at only a few spots during discharge. This accounts for the fluctuations in potential during discharge until the last anode (activated by HCl) was added. It is characteristic of anodic inhibitors to aggravate the local corrosion (7) when they are not present in sufficient concentration.

In spite of the unexpected behavior of the chloranil toward the anodes of these cells, the two electrochemical systems in acid electrolytes showed inclination toward flat discharge curves, good capacity, and resistance to anode corrosion during open-circuit storage. Taking all the observations on these preliminary tests into consideration, chloranil offers interesting prospects as a cathode depolarizer and an anodic corrosion inhibitor for zinc.

Acknowledgment

Financial support for this program from the Power Sources Branch of Signal Corps Engineering Laboratories under Contract No. DA-36-039-SC-42682 is gratefully acknowledged. The authors wish to express their thanks to the sponsoring agency for permission to publish portions of the work done under that contract.

Manuscript received March 18, 1957. This paper was prepared for delivery before the Buffalo Meeting, Oct. 6-10, 1957.

Any discussion of this paper will appear in a Discussion Section to be published in the December 1958 JOURNAL.

REFERENCES

1. J. B. Conant and L. F. Fieser, *J. Am. Chem. Soc.*, **45**, 2207 (1923).
2. J. W. Mellor, "A Comprehensive Treatise on Inorganic and Theoretical Chemistry," Longmans, Green and Co., London, Vol. **12**, Chapter LXIV, p. 429 (1932).
3. *Ibid.*, Vol. **12**, Chapter LXVI, pp. 931 and 934.
4. W. M. Latimer, "Oxidation Potentials," 2nd ed., p. 237, Prentice-Hall, Inc., New York (1952).
5. K. Vetter and G. Manecke, *Z. physik., Chem.*, **195**, 270 (1950).
6. W. O. Arsem, U. S. Pat. 2,306,927, Dec. 29, 1942.
7. U. R. Evans, "Metallic Corrosion, Passivity and Protection," 2nd ed., p. 545, Longmans, Green and Co., London (1946).

Kinetics of Reaction of Steel with Hydrogen Sulfide-Hydrogen Mixtures

Andrew Dravnieks and Carl H. Samans

Engineering Research Department, Standard Oil Company (Indiana), Whiting, Indiana

ABSTRACT

The kinetics of the reaction of steel with pure hydrogen sulfide at 250°-500°C may be interpreted in terms of consecutive linear and parabolic rates. In hydrogen sulfide-hydrogen mixtures similar reactions exist, but the reaction rate decreases as the thermodynamic equilibrium line ($Fe + H_2S \rightleftharpoons FeS + H_2$) is approached, in a manner which is approximately proportional to the decrease in the thermodynamic driving force. Increase of pressure up to 20 atmospheres increases the reaction rate by a fractional power of the pressure. In the presence of traces of oxygen, the linear rate component is minimized. The observed kinetics can be explained in terms of three steps: adsorption, rate of formation of diffusing species, and diffusion.

Iron reacts readily with sulfur and with sulfur compounds to form iron sulfides. The kinetics of the reaction of low carbon steel with elemental S has been investigated (1-4) and has been found to obey a parabolic law, with a deviation in long-range corrosion vs. time curves, believed to be due to microcracking of the scale. In the reaction of low carbon steel with H_2S, the reaction mechanism is complicated by the presence of hydrogen, since hydrogen is one of the reaction products and must leave the surface of the sulfide scale before the reaction can proceed. These complications are even more pronounced in the reaction of low carbon steel with mixtures of H_2S and H_2. The thermodynamics of the steel-hydrogen sulfide reaction has been clarified by the recent work of Rosenqvist (5), among others. The kinetics has been studied by many investigators (6-14) for various sets of conditions. Sorell and Hoyt (15) have summarized this work well and have made some correlations. However, the field has not yet been explored over a sufficient range of experimentally comparable conditions to obtain a

clear picture of the rate processes involved. The present work was undertaken to amend this shortcoming.

Experimental Methods

Several experimental techniques were used.

For experiments with pure H_2S-H_2 mixtures, electrolytic hydrogen was passed through a commercial catalyst cartridge to change oxygen to water, and through a silica gel tower to remove water vapor.

To introduce H_2S at various concentrations, three methods were used: (*A*) for the higher concentration, metered quantities of H_2S and hydrogen were taken from gas cylinders; (*B*) for the lower concentrations, purified hydrogen was bubbled through molten sulfur at a constant temperature to charge it with a constant amount of sulfur vapor; the resulting hot mixture of hydrogen and sulfur vapor then was passed through an alundum column at 510°-540°C to react the sulfur vapor completely with the hydrogen, producing a corresponding amount of H_2S (5); (*C*) for still lower concentrations, the most dilute mixture prepared by the above molten sulfur procedure was diluted still further with pure hydrogen. In most cases, continuous mixing was employed. For experiments at higher pressures, H_2S and H_2 were premixed in a steel gas cylinder.[1]

Reaction vs. time curves were obtained by two methods: (*a*) electrical resistance measurements on corroding strips of metals (1, 16); and (*b*) weight-gain measurements with specimens hung on a quartz spring balance suspension in the flowing gas mixture in a furnace. In addition, rates of reaction were measured by the conventional weight-loss method.

In all cases, the linear flow of the gas mixture past the specimens was maintained sufficiently high, of the order of 150-450 cm/min, to prevent any slowdown of corrosion by exhaustion of the H_2S in the mixture. The drag on the specimens hung on the quartz spring was found to produce a lift of 0.10-0.15 mg. To minimize the effect of the error caused by the drag, gas flow velocities were kept constant. Most samples were run at least in duplicate.

Figure 1 represents the equipment used for tests at atmospheric pressures. For the continuous weighing method, a quartz spring was used instead of the specimen holder shown. Figure 2 represents the equipment used for tests at pressures up to 21 atm. The end of the reaction tube was modified to carry sealed electrodes so that measurements of the change in electrical resistance could be made on the specimens, for continuous studies of the reaction.

Temperatures constant to ±2°C were maintained by means of heated Al cylinders with holes for inserting the reaction tubes. Specimens were made of low carbon steel with a nominal percentage composition of: C 0.06; Mn 0.37; P 0.018; S 0.031; Si 0.002; Cu 0.02; Ni 0.06; Sn 0.25. Annealing seemed

[1] It was found that oxygen had to be removed in making such mixtures. In the presence of oxygen, which occurs in small quantities in commercial bottled hydrogen, H_2S at low levels slowly disappeared from the mixture, apparently by reaction with the oxygen to form water and sulfur. Also, to accelerate mixing of the H_2S and the hydrogen in the cylinder, the cylinders were laid flat and lifted in succession several times. Without this procedure, an interval of 2-3 days was required to homogenize the contents of the cylinder.

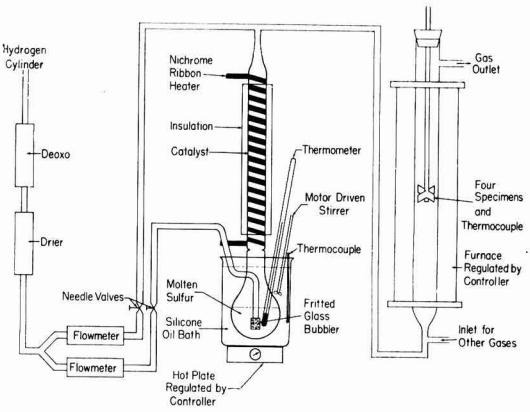

Fig. 1. Experimental setup for corrosion studies in H_2S/H_2 mixtures at atmospheric pressures.

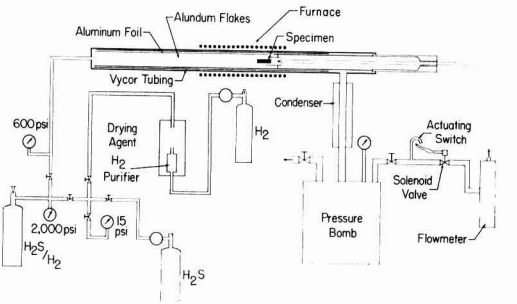

Fig. 2. Experimental setup for corrosion studies in naphtha, H_2S, and hydrogen mixtures at elevated pressures.

to have no pronounced influence on the reaction rates. However, to avoid possible strain effects, annealed specimens (1 hr at 650°C, in vacuum) were used in obtaining all reaction vs. time curves.

To obtain weight losses on single specimens, the sulfide layer was pealed off mechanically and the sulfide still adhering to the specimen was dissolved by pickling in inhibited 15% HCl for 2 min. With the commercial pickling inhibitor used, the weight loss by acid attack of the steel itself was found to be less than 0.1 mg per specimen.

Gases were analyzed by passing a metered quantity through a bubbler containing aqueous NaOH, and titrating the resultant Na_2S potentiometrically with ammoniacal $AgNO_3$ solution, using a silver sulfide-coated silver wire and a calomel cell as electrodes.

Results and Discussion

Initial Reaction Kinetics

Figure 3 gives the initial range for a number of typical time-sulfidization reaction curves. Data were obtained in pure H_2S and in H_2S-H_2 mixtures, at atmospheric pressures and at elevated pressures. In all cases, the reaction rates decrease with time. This decrease, however, is slower than if only the parabolic law were obeyed, indicating that a more complex form of corrosion reaction is involved.

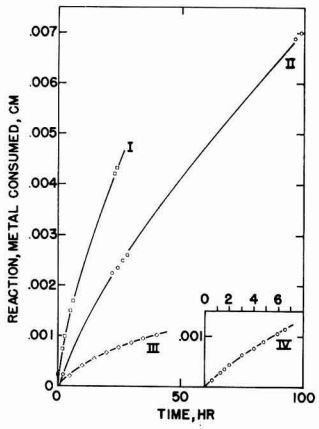

Fig. 3. Initial range of typical reaction curves of steel with H_2S and with H_2S/H_2 mixtures.

Curve	Temp, °C	Pressure atm.	H_2S/H_2	Technique
I	530	1	pure H_2S	Cont. weighing
II	450	1	7.5×10^{-4}	Elect. resist.
III	250	1	pure H_2S	Elect. resist.
IV	530	21	8×10^{-4}	Elect. resist.

The data were analyzed by the graphic-kinetic technique of Fischbeck (17) and Wagner (18). According to this method, the corrosion reaction is assumed to proceed by two consecutive reaction steps: a linear interface reaction, followed by a diffusion through the scale.

Each of these reaction steps has its own "resistivity" defined as $1/k_1$ for the interface reaction, where k_1 is a linear reaction constant, and as y/k_2 for the diffusion step, where k_2 is the parabolic rate constant, and y is the thickness of the reaction product scale through which the diffusion occurs. The total reaction rate is then:

$$\frac{dy}{dt} = \frac{C}{1/k_1 + y/k_2} \qquad (I)$$

where C is a constant. Integrated and rearranged, this becomes

$$\frac{t}{y} = \frac{1}{Ck_1} + \frac{y}{2Ck_2} \qquad (II)$$

Consequently, a plot of t/y vs. y should be linear, with $1/Ck_1$ as the intercept, and $1/2Ck_2$ as the slope. Such a plot of typical data is given in Fig. 4. Thus, the initial kinetics may be explained in terms of two consecutive rate-limiting steps: a linear step, presumably limited by an interface reaction; and a parabolic step, probably controlled by the rate of diffusion of the reactants through the sulfide layer.

If a small amount of O_2 is introduced into the H_2S-H_2 mixture just ahead of the specimen exposure tube, it reacts readily with the H_2S to form sulfur vapor and water vapor. The reaction rate of sulfur with H_2 is relatively slow under these conditions so that the sulfur vapor is carried through the experimental equipment and has been observed to deposit on the cooler parts beyond the furnace. In the presence of this sulfur vapor the reaction becomes faster (Fig. 5) but the linear component, characterized by the intercept on the time/reaction axis of the Fischbeck-Wagner plot, either becomes quite small or disappears. The addition of water vapor alone did not influence the rate of sulfide scale growth. The previously found parabolic rate curves for the corrosion of steel in molten sulfur (1, 2), similarly, did not show any intercepts on the time/reaction axis. Thus the sulfidization of Fe follows effects similar to those found for the sulfidization of Ag (19) where the parabolic law is observed principally in the Ag-S system, but a linear law is followed in the Ag-H_2S system.

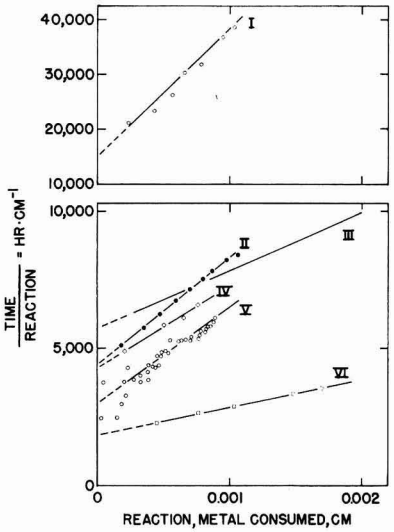

Fig. 4. Graphic kinetic analysis of reaction curves, initial range.

Curve	Temp, °C	H_2S/H_2	Pressure, atm.
I	250	Pure H_2S	1
II	315	Pure H_2S	1
III	450	8×10^{-4}	1*
IV	480	Pure H_2S	1
V	530	5.5×10^{-4}	21
VI	530	Pure H_2S	1

* Curve III is an extrapolation of Curve II from Fig. 5.

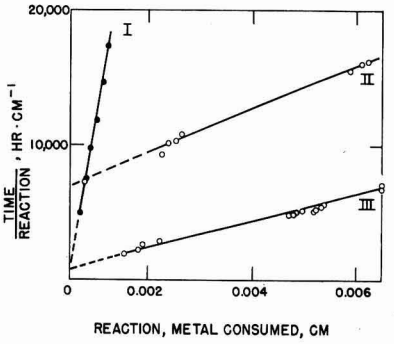

Fig. 5. Graphic kinetic analysis of the influence of oxygen on the reaction of steel with H_2S mixtures. Curve I, steel in molten sulfur at 325°C; II, steel in $H_2S/H_2 = 8 \times 10^{-4}$ at 450°C; III, same as II but with 0.1% O_2 added to the gas stream ahead of the specimen.

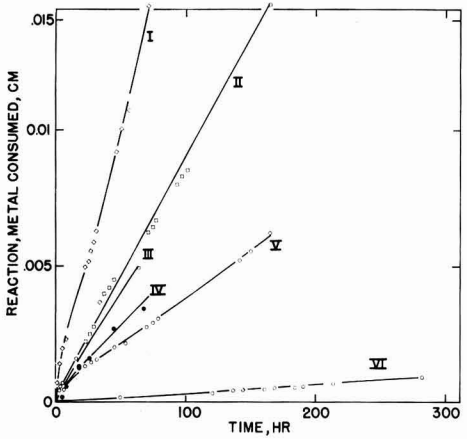

Fig. 6. Typical long-time reaction curves—I, pure H_2S, 530°C; II, pure H_2S, 480°C; III, $H_2S/H_2 = 0.33$, 440°C; IV, $H_2S/H_2 = 1 \times 10^{-3}$, 520°C (weight loss on separate specimens); V, pure H_2S, 380°C; VI, $H_2S/H_2 = 512 \times 10^{-4}$, 370°C. All pressures atmospheric.

These observations indicate, therefore, that the surface of the sulfide scale is the most likely site of the rate-limiting linear step. It must be noted that in a certain fraction of the experiments the parabolic element was poorly defined.

Long-Time Reaction Kinetics

The initial kinetics discussed above held only for a limited period, up to an extent of reaction corresponding approximately to a metal loss in thickness of $2\text{-}3 \times 10^{-3}$ cm. Typical long-time reaction curves are shown in Fig. 6. As a first approximation, these may be considered to be linear after a short initial stage. Thus, the initial linear-parabolic kinetics cannot be used with validity to extrapolate to reactions of long duration.

The long-time average rates were approximately those established at the time when the usual linear-parabolic kinetics broke down.

Variation of reaction rates with hydrogen sulfide: hydrogen ratio and temperature.—To obtain a complete quantitative picture of the separate variation of the linear and the parabolic rates with the $H_2S:H_2$ ratio and with temperature is a formidable experimental task. Most of the work was conducted with 16 to 18-hr exposures and was interpreted as an average rate of metal consumption in centimeters per hour. This simplification still permitted some generalization of the kinetics.

Figure 7 gives isokinetic curves for a field covering a wide range of temperatures and $H_2S:H_2$ ratios. The two solid straight lines represent the thermodynamic existence limits for FeS and for FeS_2 taken from the work of Rosenqvist (5). Between these lines, FeS of varying composition is stable thermodynamically. Three of the isothermal cross sections, which served to prepare the plot, are shown in Fig. 8. Toward the low concentration end, these curves were drawn so as to be consistent with the thermodynamic data of Rosenqvist (5). The decrease in the reaction rates as the limit of existence of the FeS phase is approached is clear. Therefore, at a constant $H_2S:H_2$ ratio, the reaction rates first increase and then rather abruptly decrease with increasing temperature. From the data of Fig. 7, a rough estimate of the over-all activation energy (Arrhenius) gave a value of 19.3 kcal/mole, at constant $H_2S:H_2$ ratio and in the ratio-temperature range sufficiently far away from the equilibrium line to give a linear relationship.

Effect of oxygen on reaction rates.—Table I illustrates the effect of O_2 on the rates of reaction at various locations of the plot of Fig. 7. Oxygen, introduced into the H_2S-H_2 mixtures, forms elemental sulfur as discussed previously. This accelerates the sulfidization rates, and initiates and supports sulfidic attack in a range where, in the absence of O_2, i.e., from H_2S-H_2 mixtures alone, the formation of FeS is impossible thermodynamically. The presence of elemental sulfur vapor accounts for this effect.

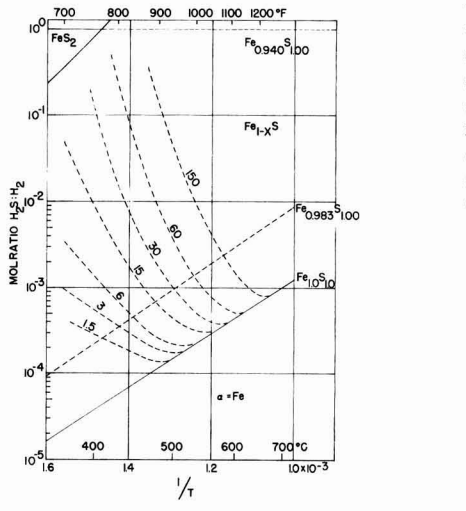

Fig. 7. Isokinetic curves and phase existence limits for the reaction of steel with H_2S mixtures at atmospheric pressure. The existence fields of Fe, $Fe_{1-x}S$, and FeS_2 are from the work of Rosenqvist (4). The numbers on the isokinetic curves indicate rates of reaction in units of $cm \cdot 10^{-6} \cdot hr^{-1}$ of metal consumed; 1.5 $cm \cdot 10^{-6} \cdot hr^{-1}$ corresponds approximately to 0.005 ipy.

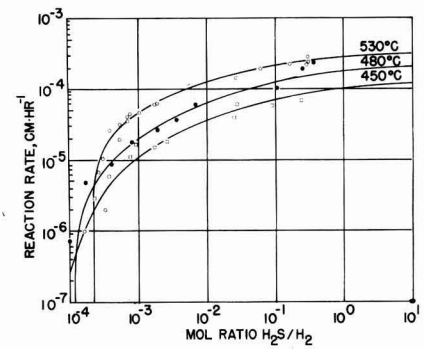

Fig. 8. Three typical experimental isothermal cross sections of Fig. 7.

Table I. Influence of Oxygen on Rates of Reaction of Steel with Hydrogen Sulfide-Hydrogen Mixtures

Temp, °C	Mole ratio, $H_2S:H_2$	Reaction rate, $cm \cdot 10^{-6} \cdot hr^{-1}$	
		No O_2	0.1 vol. % O_2 added
330	7.5×10^{-4}	17	30
375	7.5×10^{-4}	17	100
560	11×10^{-4}	48	440
530	1×10^{-4}	0	88
530	0.5×10^{-4}	0	30

A quantitative evaluation of the O_2 effect was not attempted since this would require detailed knowledge of the rates of reaction of H_2S with O_2 and of S with H_2 in the flowing gas mixture in order to determine the specific concentrations of S at the point of specimen exposure.

Variation of reaction rates with pressure.—Increasing the total pressure without changing the $H_2S:H_2$ ratio accelerates the sulfidization rate of steel, as shown in Fig. 14. This acceleration, however, is less than directly proportional to the total pressure. The data available, if analyzed by the Fischbeck-Wagner method (cf. Fig. 4), indicate that the rate change occurs principally by acceleration of the linear surface reaction, and that the parabolic rate constant is relatively unchanged.

Small amounts of O_2, if not excluded meticulously, distort the pressure-sulfidization rate relationship considerably, since concurrently with the partial oxidation of H_2S to water vapor and S, which promotes the sulfidization rate, there proceeds the slower reaction of S with H_2 to form H_2S. Under these conditions increased pressure, by causing a longer exposure of the flowing gas mixture to high temperatures in the experimental equipment, occasionally decreases the concentration of free S vapor at the specimen site. Consequently, the rate of sulfidization of steel at a certain site may even decrease with pressure if O_2 is not eliminated meticulously.

Physical structure of sulfidic scale.—Metallographic examination of the sulfidic scales shows that they may consist of several layers. However, during the early stages there appears to be only two layers, as illustrated in Fig. 9. Layer A, next to the metal, is dense and fine grained. Layer B, between layer A and the gas, is composed predominantly of coarse columnar grains which have their longest dimension roughly normal to the scale surface. The grains in layer B are separated by relatively large pores which extend from layer A to the free surface. During the early stages, layer A is approximately one-half to one-third as thick as layer B.

After the reaction is more advanced, evidence has been noted in some specimens of a third layer, C, lying between the other two. This layer also is porous and relatively coarsely crystalline although not so much so as layer B. Layer C may be nothing more than a variation of layer B. The ratio of the thickness of layer A to that of layer B (and C) decreases as the reaction advances. Apparently the outer layer increases in thickness whereas the thickness of layer A approaches a limiting value.

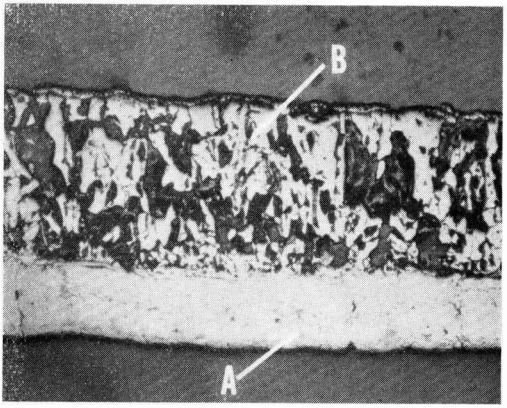

Fig. 9a. Cross section through FeS scale on iron showing the two main layers. Layer A (lower) is the dense, fine crystalline material formed next to the metal. Layer B (upper) is the porous, columnar-crystalline material found between the dense layer and the gas. Photograph taken with sensitive tint plate (X100) so pores and cavities appear gray.

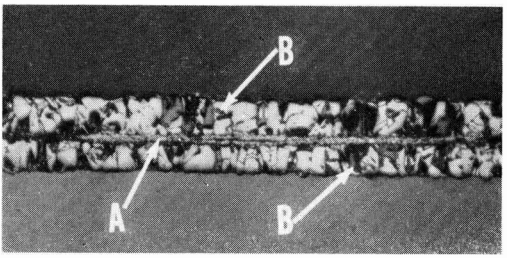

Fig. 9b. Structure of cross section of thin specimen of low carbon steel after 18-hr exposure to pure H_2S at 530°C. The metal has been completely consumed and the two layers, (A) dense fine-crystalline and (B) porous coarsely crystalline, appear on either side of the center line. Photograph taken with sensitive tint plate (X100) so pores and cavities appear gray.

The striking difference in the texture of layer A, as compared with that of layers B and C, points to different modes of nucleation and growth. Both layers were FeS.

Mechanism of the Sulfidization of Steel

The following sequence of reaction steps seems to be the simplest consistent with the experimental observations; there may be other possibilities.

Step 1. Surface adsorption: $(H_2S)_{gas} \rightleftharpoons (H_2S)_{adsorbed}$ This step may be assumed to be fast, so that an equilibrium exists essentially between the adsorbed and the gaseous H_2S, at least at the higher temperatures. The surface concentration of H_2S molecules then is determined (through an adsorption isotherm) by the partial pressure of H_2S in the gas phase.

Step 2. Formation of diffusing species at the gas-iron sulfide interface: According to the usually accepted concepts (3, 20) the diffusing species in FeS is a cation vacancy. For such a mechanism, the re-

action for Step 2 may be written, at least for a sulfur-rich composition range:

$$H_2S_{adsorbed} + 2Fe^{++}{}_{scale} + 2S^{=}{}_{scale} \rightarrow H_2 + 2Fe^{+++}{}_{scale} + V_c + 3S^{=}{}_{scale}$$

where V_c denotes a cation vacancy. For this step, the rate may be written

$$\frac{dV_c}{dt} = \dot{y} = a[H_2S_{adsorbed}] \qquad (III)$$

where a is a constant and y is the amount of reaction in terms of metal thickness consumed, and is assumed to be, as the simplest form, of first order with respect to the adsorbed H_2S. Hauffe and Pfeiffer (21, 22) used a similar concept in explaining the linear law found in the oxidation of Fe by CO_2-CO mixtures.[2] If the diffusing species is of a different kind, Eq. (III) still would apply since it is not committed to any definite species.

Step 3. Diffusion through the sulfide scale: Cation vacancy diffusion, with Fe^{++} ions moving from the metal through the scale to the gas-scale interface, is the usually accepted mechanism (4). However, it is not possible to explain the coexistence of two distinctly different types of layers in the scale by means of this particular diffusion mechanism alone. Also it cannot explain the long-range linear rates satisfactorily. Hence it is postulated that two diffusion mechanism act:

(*a*) In the porous columnar layer, B, the diffusion, so far as the FeS phase is concerned, is by the mechanism of cation vacancies. Of course, gaseous diffusion in the pores also occurs.

(*b*) In the dense fine-crystalline layer, A, the diffusing species is different; sulfur ions or atoms may be the diffusing species there. Thus, layer A would grow at the metal-scale interface, filling the zone of metal consumption (24), whereas layer B would grow at the gas-scale interface, by diffusion of Fe^{++} ions through vacancies from the boundary between A and B to this interface.

The diffusion limitation resides mainly in layer A.

Excursus on support for the second postulate in Step 3.—The second postulate given above may be supported by several arguments.

The total driving force of the reaction is

$$G = +RT \log \frac{r}{r_o} \qquad (IV)$$

where r is the H_2S:H_2 ratio for the given experimental conditions, and r_o is the same ratio for the equilibrium conditions at the temperature, T, in the FeS/Fe system, and R is the gas constant. This driving force is applied across the sum of all of the reaction steps. Thus, a fraction of this driving force may be assigned to each of the consecutive steps. Since, as further discussion will show, Step 2 probably is the principal rate-limiting step, it may use up most of the driving force available, leaving only a relatively small remainder to be applied across the sulfide phase proper. This would place the composition of the growing sulfide film, layer A, in the immediate vicinity of the FeS/Fe equilibrium line shown in Fig. 7. Now:

(*A*) If the surface reaction, Step 2, uses up most of the driving force for the reaction, the composition of the dense layer, while it is growing, is close to that of FeS in equilibrium with Fe; thus, very few cation vacancies exist, and another diffusing species could take over easily.

(*B*) FeS in equilibrium with Fe appears to have a slight S deficiency (5) thus indicating the possible existence of some mode of disorder other than the cation vacancy.

(*C*) Pfeiffer and Ilschner (25) report considerable S mobility in the FeS scale. The mobility of anions in a divalent oxide (MgO) also is apparent from the work by Winters and Houghton (26, 27).

The first argument hinges on a large decrease in driving force across the surface reaction step. Figure 10 compares the data of Hauffe and Rahmel (3), obtained at 10 mm S vapor pressure, with the parabolic rate constant derived from the slopes of curves, such as those in Fig. 4, for the reaction of steel with pure H_2S. The chemical potential, that is, the partial molar free energy, of S in pure H_2S at 530°C corresponds approximately to a sulfur (S_2) vapor pressure of 5 mm. The dashed line (III) in Fig. 10 shows the present experimental data curve after correction to a constant S_2 pressure of 5 mm by means of the $p^{1/4}$ relation found by Hauffe and Rahmel. The extrapolated curve of Hauffe and Rahmel would predict a very much higher reaction rate. Hence, sulfide film growth in pure H_2S occurs as if the chemical potential of S on the gas phase side of the sulfide film were very much lower than that which actually exists in the gas phase. In other words, the outer layer of the sulfide film "sees" a much lower chemical potential of S than that which

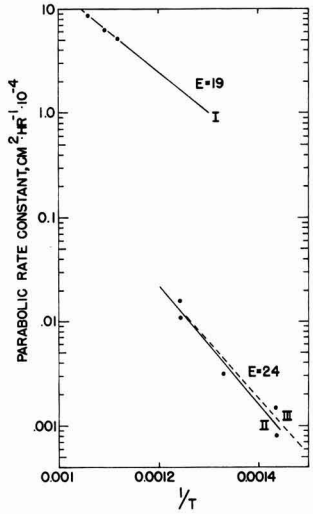

Fig. 10. Comparison of parabolic rate constants in S vapor and in H_2S. Curve I, Hauffe and Rahmel's results in S vapor at P_{S_2} = 10 mm; II, present results in pure H_2S; III, curve II corrected to one (4.7 mm) equivalent S pressure.

[2] Wagner (23) has proposed a dissociation of adsorbed CO_2 into CO and adsorbed O or $O^{=}$ as the rate-limiting step in this case; such treatment also leads to a correct mathematical form.

exists in the gas, a stituation also observed, for example, in the sulfidization of Ag by H_2S (19). This indicates a sizable decrease in the available driving force in Step 2. At the same time, the activation energies (Arrhenius) are roughly the same, viz., 19-24 kcal/mole.

A cursory x-ray examination of the sulfidic scale both for layer A and for layer B supported the thesis that the composition of the scale, even that formed by the sulfidization of steel in pure H_2S, indeed corresponds to FeS with a composition in the vicinity of the Fe-FeS equilibrium line. The following x-ray findings may be cited: (*a*) Even when H_2S alone was used, no FeS_2 was found. (*b*) Interplanar spacings, computed from planes with Miller indices: (100), (002), (101), and (102), which could be identified beyond doubt by comparison with the data of Hagg and Sucksdorff (20), were within a fraction of a per cent the same for scale formed in pure H_2S and for scale formed in a mixture in which the H_2S:H_2 ratio was 1.1×10^{-3}. This indicates that, even in pure H_2S, the scale does not contain more than a per cent or so of surplus S. (*c*) Besides the basic cell spacings, extra lines were present in the pattern of the scale formed in pure H_2S; some of the lines approximating Hagg's superlattice lines. According to Hagg, the existence of a superlattice is confined to the compositions between Fe_1S_1 and approximately $Fe_{0.93}S_1$; this is to be compared with compositions of the order of $Fe_{0.89}S_1$ which are thermodynamically possible in pure H_2S. (*d*) The lines in the x-ray patterns were not broad, and thus were more representative of a homogenous narrow range of composition than of a wide continuous composition range.

Aside from lines which could be clearly identified with Hagg's data, other lines were present, and some of Hagg's lines were absent. This might be the result of certain minor changes in the lattice cells of FeS and indicates that a more thorough x-ray investigation of the reaction products would aid in explaining the diffusion mechanisms.

Similarly, the scale formed in pure H_2S contained only very slightly magnetic or nonmagnetic fractions as tested by a hand magnet. The fractions described as "magnetic" did not exceed, by a crude comparison, on gently crushed scale, the paramagnetic susceptibility which was observed for $MnCl_2$ ($\kappa = 107 \times 10^{-6}$ cgs e.m. units). This would place the scale composition in the range close to stoichiometric FeS on the basis of Haraldsen's data (28, 29).

Step 4. Reaction at the metal-sulfide interface: There appears to be no immediate need to consider the reaction at the metal-sulfide interface to be rate-limiting. In the light of the postulates discussed under Step 3, this reaction may be one of sulfur atoms in the FeS lattice forming bonds with the iron atoms on the metal surface and then gradually penetrating into the metal.

Step 5. Processes in the contact zone between layers A and B: Occurrences in the contact zone between layers A and B also should be considered. With the above postulates, in this zone the transport process changes from that of S diffusion to that of Fe diffusion by means of cation vacancies. As sulfur atoms move through layer A toward the metal, iron ions, becoming surplus in the outer part of layer A, migrate through the columnar crystals of layer B toward the gas-scale interface. The cation diffusion coefficient should increase in this zone quite rapidly as the cation vacancies become more numerous. Formation of cation vacancies also causes a lattice shrinkage (Fig. 11).

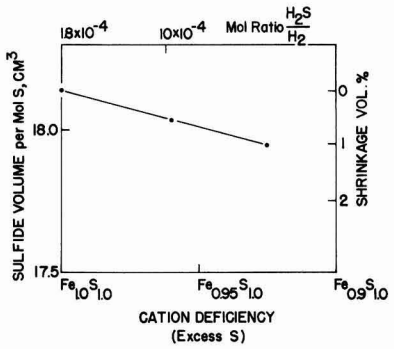

Fig. 11. Shrinkage of FeS volume with H_2S/H_2 mole ratio and with S content at 530°C (based on data of Hagg and Sucksdorff and of Rosenqvist).

Layer B should become prominent as soon as the increasing retardation of the diffusion rate through the scale by Step 3 brings the chemical potential of S in the outer regions of layer A into the existence range of cation vacancies. Accordingly, the long-time linear growth rates should become established as soon as layer A reaches a certain thickness. This is in at least qualitative agreement with the observations.

In the presence of Cr, e.g., in a 5% Cr-½% Mo steel, the linear long-range rate becomes established at a much smaller scale thickness. On the basis of a vacancy diffusion mechanism, the incorporation of Cr^{+++} ions into the FeS lattice will generate vacancies, since Cr^{+++} can act like Fe^{+++} in the equation shown in Step 2. Therefore, layer B can start forming at a lower chemical potential of S.

Cavity stabilization in Layer B.—The persistence of cavities in layer B is readily understood. The cavities communicate with the gas phase, and H_2S is consumed and H_2 generated in the cavities, thereby decreasing the H_2S:H_2 ratio. The cavity cannot close, since, if arrival of fresh H_2S is hindered, the gas phase in the cavity rapidly approaches the FeS/Fe equilibrium line and becomes less and less sulfidizing. On specimens prepared in S vapor, cavities were not observed.

On the basis of this and previous considerations, the composition of FeS in the columnar layer should be quite uniform, with a relatively small cation vacancy concentration gradient over the thickness of the layer.

Influence of Hydrogen Sulfide:Hydrogen Ratio and of Pressure

The kinetic relations are explainable on the basis of the above steps. The sum of the resistances im-

posed by Steps 2 and 3 determine the sulfide film growth rate. Under the conditions for which the kinetics is mixed linear-parabolic it may be considered, by analogy with Ohm's law (Fischbeck), that:

$$\dot{y} = \frac{E}{R_1 + R_2} \qquad (V)$$

where $\dot{y}$ is the reaction rate, E is a constant proportional to the driving force for the reaction, R_1 is the resistance (proportional to $1/k_1$) imposed by the gas-scale interface reaction, and R_2 is the resistance (proportional to y/k_2) imposed by the diffusion step. The reaction resistances, of course, are proportional to the reciprocals of the reaction rate constants. The resistance R_1 is dependent only on the surface concentration of adsorbed H_2S [Eq. (III)], but the resistance R_2 is proportional to the amount of reaction, y, since the length of the diffusion paths increases with y.

Once layer A has attained a substantially constant thickness as was observed in the case of the long-time rates, the resistance R_2 is limited predominantly by the diffusion in layer A; R_2 then becomes substantially constant. Under these conditions, Eq. (V) may be combined with Eq. (III) and (IV) and rewritten:

$$\dot{y} = \frac{A \cdot RT \log (r/r_o)}{\frac{B}{(H_2S_{adsorbed})} + C}$$

$$\approx \text{const} \cdot (H_2S_{adsorbed}) \cdot (\log r/r_o) \qquad (VI)$$

where A, B, and C are constants. For a constant temperature, the logarithmic term now gives the driving force, and the rate of the linear reaction has been made proportional to, i.e., the resistance is made inversely proportional to, the surface concentration of adsorbed H_2S. This new reaction rate, however, will be smaller than that controlled by the linear component alone, as was the case during the initial stages of the growth of layer A. This is consistent with the results obtained.

To test the compliance of the experimental data with the above mathematical form (VI), three curves of Fig. 4 are replotted in Fig. 12 in terms of log r/r_o as the abscissa, without any correction for the adsorption isotherms. At 530°C the plot is almost linear and, thus, the reaction rate is almost directly proportional to the driving force. For the two other temperatures, the lines are curved. These two, however, can be straightened out, cf. Fig. 13, by correcting for the adsorption isotherm. A Freundlich type function:

$$s = \text{const} \cdot p^{1/n} \qquad (VII)$$

has been used, with $n = 10$, to account for adsorption. This magnitude of n suggests a relatively high coverage of the surface with adsorbed H_2S.

The increase in the reaction rate with pressure at constant H_2S:H_2 ratio, shown in Fig. 14 (a) on a logarithmic scale, replots well in terms of the Langmuir adsorption isotherm, cf. Fig. 14 (b). The Langmuir isotherm was not used in making the correction in Fig. 13 because of its more complex form.

Thus, the variation of the reaction rate with the H_2S:H_2 ratio, and with the pressure, follows kinetics explainable in terms of adsorption, surface reaction, and diffusion steps. The short-time rate has a linear component, explained by the reaction of adsorbed H_2S to form a diffusing species at the gas-scale interface, and a parabolic component, ex-

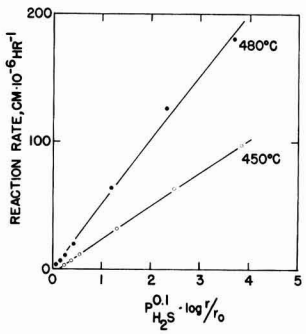

Fig. 13. Data of Fig. 12 modified by introduction of adsorption term.

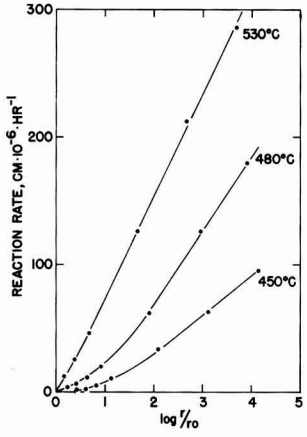

Fig. 12. Variation of reaction rate with driving force

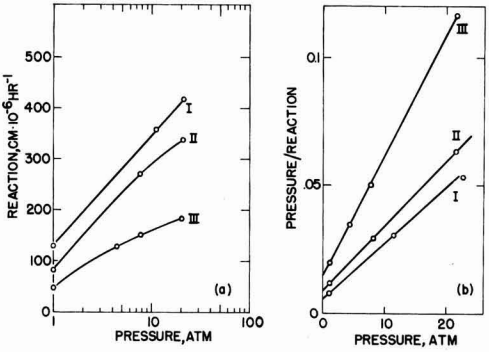

Fig. 14. Variation of the reaction rates at 530°C with total pressure, at a constant H_2S/H_2 mole ratio. (a) (left): semilogarithmic plot; (b) (right): plot for an isotherm of the Langmuir type. H_2S/H_2 mole ratios: curve I, 22 x 10^{-4}; II, 11 x 10^{-4}; III, 8 x 10^{-4}.

plained by the diffusion resistance of a growing dense layer of FeS. The long-time linear rate may be explained, at least qualitatively, by the coexistence of two diffusion mechanisms and the consequent formation of two layers—a porous one which presents no diffusion barrier and a dense one which becomes substantially constant in thickness and thus presents substantially a constant diffusion barrier.

Acknowledgment

The authors are indebted to Bernard Ostrofsky for his x-ray interpretations. The experimental help of Cecelia Husen and Gerald Van Hees is gratefully acknowledged.

Manuscript received Dec. 10, 1956. This paper was prepared for delivery before the Cleveland Meeting Sept. 30-Oct. 4, 1956.

Any discussion of this paper will appear in a Discussion Section to be published in the December 1958 JOURNAL.

REFERENCES

1. A. Dravnieks, *Ind. Eng. Chem.*, **43**, 2897 (1951).
2. A. Dravnieks, *This Journal*, **102**, 435 (1955).
3. K. Hauffe and A. Rahmel, *Z. Physik. Chem.*, **199**, 152 (1951).
4. R. A. Meussner and C. E. Birchenall, Metallurgy Report No. 7, Princeton University (1956).
5. T. Rosenqvist, *J. Iron Steel Inst. London*, **176**, 37 (1954).
6. M. Farber and D. M. Ehrenberg, *This Journal*, **99**, 427 (1952).
7. R. E. Wilson and W. H. Bahlke, *Ind. Eng. Chem.*, **17**, 355 (1925).
8. E. Dietrich, *Chem. Fabrik*, **6**, 25 (1933).
9. E. Dietrich, *ibid.*, **10**, 145 (1937).
10. C. F. Prutton, D. Turnbull, and G. Dlouhy, *Ind. Eng. Chem.*, **37**, 1092 (1945).
11. E. B. Backensto, R. D. Drew, and C. C. Stapleford, *Corrosion*, **12**, 22 (1956).
12. E. B. Backensto, R. D. Drew, R. W. Manuel, and J. W. Sjoberg, *Corrosion*, **12**, 235 (1956).
13. C. Phillips, Jr., "High Temperature Sulfide Corrosion in Catalytic Reforming of Light Naphthas," presented at South Central Region meeting of N.A.C.E., San Antonio, Texas (Oct. 1956).
14. F. J. Bruns, "Effect of Hot H_2S Environments on Various Metals," *ibid.*
15. G. Sorell and W. B. Hoyt, *Corrosion*, **12**, 213 (1956).
16. A. Dravnieks, *J. Am. Chem. Soc.*, **72**, 3761 (1950).
17. K. Fischbeck, L. Neundenbel, and F. Salzer, *Z. Elektrochem.*, **40**, 517 (1934).
18. C. Wagner and K. Grunewald, *Z. Physik. Chem.*, **B40**, 455 (1938); cf. W. Jost, "Diffusion in Solids," p. 353, Academic Press, Inc., New York (1952).
19. H. Reinhold and H. Seidel, *Z. Elektrochem.*, **41**, 499 (1953).
20. G. Hägg and I. Z. Sucksdorff, *Z. Physik. Chem.*, **B22**, 444 (1933).
21. K. Hauffe and H. Pfeiffer, *Z. Elektrochem.*, **56**, 390 (1952).
22. K. Hauffe and H. Pfeiffer, *Z. Metallkunde*, **44**, 27 (1953).
23. C. Wagner, Private communication.
24. A. Dravnieks and H. J. McDonald, *J. (and Trans.) Electrochem. Soc.*, **94**, 139 (1948).
25. H. Pfeiffer and B. Ilschner, *Z. Elektrochem.*, **60**, 424 (1956).
26. E. R. S. Winters and G. Houghton, *Nature*, **164**, 1130 (1949).
27. E. R. S. Winters and G. Houghton, "Mass Spectrometry," p. 127, The Institute of Petroleum, London (1952).
28. H. Haraldsen, *Z. anorg. u. allgem. Chem.*, **246**, 169, 195 (1941).
29. P. W. Selwood, "Magnetochemistry," p. 246, Interscience Publishers, New York (1943).

Corrosion Inhibition by Organic Amines

Helmut Kaesche[1] **and Norman Hackerman**

Department of Chemistry, The University of Texas, Austin, Texas

ABSTRACT

The corrosion of pure iron in 1*N* HCl is discussed in terms of the theory of mixed potentials and the theory is applied to inhibition by organic compounds. Corrosion rates with and without inhibition by aniline, several aniline derivatives, and alkylamines were determined by cathodic polarization measurements as well as by colorimetric analysis of the solution. It is shown that all compounds show a maximum inhibitor efficiency at a concentration of approximately 0.1 mole/l, that with one exception all are cathodic as well as anodic inhibitors, and that in most cases they are predominantly anodic inhibitors. An interpretation of the data on cathodic inhibition is suggested on the basis of the assumption of a uniform metal surface and uniform adsorption. The interpretation of anodic inhibition is found to be difficult due to a lack of satisfactory experimental data.

There is little question that organic compounds acting as inhibitors of wet corrosion do so by forming an adsorbed layer at the metal-solution interface. There is still considerable difference of opinion as to the details of the mechanism of inhibition. Also, while an extensive literature on inhibition exists, detailed knowledge of the influence of the nature of the inhibitor is still lacking. Therefore it is desirable to accumulate more data on the inhibition efficiency of simple organic compounds with fairly well-known molecular properties. It is for this reason that some experiments with simple aniline derivatives and

[1] Present address: Bundesanstalt fuer Materialpruefung, Berlin-Dahlem, West Germany.

alkylamines have been carried out and are presented in this paper.

The corrosion of pure Fe in air-free 1*N* HCl was chosen for the investigation. The over-all corrosion reaction may be split into the anodic and cathodic "partial" reactions:

$$Fe \rightarrow Fe^{++} + 2e^-; \qquad 2H^+ + 2e^- \rightarrow H_2$$

The electrochemical behavior of the Fe specimen as an electrode, including corrosion, is then determined by the kinetics of the partial reactions, these being characterized by their overvoltage curves. This leads to the concept of the superposition of the "partial overvoltage curves" to the "total current-voltage curve" originally given by Wagner (1) and recently applied to the corroding Fe electrode by Uhlig (2), Stern (3), Bonhoeffer (4), and Heusler (5). The following two paragraphs give a short summary of the terms involved. For more detail the papers cited above should be used.

Neglecting the reverse reactions (Fe deposition and H dissolution), the two partial reactions are assumed to have exponential overvoltage curves of the form

$$j_{Fe} = (j_o)_{Fe} \exp\left[-\frac{1}{b'_{Fe}}(E_{Fe} - E)\right] \qquad (I)$$

$$j_H = (j_o)_H \exp\left[\frac{1}{b'_H}(E_H - E)\right] \qquad (II)$$

Here j_{Fe} and j_H are the apparent anodic and cathodic current densities based on projected surface area; $(j_o)_{Fe}$ and $(j_o)_H$ are the current values at the equilibrium potentials E_{Fe} and E'_H, b'_{Fe}, and b'_H are the "Tafel" slopes; and E is the measured electrode potential. Regardless of their actual physical significance $(j_o)_{Fe}$ and $(j_o)_H$ are called exchange currents.

At any value of a polarizing current, j

$$j = j_{Fe} - j_H \qquad (III)$$

This is the equation of the total current-voltage curve which can be measured by external polarization. At $j = 0$, $E = E_{corr}$ and

$$|j_{Fe}| = |j_H| = j_{corr}$$

Here j_{corr} is the corrosion rate in terms of an apparent current density, and E_{corr} the corrosion potential (open circuit potential). With Eqs. (I), (II), and (III) both the corrosion rate and the corrosion potential are completely determined by the overvoltage properties of the partial reactions. The simultaneous measurements of j, j_{Fe}, and j_H should therefore yield complete knowledge of the electrode behavior in a given surrounding medium. This procedure involves laborious analytical determinations of the amount of dissolved iron or deposited hydrogen. Alternatively the electrode may simply be polarized to potential regions where either j_{Fe} or j_H becomes very small so that $j \cong j_H$, or $j \cong j_{Fe}$. Then the total current voltage curve becomes practically identical with one or the other of the partial overvoltage curves. Provided no change of the rate-determining step of the partial reaction occurs between this potential region and E_{corr}, the partial curve in the vicinity of the latter potential can then be obtained by extrapolation.[2] This simple geometrical operation is illustrated by Fig. 1. Moreover, extrapolation to E_{corr} yields the value of j_{corr}. Stern (3) has shown that the corrosion rates obtained by extrapolation of the cathodic partial overvoltage curve check well with those determined by analysis of the amount of dissolved Fe. The same method is used throughout the present investigation. So far it appears to be difficult to measure the anodic partial curve in this way, but in the vicinity of E_{corr} a part of this curve may be obtained from corresponding values of j and j_H by application of Eq. (III).

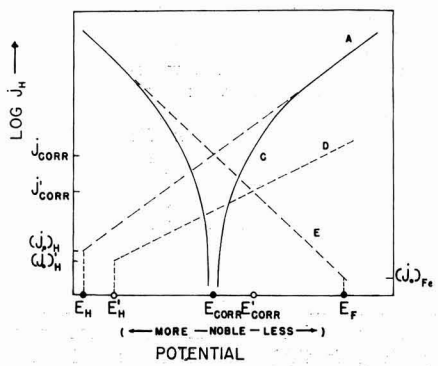

Fig. 1. Schematic representation of the partial overvoltage curves (dashed curves) and the total current voltage curve (solid curve C) of iron corroding in nonoxidizing acids. (A)—cathodic partial curve; (D)—cathodic partial curve in the presence of a cathodic inhibitor; (E)—anodic partial curve. Other symbols as defined in the text.

The organic inhibitors used for the present investigation do not change the over-all reaction. The lowering of the corrosion rate must therefore be brought about either by a decrease of the difference between the equilibrium potentials E_H and E_{Fe}, which can only be brought about by changes of the bulk concentration of the species taking part in the corrosion reaction, or by an increase of the overvoltage of one or both partial reactions. With respect to their action on one or both partial reactions, inhibitors are often classified as being of an anodic, cathodic, or mixed type. The general result of strictly cathodic inhibition is shown in Fig. 1 by the shift of the cathodic partial curve (A) without inhibition to (D) with inhibition. The inhibition is assumed to decrease the H-equilibrium potential from E_H to E'_H, the exchange current from $(j_o)_H$ to $(j_o)'_H$ and to increase the Tafel slope. At the same time the corrosion rate decreases from j_{corr} to j'_{corr}. Whether one, two, or all the possible changes occur, E_{corr} must always change to a less noble value E'_{corr}. Similarly, a reverse change of E_{corr} indicates some anodic inhibition. However, observation of the decrease of j_{corr} and the shift of E_{corr} alone simply indicates predominance of anodic or cathodic inhibition since a small effect on the opposite partial reaction may also exist. That is, the inhibition is actually of the mixed type.

Local cell action between fixed anodic and cathodic areas cannot be affected seriously by the ohmic resistance of the adsorbed layer as long as this polarization method gives the same value for the

[2] This also requires that no other oxidation or reduction process becomes operative in this potential span.

corrosion rate as does a direct analytical method. The former is based on the assumption of a virtually uniform electrode potential and must lead to serious errors if iR drops of the order of $\geqq 5$ mv exist along an average current path between local electrodes. Correct polarization values of j_{corr} indicate either very short local current paths or low values of the specific resistance of the adsorbed layer. Hoar (6) has suggested that practically the whole electrode surface is capable of acting as a cathodic area, whereas the anodic area should be represented by the sum of all atomic sites undergoing dissolution at any given moment, e.g., where the sites might be the ends of incomplete atom rows. With any nonideal crystal, lattice distortions and impurity atoms may also give rise to anodic spots. Thus, with respect to the relative size of anodic and cathodic areas, as well as to the distribution of anodic spots, the condition of the corroding iron surface is similar to the condition of the surface of a corroding liquid amalgam. In the latter case the cathodic area is identical with the total surface and the anodic area is given by the sum of atoms of the amalgamated metal in the surface of the Hg. Since at any moment predictions can be made that the next Fe atom being transferred across the phase boundary should come from the same incomplete atom row or lattice distortion, Fe dissolution is still not as truly statistical as the dissolution of an amalgamated metal. Nevertheless, the condition of the corroding amalgam surface should be a better model for the condition of the surface or corroding Fe, especially in acid solutions, than is the frequently used model of a checkerboard-like pattern of local electrodes. Therefore, the concept of a uniform metal surface undergoing statistical dissolution is used for the discussion of inhibition. It is obvious that this concept, if justified for pure Fe, is not immediately applicable to steel surfaces where secondary phases may have considerable influence.

If the electrode surface is uniform, inhibitor adsorption should be general. As has been pointed out by Hoar (7), and Hackerman and Makrides (8), the theory of adsorption of cationic inhibitors on cathodic sites only, for some time widely accepted (9), is objectionable even if local cells are operating on the corroding surface, the obvious argument being the uniformity of the electrode potential. The possibility of cation adsorption by means of electrostatic forces is determined by the electric charge of the electrode with respect to the solution, i.e., by the position of the electrocapillary maximum with respect to E_{corr}, not by the charge of one electrode with respect to another electrode, as with local anodes and cathodes. Little is known about the electrocapillary maximum of Fe, and Frumkin's value of 0.37 v in $10^{-3}N$ H_2SO_4 (10) does not indicate that Fe corroding in $1N$ HCl ($E_{corr} = 0.25$ v) has a positive charge at the corrosion potential. The electrocapillary maximum may be shifted to considerably more noble potentials by chemisorption of Cl^-, analogous to observations reported by Iofa and coworkers (11) for I^- and Br^- at very low concentrations. At present, therefore, the possibility of strong cation adsorption on corroding Fe is undecided. This is important with respect to the theory of chemical rather than physical adsorption suggested by Hackerman and Makrides (8). According to this concept, cationic organic inhibitors are deionized at the metal-solution interface; therefore, in the case of amine-hydrochlorides the adsorbed species should be the free amine. The establishment of a more or less well-defined chemical bond between the inhibitor and the Fe should result in a decrease in apparent reactivity of the Fe in the electrode surface [Hackerman (12)]. This leaves E_{Fe} unchanged, but it may greatly decrease the exchange current of the anodic partial reaction.

Material and Apparatus

Iron electrodes were cut out of 99.99% Armco iron sheets, 1 mm in thickness, in the shape of little flags of about 4-5 cm^2 geometric surface area. The handle of these flags was soldered to a copper wire and sealed into a glass holder with polyethylene. Before immersion, the electrodes were abraded with No. 1 through 4/0 emery paper, and rinsed with benzene, acetone, and water.

$1N$ HCl solutions were prepared from C.P. concentrated HCl and double-distilled water. No change of the corrosion rate was observed when gaseous HCl distilled into water was used instead.

Except for methylamine- and ethylamine-hydrochloride, which were used without further purification of the high-grade compound, all inhibitors were redistilled one to three times under reduced pressure, until a colorless product of constant boiling point was obtained. The inhibitors were then dissolved in the appropriate amount of concentrated HCl to give a $1N$ HCl solution of the hydrochloride. No inhibitor solution was used later than three days after preparation.

Electrolytic hydrogen was passed through pyrogallic acid in alkaline solution, sodium plumbite in alkaline solution, concentrated H_2SO_4, a trap cooled with liquid nitrogen, and finally a 50-cm column of $1N$ HCl before being bubbled through the test solution. Omitting this procedure resulted in a marked decrease of the corrosion rate.

The apparatus used throughout the experiments is shown in Fig. 2. All parts were made of Pyrex, with stoppers and stopcocks very lightly greased with silicone grease. The test vessel A, the Ag/AgCl-electrode B, and the Pt-electrode C, were filled with $1N$ HCl up to the dotted lines. Three iron electrodes, D, of which only one is shown, were used at the same time.

The outlet of burette F was sealed into the ground joint E and on top of F a flask G served as a reservoir for inhibitor solutions. A second burette H was also sealed into E and was extended via capillary tubing into the test solution. Hydrogen entered the apparatus at I and left it at K, thus keeping all parts air-free and also slightly agitating the solution. If hydrogen was bubbled through the solution more vigorously the corrosion potential and the corrosion rate did not change by more than 1 mv and 1 $\mu a/cm^2$. The test vessel was placed in a thermostat kept at $30 \pm 0.5°C$. The volume of the test solution in A

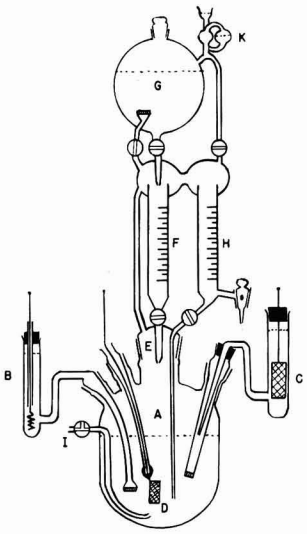

Fig. 2. Apparatus used for the measurement of overvoltage properties and corrosion rates.

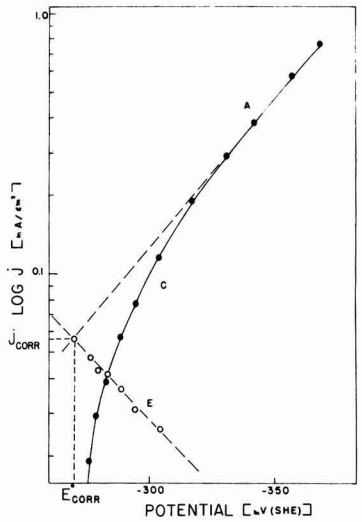

Fig. 3. Total current-voltage curve and partial overvoltage curve determined by cathodic polarization of an iron electrode in 1N HCl without inhibition. Symbols as given in the caption of Fig. 1; other symbols as defined in text.

was 500 cc; all pH changes due to the corrosion reaction were negligible.

The potential difference between the Fe-electrode and the Ag/AgCl-reference electrode was measured with a student-type potentiometer within ±1 mv. In order to be able to make quick readings during polarization measurements, an oscilloscope was used as zero indicator. Polarizing currents were applied between the Fe- and the Pt-electrode, using a 220 v dry battery in series with a resistance box and a milliammeter. Current readings were taken with a precision of ±5 μa at currents between 1 and 3 ma and ± 2μa at currents less than 1 ma. The resistance of the electrode system was small compared with the external ohmic resistance, the polarizing currents were therefore constant during the polarization time.

Procedure and Results

After the electrodes had been immersed in air- and inhibitor-free 1*N* HCl, a period of 3-5 hr was required for both E°_{corr} and j°_{corr}[3] to become constant. After 5 hr, E°_{corr} and j°_{corr} were constant in most cases except for random changes of ±1 mv/hr and ±3 μa/cm²/hr, respectively. The polarization behavior of all electrodes was checked at one-hour intervals throughout the immersion time, but only the readings taken between 5 and 7 hr after immersion were used for the final determination of the overvoltage properties. A considerable number of runs had to be discarded because of (*a*) corrosion rates more than 5 μa/cm² lower or higher than the average of all measurements, (*b*) nonconstant values of E_{corr} and j_{corr} after 5 hr, (*c*) potential drifts during polarization. Any drift greater than 1 mv/10 sec observed later than 10 sec after switching on the polarizing current was regarded as abnormal and attributed to contamination of the acid. In all cases of erratic behavior the electrodes were freshly sealed to the glass holder, freshly abraded and rinsed, and the test solution replaced by freshly prepared solution. No inhibition experiment was carried out until a given set of electrodes exhibited "normal" behavior, with $E_{corr} = -260 \pm 10$ mv (vs. S.H.E.), $j_{corr} = 50 \pm \mu$a/cm² and nondrifting potentials during cathodic polarization.

A typical example of a single polarization measurement with an uninhibited specimen is shown in Fig. 3. E_{corr} was measured immediately before the first polarization (immediately afterwards E_{corr} is usually 1-2 mv more noble than before, but the original value is reestablished within a minute). Cathodic currents of various strength were applied at 30-sec intervals and the polarized potentials E measured with the potentiometer (solid circles) 5-10 sec after switching on the current. The total current-voltage curve obtained as E vs. log j (solid curve) was always found to have a linear section in the current range $0.2 \leqq j \leqq 0.7$ ma/cm² which could easily be extrapolated to E°_{corr} (dashed curve). From this curve, presumably the cathodic partial overvoltage curve, j°_{corr} and b°_{H} ($=b^{o\prime}_{H}/2.303$) were determined graphically. In a few cases the nonlinear part of the logarithmic total current voltage curve was also measured to obtain examples of the anodic partial overvoltage curve by application of Eq. (III) (open circles and broken line). Thus the slope b°_{Fe} of the anodic curve was found to be of the order of 0.075 ± 0.01 v/log j which may be compared with Stern's (13) value 0.068, determined by the same method in NaCl + HCl solution of pH 1.5 at 25°C. The exchange current $(j_o)^{\circ}_{Fe}$ was calculated to be of the order of 0.04 to 0.1 μa/cm² which agrees fairly well with Stern's value of 0.04 μa/cm². However, any single determination of $(j_o)_{Fe}$ is good only to ±0.02 and any attempt to calculate the change of the exchange current due to weak inhibitor action is useless.

[3] o designates uninhibited properties.

Table I. Comparison of the average total corrosion rate of 3 electrodes obtained by cathodic polarization (i_1) and by colorimetric analysis (i_2)

Inhibitor	C (mole/1)	i_1 (μa)	i_2 (μa)
—	0	820 ± 20	840 ± 50
N-Methylaniline	0.06	720 ± 20	700 ± 20
N-Ethylaniline	0.05	490 ± 10	490 ± 10
N-Propylaniline	0.12	355 ± 10	350 ± 20

In order to avoid erroneous results caused by slow drifts of the electrode properties during immersion over several days, all electrodes were again abraded and rinsed before addition of inhibitors to the solution. Also, usually after two complete series of experiments for one inhibitor new electrodes were prepared. Otherwise the measurements in inhibited solutions were carried out exactly as were those without inhibitors. In these systems the cathodic partial current of the inhibited electrode at E°_{corr}, j', was also determined.

Especially after addition of the more effective inhibitors a slow drift of the potential of externally-polarized electrodes to less noble potentials could not be eliminated. It was probably caused by changes of the adsorption concentration of the inhibitor. Nevertheless, correct values of j_{corr} were obtained by using the potentials obtained 5-10 sec after switching on the polarization current, allowing 1-min intervals between two consecutive polarizations, and also limiting the polarizing currents to 0.5 ma/cm² in cases where the logarithmic total current-voltage curve became linear at 0.15-0.17 ma/cm² because of the lowered j_{corr}. This was shown by independent analytical measurements. For this control, polarization measurements were carried out between 2 and 8 hr after immersion in separate runs at one-hour intervals, and samples of the solution were taken at the same time. The Fe^{++} concentration of the samples was then determined colorimetrically, using o-phenanthroline. The average values of the corrosion rate obtained by polarization checked well with the corrosion rate determined by analysis (Table I).

Usually 3-4 runs at inhibitor concentrations between 0.05 and 0.2 mole/l were carried out. For each inhibitor concentration final values of j_{corr}, j', b_H, and E_{corr} were obtained by obtaining the algebraic mean of six single measurements, two per electrode. A typical example of the resulting curves of the electrode properties as a function of concentration is shown in Fig. 4 for *m*-toluidine. At $C \geqq 0.08$ to 0.1 mole/l, all inhibitors showed a maximum effect on the electrode properties independent of further increase of concentration up to 0.2 mole/l, the highest concentration investigated. As no attempt was made to measure fully the changes of the electrode properties at concentrations $0 \leqq C \leqq 0.1$, Table II lists only the electrode properties at maximum inhibitor effect obtained graphically from plots of the experimental values against concentration. With propylamine as inhibitor the slope b^{m}_{Fe} of the anodic partial overvoltage curve was determined at maximum inhibitor effect and found to be of the order of 0.080 ± 0.01 v/log *i*.

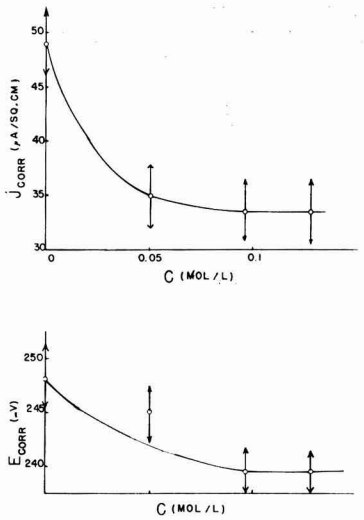

Fig. 4. The variation of the corrosion potential E_{corr} and the corrosion rate j_{corr} of a set of 3 Fe electrodes as function of the concentration of m-toluidine hydrochloride.

The error limits given in the tables are caused by differences in the behavior of different electrodes. Compared with these differences the limited precision of the measurements has little significance. This includes the error introduced by the resistance between the tip of the reference electrode and the iron electrodes about 2 cm away. It does not include the error limit of the colorimetrically determined values of j_{corr}.

Discussion

Inhibition of the cathodic partial reaction.—Table II shows that j' is lower than j°_{corr} for all the inhibi-

Table II. Average value of the corrosion potential E_{corr}, the corrosion rate j_{corr}, and the cathodic Tafel slope b_H of three electrodes with no inhibition (O) and at maximum inhibition (m), also the cathodic current at maximum inhibition at E°_{corr}

Inhibitor		E°_{corr} E^{m}_{corr} (mv)	b°_H b^{m}_H (v/log i)	j°_{corr} j^{m}_{corr} (μa/cm²)	j' (μa/cm²)
Aniline	O	−249	0.091	47	
	m	−237	0.090*	30	40
m-Toluidine	O	−248	0.092	48	
	m	−239	0.093	33	42
o-Toluidine	O	−257	0.086	51	
	m	−240	0.091	29	44
N-Methylaniline	O	−249	0.092	51	
	m	−241	0.089	38	46
N-Ethylaniline	O	−269	0.088	53	
	m	−260	0.094	37	46
N-*n*-Propylaniline	O	−267	0.089	49	
	m	−258	0.095*	32	38
N-Dimethylaniline	O	−249	0.085	53	
	m	−231	0.085	31	47
N-Diethylaniline	O	−268	0.083	54	
	m	−255	0.093	25	34
N-Di-*n*-propylaniline	O	−266	0.084	53	
	m	−252	0.093	24	29
Methylamine	O	−265	0.086	52	
	m	−268	0.086	45	43
Ethylamine	O	−268	0.091	54	
	m	−268	0.091	42	42
Propylamine	O	−269	0.085	55	
	m	−267	0.091	42	44
Error limit		±2	±0.002-3	±2	±3

* To ±0.004 in these cases.

tors and in many cases b^m_H (inhibited) is larger than b°_H. Therefore, all inhibitors investigated exhibit cathodic inhibitor action. To obtain a quantitative measure of this action recall that, with b_H constant, j'/j_{corr} must equal $(j_o)^m_H/(j_o)^\circ_H$, and therefore be a measure of the decrease of the cathodic exchange current. Even for small values of Δb_H ($= b^m_H - b^\circ_H$) the same relationship holds to a first approximation and was therefore calculated for each inhibitor. Following common usage in inhibitor research, instead of j'/j°_{corr} itself, Table III lists the quantity $(I - j'/j^\circ_{corr}) \cdot 100\% = I_c$. Neglecting the influence of Δb_H this quantity is called the "cathodic inhibitor efficiency" (not identical with the inhibitor efficiency which would be observed with a given I_c in the absence of all anodic inhibition). The values of Δb_H and the "total inhibitor efficiency" $I_T = (1 - j^m_{corr}/j^\circ_{corr}) \cdot 100\%$ are also tabulated. It is seen that I_c is practically constant for the first group and the last group (the alkylamines). With increasing chain length of the substituent of *N*-alkylanilines, inhibition increases, more noticeably in the *N*-dialkylanilines than in the *N*-monoalkylaniline series.

Remembering that all numbers are limiting values for maximum inhibition and therefore probably maximum adsorption, it can be expected that the adsorbed molecules are oriented nearly perpendicularly to the surface. If this is true, then the observed tendencies of the change of I_c strongly suggests an effect of the projected area per molecule. For perpendicularly oriented molecules the projected area of straight chain alkylamines is independent of the chain length and equals the projected area of the amine group. On the other hand, perpendicular adsorption of a *N*-substituted aniline means that all substituents form an angle smaller than 90° with the metal surface. An increase of chain length consequently increases the projected area. Also, with *N*-dialkylanilines a larger increase of the projected area is to be expected since two alkyl groups are added instead of one as in the case of *N*-monoalkylanilines. While no quantitative interpretation is possible it is clear that, for alkylamines and *N*-alkylamines, changes of I_c parallel changes of the projected area within each group. As I_c is the same for aniline and the toluidines it follows that only substitution for H on the amino group is effective, that is, close to the surface of the underlying metal. It is also possible that a smaller effect would be observed on increasing the chain length of the substituent on the benzene ring.

If all types of aniline derivatives investigated have the same maximum number of moles adsorbed per sq cm of the metal, then the total projected area should increase in the series aniline, *N*-methylaniline, *N*-dimethylaniline, and I_c should also increase. Actually I_c is greater for aniline than for either *N*-methyl- or *N*-dimethylaniline, and is about the same for these two compounds. Experimental data for the maximum adsorbed amount are not available, but it is reasonable to predict a decrease with increasing branching of the substituents due to steric hindrance. Therefore it is likely that, while the projected area per molecule increases, the total projected area decreases from aniline to *N*-methylaniline because of a decrease of the number of adsorbed moles. Thus the decrease of I_c here is not contradictory.

The decrease of $(j_o)_H$ is usually ascribed to a decrease of the true surface area available for hydrogen deposition (6, 7, 9). The observed changes of b_H, neglected in the discussion just above, is of importance here. In principle, changes of b_H can indeed be caused by mere changes of the true surface area available. This follows not only for the case of competing adsorption of inhibitor and H-atoms but also because of competing parallel reaction paths for H-deposition, depending to different degrees on the H-concentration of the surface. However, this requires very special assumptions not justified by experimental evidence.

A preferable less elaborate assumption is that both partial reactions are controlled by an energy barrier at the phase boundary which requires a slow discharge mechanism for the cathodic partial reaction. According to the H-overvoltage theory, b_H should then be of the form $2.303RT/\alpha z\mathbf{F}$, where R is the gas constant, T the absolute temperature, α a factor between 0 and 1, z the electron number, and $\mathbf{F}$ the Faraday. For Fe in different inhibitor-free solutions values of b_H between 0.08 and 0.15 v/log i have been observed by different authors (3, 5, 13, 14) indicating values of α ranging from 0.7 to 0.4. The average value of b_H found during the present investigation is 0.088 ± 0.004; α therefore is 0.66. The theory of slow discharge predicts $\alpha = 0.5$ for the case that exactly half of the overvoltage is used to lower the activation energy of the forward reaction, the other half being used to increase the activation energy of the reverse reaction. However, this ideal symmetry need not be followed in every case and, with a different α, slow discharge (or the electrochemical mechanism) may still be rate-determining. If this is accepted for the cathodic partial reaction it follows that an increase of b_H indicates a decrease of α and therefore a decrease in the fraction of the cathodic overvoltage used to lower the activation energy of the H^+ transfer across the phase boundary. This requires a distortion of the potential distribu-

Table III. Total, cathodic, and anodic inhibitor efficiency calculated for each inhibitor from j^m_{corr}, j', and j'', respectively; and j°_{corr} as found in uninhibited solution with the same set of electrodes; also $\Delta b_H = b^m_H - b^\circ_H$ calculated in the same way.

Inhibitor	I_T (%)	I_c (%)	Δb_H (v/log i)	I_a (%)
Aniline	36	15	−0.001	55
m-Toluidine	31	13	+0.001	46
o-Toluidine	43	14	+0.005	65
N-Methylaniline	25	10	−0.003	41
N-Ethylaniline	30	13	+0.006	47
N-*n*-Propylaniline	36	26	+0.006	53
N-Dimethylaniline	41	11	0.000	66
N-Diethylaniline	54	37	+0.010	68
N-Di-*n*-propylaniline	57	40	+0.008	71
Methylamine	13	18	0.000	0
Ethylamine	17	20	+0.002	20
Propylamine	23	20	+0.006	29
Error limit	4	4	0.003-4	4

tion in the phase boundary. It is then reasonable to assume that the cause of this distortion is the establishment of an additional energy barrier due to inhibitor adsorption. Consequently, the inhibitor layer is treated as a uniform film which leaves the available surface unchanged but increases the activation energy of H^+ transfer, thus decreasing the probability of this transfer. While distortion of the potential distribution may be responsible for the change of b_H lowering the transfer probability is responsible for the decrease of $(j_o)_H$. The observed influence of the total projected area is then not that of increasing surface coverage but of increasing density of the uniform inhibitor layer. The increase in density should cause a proportional increase in the activation energy. In view of the considerable error limit of the Δb_H values, a similar interpretation cannot be attempted for b_H as a function of the molecular structure of the inhibitor.

Inhibition of the anodic partial reaction.—Except for the single pair of data of b_{Fe} before and after addition of propylamine as inhibitor no other information on anodic inhibition has been obtained except the shift of E_{Fe}. Assuming b_{Fe} = constant = 0.075 for inhibited and uninhibited electrodes, an anodic partial current j'' of the inhibited electrode at E°_{corr} can be obtained from I_{corr} and I_c and a quantity $(1 - j''/j^\circ_{corr}) \cdot 100\% = I_a$ can be calculated which is comparable to I_c. This has been done graphically and the resulting values of I_a (Table III) are used instead of the shift of E°_{corr} for the discussion of anodic inhibition. In view of the arbitrary assumption b_{Fe} = constant the same error limit has to be attributed to the I_a values as to those of I_c. Within this limit I_a, if not a measure of the decrease of $(j_o)_{Fe}$, is at any rate a measure of the anodic inhibition and therefore justly called the "anodic inhibitor efficiency". Table III shows that, with the exception of methylamine, all inhibitors investigated exhibit anodic as well as cathodic inhibition and are therefore inhibitors of the mixed type. Furthermore it is also seen that all aniline derivatives are of a predominantly anodic type.

I_a is zero for methylamine and increases rapidly with increasing chain length of alkylamines. It has already been argued that the total projected area for alkylamines is constant with respect to the cathodic partial reaction. Within the concept of general adsorption and uniform electrode surface, the same must be true for the anodic partial reaction. An explanation of the increase for I_c in spite of constant total projected area, is offered by the theory of chemisorption. It has been pointed out by Hackerman and Makrides (8) that chemisorption of amines should increase with electron donor properties and that, lacking other data, the basicity of the free amine should be considered representative of these properties. As the basicities of the alkylamines used here are practically constant (15), this suggestion gives no clue to the variation of the chemisorption of these compounds. Therefore, it can only be assumed tentatively that the contribution of chemisorption to the total adsorption may increase with increasing chain length, while the total adsorbed amount, and therefore the total projected area, remains constant because of the existence of a saturated monolayer of adsorbed amines. As has been mentioned before, this can be expected to result in a decrease of the apparent reactivity of Fe in the electrode surface. If slow charge transfer across the interface is rate-determining for the anodic partial reaction, the anodic exchange current $(j_o)_{Fe}$ may then be treated as the product of the true surface area (which is constant if the concept of uniform adsorption is correct), a transfer probability (the probability of the penetration of the activation barrier across the double layer by Fe^{++}), and the iron surface reactivity. The predominance of anodic inhibition can then be interpreted as being due to the lowering of the reactivity by chemisorption, where the lowering of the transfer probability by inhibitor adsorption is roughly the same as that for the cathodic inhibition.

Aniline derivatives are much less basic than straight chain alkylamines, but they are none the less the better anodic inhibitors. The *N*-alkylanilines show a comparatively small increase of I_c with increasing chain length of the aliphatic substituent, but it is doubtful whether this can be attributed to the basicity. Basicity constants of aniline derivatives (15) in dilute solutions show that the basicity does not increase regularly with chain length of aliphatic substituents. The difference in basicity of different compounds is usually small, so that no predictions as to the basicity in concentrated solutions are possible. Both the total amount and the differences of anodic inhibition observed with aniline derivatives are therefore difficult to explain. Considering that within each group of *N*-alkylanilines the changes of I_a parallel the changes of I_c, it may be assumed tentatively that this indicates an influence of the energy barrier similar to that of the cathodic partial reaction. Whether the large total value of I_a is caused by additional strong chemisorption of the aniline derivatives cannot be decided here.

Acknowledgment

The authors are grateful to the Office of Naval Research for the financial support of this work under Contract Nonr 375(02). The authors also wish to express their appreciation to A. C. Makrides for his contributions through helpful discussions.

Manuscript received April 17, 1957.

Any discussion of this paper will appear in a Discussion Section to be published in the December 1958 JOURNAL.

REFERENCES

1. C. Wagner and W. Traud, *Z. Elektrochem.*, **44**, 391 (1938).
2. H. H. Uhlig, *Proc. Nat. Acad. Sci. U.S.*, **40**, 276 (1954).
3. M. Stern, *This Journal*, **102**, 609 (1955).
4. K. F. Bonhoeffer, Lecture given at Electrochemical Society Meeting, San Francisco, 1956.
5. K. F. Bonhoeffer and K. Heusler, *Z. physik. Chem.* (N.F.), **8**, 390 (1956).
6. T. P. Hoar and R. D. Holliday, *J. appl. Chem.*, **3**, 502 (1953).
7. T. P. Hoar, Pittsburg International Conference on Surface Reactions, 1948, pp. 127-134.

8. N. Hackerman and A. C. Makrides, *Ind. Eng. Chem.*, **46**, 523 (1954).
9. Shih-Jen Chiao and C. A. Mann, *ibid.*, **39**, 910 (1947).
10. A. Frumkin, *Z. Elektrochem.*, **59**, 807 (1955).
11. S. Iofa, *et. al., Doklady Akad, Nauk SSSR*, **69**, 213 (1949); **84**, 543 (1952); **91**, 1159 (1953).
12. N. Hackerman, *Trans. N. Y. Acad. Sci.*, [2] **17**, 7 (1954).
13. M. Stern and R. M. Roth, *This Journal*, **104**, 390 (1957).
14. A. G. Pecherskaja and V. V. Stender, *Zhur. Priklad. Khim.*, **19**, 1303 (1946).
15. N. F. Hall and M. R. Sprinkle, *J. Am. Chem. Soc.*, **54**, 3469 (1932).

Local Cell Action during the Scaling of Metals, I

Christa Ilschner-Gensch[1] and Carl Wagner[2]

Department of Metallurgy, Massachusetts Institute of Technology, Cambridge, Massachusetts

ABSTRACT

When a tantalum wire partly covered by silver is exposed to iodine vapor at 174°C, a AgI layer is formed not only on silver but also rapidly along the tantalum surface by virtue of local cell action involving migration of silver ions in AgI and migration of electrons in the tantalum wire and across the AgI layer. The observed rate of sidewise growth of the AgI layer along the tantalum surface is in accord with theoretical calculations. By and large, local cell action may increase the rate of dry corrosion when there are different phases, one of which involves easy flow of ions and another involves easy flow of electrons.

Corrosion of metals in aqueous solutions at room temperature, as well as corrosion of metals in oxygen or sulfur at elevated temperatures, has been interpreted in terms of electrochemical reactions and, accordingly, the rates of both types of reactions may be calculated from electrical measurements. There are, however, significant differences between these two types of reactions. The rate of corrosion in aqueous solutions is frequently determined by the magnitude of activation polarization, and cathodic and anodic reactions may occur at different interfaces corresponding to local cell action. In contradistinction, the rate of oxidation of metals at elevated temperatures is frequently determined by the rate of diffusion in the solid reaction product rather than by the rate of phase boundary reactions, and diffusion of ions and electrons occurs in the same phase.

It is already known that local cell action takes place in solid-state reactions of type A + B = C + D, e.g., Cu + AgCl = CuCl + Ag at 230°C (1). Likewise, it can be anticipated that local cell action will be operative when metals are oxidized at elevated temperatures under conditions involving several phases, with easy flow of ions in one phase and easy flow of electrons in another phase. In particular, when the main product of an oxidation reaction has a high electronic but a low ionic conductivity, addition of another phase providing easy flow of ions may result in a much higher over-all corrosion rate. The same is true if, conversely, the main product has a high ionic but a low electronic conductivity and another phase providing easy flow of electrons is added. As an example for the latter case, the reaction between silver and iodine vapor has been investigated. According to Reinhold and Seidel (2) and Jost and Weiss (3), the rate of formation of AgI is determined by transport of electrons rather than ions across the AgI layer since AgI is mainly an ionic conductor.

[1] Present address: Zentralforschunganstalt Fried. Krupp, Essen, Germany.
[2] Present address: Max Planck Institute for Physical Chemistry, Goettingen, Germany.

Experimental

To make local cell action possible, Ta wires were covered by Ag by immersing the ends of the Ta wires in molten Ag contained in a vycor tube. After cleaning the surface, the Ta wires were placed together with dried iodine in Pyrex tubes cooled by means of dry ice. The Pyrex tubes were evacuated, sealed off, heated in boiling decane at 174°C for 15-150 min, and placed again in dry ice in order to terminate the reaction. At 174°C the vapor pressure of iodine amounts to 575 mm Hg.

It was observed that a AgI layer grows not only on the Ag surface but also spreads along the Ta surface as is shown schematically in Fig. 1. Supposedly, silver ions migrate in the AgI layer and electrons migrate in the Ta wire and across the AgI layer. The distance X' between the tip of the AgI layer and the step next to the Ag slug was measured and the estimated thickness δ of the AgI layer on the silver slug was added in order to obtain the length $X = X' + \delta$ of the AgI layer on Ta.

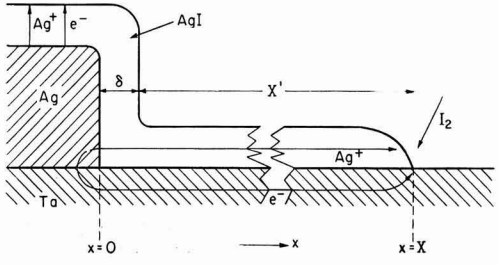

Fig. 1. Reaction of iodine vapor with Ag on Ta

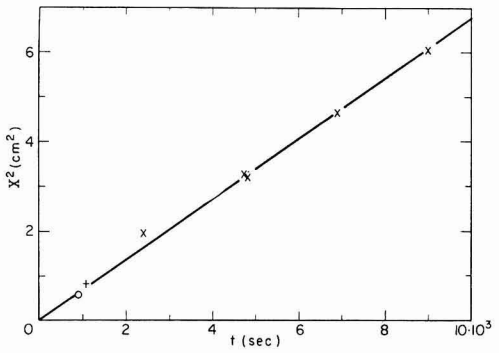

Fig. 2. Square of the length X of a AgI layer on Ta (x), Pt (o), and graphite (+) vs. time.

Results are shown in Fig. 2. In accord with Eq. [25] derived below, a plot of the square of length X vs. time t yields a straight line. Figure 2 also shows results obtained with Pt and graphite instead of Ta. These results show no significant difference, although Pt itself reacts to a minor extent with iodine vapor and yields a very thin blackish film which can be distinguished easily from the much thicker yellow AgI layer.

Some samples were sectioned and examined microscopically. The thickness of the AgI layer on Ag was found to be 0.046 cm for $t = 4740$ sec. The thickness of the AgI layer on Ta was found to decrease with increasing distance x from the Ag slug, qualitatively in accord with Eq. [20] derived below.

Theoretical Calculations

The location of the three-phase boundary Ag-Ta-AgI at $t = 0$ is supposed to be at $x = 0$ (*see* Fig. 1) and moves at $t > 0$ with respect to a hypothetical marker inside the Ta wire since Ag is consumed by the sidewise growth of the AgI layer. If the thickness of the Ag layer on the Ta wire is much greater than the thickness of the AgI layer, the shift of the location of the three-phase boundary with time is only minor and will be disregarded in what follows.

In principle, migration of silver ions, iodine ions, and electrons denoted as particles of type 1, 2, and 3 is to be considered. Practically, the migration of iodine ions is insignificant (4).

The flux j_1 of silver ions in the AgI layer on the Ta wire along the surface (x-direction) may be calculated as (5)

$$j_1 = -(\kappa_1/\mathbf{F}^2)\ (\partial\eta_1/\partial x) \text{ at } 0 < x < X \qquad [1]$$

where η_1 is the local electrochemical potential of the silver ions, $\mathbf{F}$ is the Faraday constant, x is distance as shown in Fig. 1, and X denotes the location of the tip of the AgI layer at time t. The partial conductivity κ_1 for silver ions in AgI may be written as the product of their concentration c_1, their electrical mobility u_1, and the Faraday constant,

$$\kappa_1 = c_1 u_1 \mathbf{F} \qquad [2]$$

From Eq. [2] the mobility u_1 may be calculated as

$$u_1 = \kappa_1/c_1\mathbf{F} = \kappa V_{AgI}/\mathbf{F} \qquad [3]$$

where $V_{AgI} = 1/c_1$ is the molar volume of AgI and κ is the total conductivity which is virtually equal to the cationic conductivity κ_1.

The electrochemical potential η_1 is the sum of the chemical potential μ_1 of the silver ions and the product $\phi\mathbf{F}$ where ϕ is the local electrical potential. In view of the high degree of disorder of the cations in AgI above 146°C, their chemical potential μ_1 is virtually constant. Thus the gradient of the electrochemical potential η_1 is essentially equal to the product of the gradient of the electrical potential and the Faraday constant,

$$\partial\eta_1/\partial x \cong \mathbf{F}(\partial\phi/\partial x) \qquad [4]$$

In view of Eqs. [2] and [4], Eq. [1] may be rewritten as

$$j_1 \cong -u_1 c_1(\partial\phi/\partial x) \qquad [5]$$

i.e., the driving force for the migration of silver ions in AgI results mainly from an electrical field.

The formation of AgI from silver and iodine vapor follows the parabolic rate law (2, 3)

$$\delta = (2\,k't)^{1/2} \text{ at } x < 0 \qquad [6]$$

where δ is the thickness of the AgI film at time t and k' is the rate constant of Tammann's rate law. Since the rate is determined essentially by migration of electrons, the rate depends virtually only on the gradient of the electrochemical potential η_3 of the electrons. In view of the high conductivity of Ag and Ta, η_3 is practically constant along the entire metal-AgI interface ($x >< 0$). Thus the thickness δ of the AgI layer on the Ta wire follows the same rate law after time t_x at which the tip of the AgI layer has arrived at x,

$$\delta = [2\,k'(t - t_x)\,]^{1/2} \text{ at } 0 < x < X \qquad [7]$$

corresponding to the differential equation

$$\partial\delta/\partial t = k'/\delta \text{ at } t > t_x \qquad [8]$$

and the boundary condition

$$\delta = 0 \text{ at } t = t_x \qquad [9]$$

The continuity condition requires that the amount of AgI formed per unit width is equal to the negative value of the divergence of the flow of silver ions per unit width. Thus

$$c_1(\partial\delta/\partial t) = \partial(j\delta)/\partial x \qquad [10]$$

Substitution of Eqs. [1], [2], and [8] in Eq. [10] yields

$$\frac{u_1}{\mathbf{F}}\frac{\partial}{\partial x}\left(\delta\frac{\partial\eta_1}{\partial x}\right) = \frac{k'}{\delta} \qquad [11]$$

At the tip of the AgI layer the average velocity of the silver ions equal to j_1/c_1 must be equal to the rate of advancement of the tip, dX/dt. In view of Eqs. [1] and [2] it follows that

$$\frac{dX}{dt} = \left(\frac{j_1}{c_1}\right)_{x=X} = -\frac{u_1}{\mathbf{F}}\left(\frac{\partial\eta_1}{\partial x}\right)_{x=X} \qquad [12]$$

At the two-phase boundary Ag-AgI at $x = 0$, equilibrium for the reaction

$$Ag(s) = Ag^+ (\text{in AgI}) + e^- \quad [13]$$

is supposed to be established. Thus

$$\mu_{Ag}^\circ = \eta_1(x = 0) + \eta_3 \quad [14]$$

where μ_{Ag}° is the standard chemical potential of Ag.

Along the three-phase boundary Ta-AgI-gas at $x = X$, equilibrium for the reaction

$$Ag^+(\text{in AgI}) + e^- + \frac{1}{2} I_2(g) = AgI \quad [15]$$

is supposed to be established. Thus

$$\eta_1(x = X) + \eta_3 + \frac{1}{2}\mu_{I_2} = \mu_{AgI}^\circ \quad [16]$$

where μ_{I_2} and μ_{AgI}° denote the chemical potentials of iodine in the gas phase and solid silver iodide, respectively, and the electrochemical potential η_3 of the electrons has the same value as in Eq. [14] in view of the high electronic conductivity of the metallic phases.

Upon adding corresponding sides of Eqs. [14] and [16] and regrouping, it follows that

$$\eta_1(x = 0) - \eta_1(x = X) = -\left[\mu_{AgI}^\circ - \mu_{Ag}^\circ - \frac{1}{2}\mu_{I_2}\right]$$

$$= -\Delta F = E\mathbf{F} \quad [17]$$

where ΔF is the free energy of formation of AgI and E is the emf of a galvanic cell involving formation of one mole AgI from the elements on passing one faraday as virtual cell reaction.

Since this is a semi-infinite diffusion problem, the location of the tip of the AgI layer is supposed to be proportional to the square root of time t,

$$X = 2(\gamma t)^{1/2} \quad [18]$$

where γ is a constant parameter which has the dimension of a diffusion coefficient.

In view of Eq. [18], the value of t_x introduced in Eq. [7] is

$$t_x = x^2/4\gamma \quad [19]$$

whereupon Eq. [7] becomes

$$\delta = [2\,k't(1 - x^2/X^2)]^{1/2} \quad [20]$$

Substitution of Eq. [20] in Eqs. [11] and [12] yields

$$\frac{u_1}{\mathbf{F}}\frac{\partial}{\partial x}\left\{\left[2\,k't(1 - x^2/X^2)\right]^{1/2}\frac{\partial \eta_1}{\partial x}\right\} = \frac{k'}{[2\,k't(1 - x^2/X^2)]^{1/2}} \quad [21]$$

$$\left(\frac{\partial \eta_1}{\partial x}\right)_{x=X} = -\frac{2\mathbf{F}\gamma}{u_1 X} \quad [22]$$

Upon integrating Eq. [21] once with respect to x at constant t and using Eq. [18] and [22]

$$\frac{\partial \eta_1}{\partial x} = -\frac{2\gamma\mathbf{F}}{u_1 X}\frac{\cos^{-1}(x/X)}{(1 - x^2/X^2)^{1/2}} \quad [23]$$

Upon integrating Eq. [23] between $x = 0$ and $x = X$, using Eq. [17], and solving for γ, it follows that

$$\gamma = (4/\pi^2)u_1 E \quad [24]$$

In view of Eqs. [18] and [24], the location X of the tip of AgI layer at time t is found to be

$$X = (4/\pi)(u_1 E t)^{1/2} \quad [25]$$

Equation [24] has been evaluated by using the numerical values $V_{AgI} = 38.4$ cm³/mole (6), κ_{AgI} 1.5 ohm^{-1} cm^{-1} (7), $u_1 = 6.0 \times 10^{-4}$ cm² volt^{-1} sec^{-1} calculated from Eq. [3], $\Delta F = -16{,}135$ cal/mole calculated from the heat of formation at 25°C, enthalpy increments, and entropy values (8, 9) corresponding to $E = 0.70$ v. Thus γ has been found to be 1.7×10^{-4} cm²/sec. The straight line in Fig. 2 has been drawn in accord with this value and agrees closely with the observed values. This confirms the principles of the theoretical analysis.

Concluding Remarks

The results of the foregoing experiments may be generalized. Sidewise growth of tarnishing layers may also be expected when Ta wires partly covered by Ag are exposed to chlorine or bromine gas. In view of the lower ionic conductivity of AgCl and AgBr corresponding to a lower average mobility u_1 of silver ions in AgCl and AgBr, however, sidewise growth will be less spectacular.

Especially high oxidation rates may result when an alloy yields a composite scale consisting of a melt providing easy flow of ions and a solid phase providing easy flow of electrons. Experimental investigations are in preparation.

Acknowledgment

This investigation was sponsored by U. S. Atomic Energy Commission under Contract AT(30-1)-1903.

Manuscript received July 25, 1957.

Any discussion of this paper will appear in a Discussion Section to be published in the December 1958 JOURNAL.

REFERENCES

1. C. Wagner, *Z. anorg. u allgem. Chem.*, **236**, 320 (1937).
2. H. Reinhold and H. Seidel, *Z. Elektrochem.*, **41**, 499 (1935).
3. W. Jost and K. Weiss, *Z. physik. Chem. N.F.*, **2**, 112 (1954). According to a private communication from the authors, values of the rate constants and transference numbers need to be corrected, but the main conclusions are not affected thereby.
4. C. Tubandt, *Z. anorg. u. allgem., Chem.*, **115**, 105 (1921).
5. C. Wagner, *Z. Elektrochem.*, **60**, 4 (1956).
6. E. Cohen and W. J. D. van Dobbenburg, *Z. physik. Chem.*, **A137**, 289 (1928); L. W. Strock, *ibid.*, **B25**, 441 (1934).
7. C. Tubandt and E. Lorenz, *ibid.*, **87**, 573 (1914).
8. National Bureau of Standards Circular *500* (1952).
9. K. K. Kelley, Bulletin Bureau of Mines 476 (1949).
10. C. Wagner, *Z. physik. Chem.*, **B32**, 447 (1936).
11. C. Wagner, *ibid.*, **B21**, 25 (1933).

The Effect of Temperature and Thickness on the Electrical Resistivity of Ceramic Coatings

Wm. H. Fischer

General Engineering Laboratory, General Electric Company, Schenectady, New York

ABSTRACT

Tests show that the electrical resistivity of ceramic coatings less than 3 mils thick vary with thickness, although the variation of resistivity with temperature is normal. It is believed that the resistivity-thickness variation is due to surface irregularities and metal-ceramic interface factors which together produce nonuniform, nonhomogenous coatings. Consequently, electrical characteristics of ceramic coatings intended for electrical insulation use should be evaluated only from measurements made on coatings closely approximating actual service thicknesses.

Recent demands for electrical and electronic components capable of operation at temperatures as high as 500°C have led to the investigation of ceramic materials applied in thin coatings for electrical insulation. Such coatings are of the order of 0.0005 in. or less in thickness. However, the electrical properties, particularly the resistivity, of such thin coatings are frequently lower than those reported for the same or similar material in massive forms or when applied in thicker coatings. Consequently it was thought wise to explore the resistivity vs. thickness relationship for thin coatings on the theory that factors operating at the metal-ceramic interface as well as outer surface irregularities might be expected to affect the measured resistance of very thin coatings. If this were true, it would be unwise to evaluate ceramics for design purposes on the basis of resistivity measured on thick coatings.

Strauss, Richards and Moore (1) applied ceramic type coatings to Inconel strips by dipping and studied the effects of temperature on resistivity. They concluded that the resistivity of ceramic coatings is independent of thickness over the thickness range 0.003 in. to 0.020 in.

Experimental

The experimental technique used in this investigation was similar to that of Strauss, *et al.* (1). Inconel plates 2½ in. by 1½ in. by 1/16 in. were polished and oxidized to give a surface suitable for the application of a ceramic coating. The oxidation was performed in a controlled wet hydrogen atmosphere to secure the proper type and amount of oxide to form a strong ceramic to metal bond (as determined in previous work here). Ten of these plates were coated with each of two kinds of ceramic. The nominal oxide compositions for the coatings are given in Table I. In each group two plates were coated at each of the following thicknesses: 0.005 in., 0.003 in., 0.001 in., 0.0005 in., and 0.00025 in. The ceramic frit was suspended in isopropanol and sprayed from a De Vilbiss atomizer onto one side of the plates. After air drying the coating was fired for 3 min at 1050° or 1195°C depending on formulation. A ¾ in. diameter electrode was formed on the ceramic by brushing silver paint on through a template centered on the plate. After air drying the silver paint was baked to form a smooth, adherent electrode of known area. This is essentially the same as the Bureau of Standards technique (1). Additionally, resistance measurements were made using a conducting rubber electrode. Measurements were made with direct voltage at 24°C and 50% relative humidity using a Keithley variable voltage power supply and a Keithley electronic voltmeter with a shunt which converts it to a micromicroammeter. No polarity effect was observed, nor did the resistance vary with the voltage applied. Voltage varied from 10 v on the thinnest specimens to 500 on the thickest, the increase in the voltage being necessary to achieve measurable currents with the thicker specimens. The resistance of

Table I. Ceramic coatings composition

	G-6 (1)	G-6G (1)	I-2 (1)	5210	H-147
SiO_2	27.73	28.40	49.48	48.16	39.30
B_2O_3	4.36	4.46	15.24	7.85	8.71
Al_2O_3	1.90	1.90	7.37	3.62	0.98
Cr_2O_3	28.76	28.76	—	—	—
BaO	29.53	30.29	—	18.26	33.24
CaO	2.68	2.75	5.21	1.06	2.95
ZnO	3.36	3.44	—	4.32	3.75
BeO	1.68	—	—	—	—
Na_2O	—	—	13.75	2.58	2.24
K_2O	—	—	3.54	1.08	1.60
F_2	—	—	3.44	0.10	0.77
MnO	—	—	0.76	—	—
CoO	—	—	0.56	—	—
NiO	—	—	0.65	—	—
TiO_2	—	—	—	8.40	3.46
ZrO	—	—	—	4.67	2.08
MgO	—	—	—	—	0.17
P_2O_5	—	—	—	—	0.62
Co_2O_3	—	—	—	—	0.03
MnO_2	—	—	—	—	0.05
Ni_2O_3	—	—	—	—	0.05

the specimens varied so widely that it was necessary to vary the voltage in order to maintain the current within the range of the measuring equipment. Consequently, neither constant voltage nor constant voltage gradient was maintained. The conditions more nearly approximated constant current.

In order to assess the effect of surface irregularities better, the 0.005 in. specimens were reduced progressively in ceramic thickness. This procedure would further show whether resistance was uniform throughout the thickness of the film. The specimens were ground on a metallurgical polishing wheel to successive approximate thicknesses of 0.004, 0.003, 0.002, 0.001, and 0.0005 in. Resistance measurements were made with conducting rubber electrodes at each stage.

For high temperature application, the resistivity at temperature is obviously the important property. To establish this the 0.001, 0.003, and 0.005 in. specimens were used to determine the resistivity at temperatures from 25° to 500°C.

Results

Figure 1 shows resistivity vs. thickness from this study and from that of Strauss, Richards, and Moore (1). The present data were gathered at room temperature (except for points E and F) and the others were measured at elevated temperatures. In the original resistivity vs. thickness curves of (1), there are several points scattered below the G-6, G-6G line between 0.003 and 0.005 in. which might indicate the beginning of a downward trend.

The author's data show that both ceramics decrease in resistivity as thickness decreases, the major decline being at thicknesses below 0.001 in.

Figure 2 is a plot of the resistivity vs. thickness for the ground samples. For the 5210 ceramic, the ground specimens follow the original curve closely, whereas as soon as the H-147 coating was ground from 0.005 to 0.004 in. the resistivity decreased by 3 decades.

The curves for resistivity vs. temperature obtained in this study as well as that from the Bureau of Standards (1) are all similar in shape and slope (Fig. 3). The decrease of 1½ to 2 decades in resistivity per 100°C increase in temperature indicates that the ceramics are normal at usual thicknesses and that the variation of resistivity with thickness is not peculiar to the special ceramics used in this work.

Discussion

It is apparent from Fig. 1 that the resistivities of applied ceramics are not independent of coating thickness when the thickness is below 0.003 in. While the resistivity of a tiny section of the ceramic encompassing only a few molecules in any direction may be constant, the measured resistivity must include many such sections as well as sections which are not free from the effects of the ceramic-metal interface or surface irregularities. As the over-all ceramic thickness decreases these disturbing effects must manifest themselves to an increasing degree. In thicknesses of the order of 0.0005 in. the application technique which has an effect on surface roughness and the interface characteristics overbalance the internal electrical characteristics of the ceramic. Such interface characteristics as ceramic to metal bonding (interpenetration of the ceramic and metal by each other), metal oxide characteristics, and roughness of the substrate surface, all influence the measured resistance from which resistivity must be calculated. This calculation has to be made on the basis of a nominal or general thickness measurement with a micrometer which touches only the high spots of the ceramic surface. As ceramic surface roughness increases, the actual surface area of the measuring electrode varies from the apparent

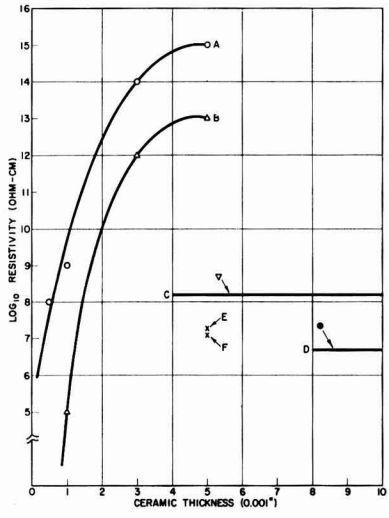

Fig. 1. Resistivity vs. ceramic thickness, measured with silver electrodes. A, 5210, room temperature; B, H-147, room temperature; C, G-6 and G-6G, 400°C (1); D, I-2, 300°C (1); E, 5210, 400°C; F, H-147, 400°C.

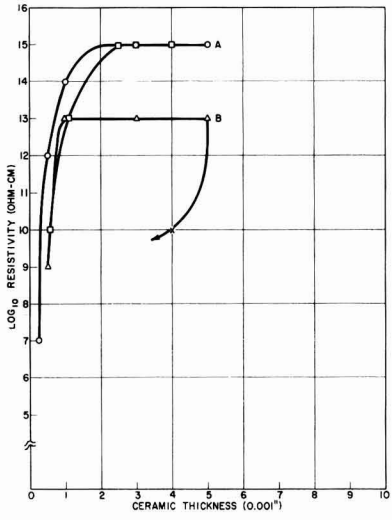

Fig. 2. Resistivity vs. ceramic thickness, measured with rubber electrodes at room temperature. A, open circle, 5210, as applied, open square, 5210, applied at 5 mils, then ground to plotted thickness; B, open triangle, H-147, as applied, x, H-147, applied at 5 mils, then ground to plotted thickness.

area based on a diameter measurement and the ceramic thickness also varies, being always less than that indicated by a micrometer measurement. As a consequence of these considerations, the electrical characteristics of ceramics intended for electrical insulation use should be evaluated only from measurements on coatings closely approximating actual service thickness.

It is believed that the explanation for the variation of resistivity with thickness lies in two effects, ceramic surface irregularities and ceramic-metal interface factors. The larger thicknesses show a higher and more constant resistivity with the rubber electrode than with the silver paint electrode (compare Fig. 1 with Fig. 2), indicating that the surface irregularities are more important at these thicknesses, since the rubber electrode does not follow these irregularities as well as does the silver paint electrode.

However, at very small thicknesses, the interface factors become more important, and these affect the resistivities determined with either electrode.

The sudden drop with only a slight decrease in thickness observed with the H-147 ceramic is related to the manner in which the ceramic was fired. This material was developed for firing in a protective atmosphere, but it was fired in air to assess the effect of such treatment. The air firing increased the substrate oxidation and hence the amount of oxide dissolved in the ceramic coating. This oxide-rich ceramic was overlain by a normal ceramic layer. Once this low oxide layer was removed, the remaining oxide rich layer exhibited its markedly lower electrical properties.

There was considerable variation in the resistance of the thinnest samples at temperatures between 25° and 200°C. Some of them showed higher resistances at 100° and 200°C than at 25°C. A second series of measurements gave a fairly good duplication of this performance.

It is believed that this behavior was caused by the penetration of the thin and imperfect ceramic films by the moisture in the 50% humidity room where the samples were conditioned and tested at 25°C. The moisture was removed by heating to 100°-200°C after which the resistance of these samples followed a normal course. When the specimens were cooled to 25°C for the repeat test moisture again penetrated the ceramic and the curves were repeated for these moisture sensitive samples. The thicker samples, of course, showed a smoothly decreasing resistance vs. temperature curve, as depicted in Fig. 3.

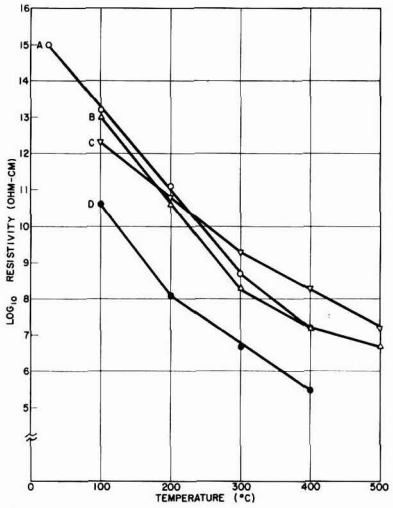

Fig. 3. Resistivity vs. temperature measured with silver electrodes. A, 5210; B, H-147; C, G-6 and G-6G (1); D, 1-2 (1).

Conclusions

1. The resistivity of ceramic coatings decreases with increasing temperature, as is to be expected.
2. The resistivity of thin ceramic coatings is affected by surface irregularities and factors existing at the metal-ceramic interface which operate to produce a nonhomogenous coating of nonuniform thickness.
3. Electrical characteristics of ceramics intended for use as electrical insulation should be evaluated only from measurements on coatings closely approximating actual service conditions.

Acknowledgments

The author wishes to thank Mr. G. R. Sewell for sample preparation, Messrs. A. Soris, J. Francoys, and R. D. Wagner who made the measurements, and Mr. H. T. McLean who suggested that the work be done and participated in the analysis of the results.

Manuscript received Nov. 4, 1957. This paper was prepared for delivery before the New York Meeting, April 27-May 1, 1958.

Any discussion of this paper will appear in a Discussion Section to be published in the December 1958 JOURNAL.

REFERENCE

1. S. W. Strauss, L. E. Richards, and D. G. Moore in "Symposium on Porcelain Enamels and Ceramic Coatings as Engineering Materials", p. 101, ASTM Special Technical Publication No. 153, Philadelphia (1954).

A New Approach to the Measurement of Coating Thickness by Fluorescent X-Ray Absorption

Fred A. Achey and Earl J. Serfass

Department of Chemistry, Lehigh University, Bethlehem, Pennsylvania

ABSTRACT

Absorption of x-ray fluorescence from the base metal of a plated sample is the most frequently used x-ray method for coating thickness determinations. If both coating and base metal yield fluorescent x-rays, it is necessary to isolate the base metal fluorescence before measurement.

Balanced filters are used for isolating the fluorescence from the base metal, and results show close agreement with crystal reflection techniques. Simplicity of the method, together with low equipment cost and high accuracy, recommend it as a useful tool in measuring plating thicknesses.

The method of measuring coating thicknesses by fluorescent x-ray absorption involves irradiating a sample with an incident x-ray beam of sufficient energy (1) to excite base metal fluorescence. The thickness of the coating layer is determined by observing, with a Geiger counter, the absorption of base metal fluorescence as it passes through the coating.

If the base metal is of lower atomic number than the coating, interference from coating fluorescence can be eliminated by adjustment of the incident x-ray tube potential (1). This was demonstrated by Beeghly (2) in his determination of tin coating thickness on steel, where the x-ray tube potential was held below that required to excite tin.

In samples where the coating is of lower atomic number than the base metal, both coating and base metal will be excited by the incident x-ray beam. Therefore, it is necessary to isolate base metal fluorescence from that of the coating before measurements are taken. Zemany and Liebhafsky (3) have shown that coating thicknesses can be determined by absorption procedures using good collimation and crystal reflection for isolation of base metal fluorescence.

The proposed technique, based on absorption of base metal fluorescence by the coating, is independent of atomic number relationships between coating and base metal, and completely eliminates the need for precise crystal reflection procedures. A differential filter system, first developed by Ross (4) and recently used in coating fluorescence measurement (5), isolates the base metal fluorescence from any interfering radiation. This affords a simple method of monochromatization with a great gain in intensity over crystal reflection procedures (6), and its use corrects for background errors normally encountered using other methods of monochromatization.

Apparatus

A General Electric XRD-3 x-ray unit was used for the coating thickness determinations. The x-ray tube was a tungsten target Machlett AEG-50T, used in conjunction with the General Electric fluorescent sample chamber. The Geiger counter of the unit was placed directly opposite the collimator of the sample chamber, and an accurately machined slide used to place the filters alternately in the fluorescent beam. No crystal reflection was employed, and only soller-type collimators were used [*see* (5) for more details].

Experimental

To test the use of a differential filter system for coating thickness determinations, samples were prepared using iron foil as the coating, and zirconium and silver as the base metals (Table I). These choices were made so that a direct comparison could be obtained with recent experiments by Zemany and Liebhafsky who utilized crystal reflection procedures (3). The use of iron foil simplified the preparation of accurate thickness coatings, and provided an example where the fluorescence from the coating could not be eliminated by selection of x-ray tube potential.

Before making measurements it is necessary to select and prepare the filters used for isolation of the characteristic radiation of the base metal. The

Table I. Experimental data

Thickness of iron coating (mils)	Silver fluorescence (cps)	Zirconium fluorescence (cps)
0.0	9654	36680
0.5	6404	12320
1.0	4250	3502
1.5	2029	1107
2.0	1370	342
2.5	868	104
3.0	535	35
3.5	339	11
4.0	199	3
4.5	122	1
5.0	69	—
5.5	47	—
6.0	24	—

elements selected for filters are chosen so that their K edges fall on both the long and short wave length side of the characteristic K radiation to be measured (base metal fluorescence). These filter elements, in elemental or compound form, are mixed thoroughly with polystyrene flour and pressed in a die heated to 350°F, forming a rigid filter disk with the element or compound uniformly dispersed throughout. The appropriate filters are balanced by sanding so that they transmit the unwanted radiation (coating fluorescence) equally. Filters used in this experimental work were balanced to ±0.3%, and their selection was based on data given in Table II. The balancing procedure eliminated the interference from coating fluorescence and background radiation.

In taking a measurement of a particular sample, filters are placed alternately in the beam consisting of fluorescent radiation from both the coating and base metal. Since previous filter balance equalized transmission of coating fluorescence, the difference in observed intensity with the two filters in the beam is due to the characteristic K radiation from the base metal, which falls in the wave-length interval, or pass band, between the two filter K edges. The high transmission of the filters reduced the power requirements of the x-ray tube to 35 kvp, 20 ma.

Discussion

As shown in Fig. 1, straight line relationships between observed base metal intensity and coating thicknesses are obtained directly by experiment and do not involve any corrections for background interference. This is possible because of the balancing procedure, which involves equalizing the transmission of the two filters for both the coating fluorescence and the background radiation. Subtraction of intensities obtained with the two filters eliminates the effects of coating fluorescence and background radiation, and yields only the net intensity of the radiation in the previously selected pass band. The high transmission of the differential filter system reduced the power requirements to 35 kvp, 20 ma.

Table II. Filter selection

Filter	K edge (Å)
Iron coating on silver base metal (Ag fluorescence = 0.56Å)	
Mo	0.618
Rh	0.533
Iron coating on zirconium base metal (Zr fluorescence = 0.78 Å)	
Rb (as RbCl)	0.814
Sr (as $SrSO_4$)	0.768

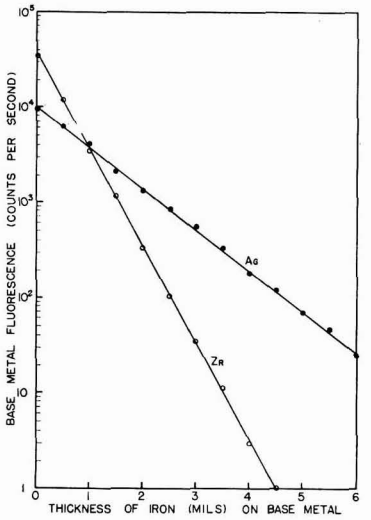

Fig. 1. Experimental results for the measurement of base metal fluorescence with balanced filters.

The straight line logarithmic relationships obtained in measurements of both the silver and zirconium base metal fluorescent intensities indicate adherence to the well known x-ray absorption laws, confirming that the intensity difference obtained with the two filters is essentially monochromatic beam.

A comparison of the proposed balanced filter method and the crystal reflection technique of Zemany and Liebhafsky (3) shows close agreement obtained between the two methods of analysis. Ultimately, however, balanced filters do not afford as critical a wave-length isolation as reflection methods, but their use in coating thickness determinations reduces equipment costs, simplifies power requirements, and automatically compensates for background radiation with no significant loss in accuracy.

Manuscript received Sept. 20, 1957.

Any discussion of this paper will appear in a Discussion Section to be published in the December 1958 JOURNAL.

REFERENCES

1. W. T. Sproull, "X-Rays in Practice," 1st ed., McGraw-Hill Book Co., New York (1946).
2. H. F. Beeghly, *This Journal*, **97**, 152 (1950).
3. P. D. Zemany and H. A. Liebhafsky, *ibid.*, **103**, 157 (1956).
4. P. A. Ross, *Phys. Rev.*, **28**, 425 (1926).
5. F. A. Achey and E. J. Serfass, 43rd Annual Technical Proceedings, American Electroplaters' Society, p. 41 (1956).
6. P. Kirkpatrick, *Rev. Sci. Instr.*, **10**, 186 (1939).

The Lead Oxide-Lead Sulfate and Lead Oxide-Lead Selenate Systems

R. O. Jones and S. Rothschild

Mullard Research Laboratories, Cross Oak Lane, Salfords, Nr. Redhill, Surrey, England

ABSTRACT

The lead oxide-lead sulfate and lead oxide-lead selenate systems have been investigated using the room temperature x-ray powder method. The two systems are very similar and the preparation and x-ray powder patterns are given of lead sulfate $PbSO_4$, lead monoxysulfate $PbO.PbSO_4$, lead tetroxysulfate $4PbO.PbSO_4$, lead selenate $PbSeO_4$, lead monoxyselenate $PbO.PbSeO_4$, and lead tetroxyselenate $4PbO.PbSeO_4$. The lead oxyselenates are isomorphous with the corresponding lead oxysulfates and the pattern of lead monoxyselenate has been indexed on the basis of a monoclinic unit cell of dimensions. a = 13.94Å, b = 5.78Å, c = 7.25Å, β = 115.9°.

The lead oxide-lead sulfate system has been investigated by a number of workers but without much agreement as to the chemical formulae of the various lead oxysulfates present. The compounds reported by the various authors are listed in Table I.

The x-ray powder patterns of the lead oxysulfates detected have been published by Clark, *et al.* (3), Lander (4), and by the Shell Petroleum Co., Ltd. (5).

The structures of lead sulfate, $PbSO_4$, and lead monoxysulfate, $PbO.PbSO_4$, which occur naturally as anglesite and lanarkite, respectively, have been described (6,7).

The lead oxide-lead selenate system has not been investigated previously. The present work was carried out to re-investigate the compounds present in the lead oxide-lead sulfate system and their x-ray patterns, and to determine the compounds present in the lead oxide-lead selenate system and their powder patterns.

Experimental

Series of lead oxide-lead sulfate and lead oxide-lead selenate materials of known compositions were prepared. X-ray powder patterns were recorded at room temperature using a Philips 114.83 mm diameter cylindrical camera and CuK α radiation, the specimen being coated on a thin glass fiber at the center of the camera. Suppose materials of x, y, and z molecular % $PbSO_4$ show on the x-ray powder patterns the presence of PbO + compound A, compound A + compound B, and compound B + $PbSO_4$, respectively. It follows that pure A must contain between x and y % $PbSO_4$ and pure B similarly lies in the range $y - z$. Other materials in the range $x - y$ can now be selected until a composition is found which gives only the lines associated with A: this will be the composition of pure A. It should be noted that the method detects only those compounds that are stable at room temperature.

The x-ray powder patterns are given below in the form of tables of the interplanar spacing d (in Å) and intensity I of each line of the pattern. The interplanar spacings were determined by measurement of the distance between lines on the film and the estimated accuracy of d is given in Table II.

The intensities of the lines were generally estimated visually and are given in terms of the scale vvs (100-90), vs (90-70), s (70-40), ms (40-30,) m (30-20), mw (20-15), w (15-10), vw (< 10). The figures in brackets denote the approximate relative intensities.

In some cases the lines were also microphotometered and the values of relative intensities obtained in these cases are given as figures in the intensity column of the tables.

Results

Lead Oxide PbO (red)

The red (tetragonal) form of lead oxide was prepared by heating lead nitrate in air at 500°C for 30

Table I

Authors	Compounds reported			
Jaeger and Germs (1)		$3PbO.PbSO_4$	$2PbO.PbSO_4$	$PbO.PbSO_4$
Schenck (2)		$3PbO.PbSO_4$	$2PbO.PbSO_4$	$PbO.PbSO_4$
Clark, *et al.* (3)	$4PbO.PbSO_4$	$3PbO.PbSO_4$	$2PbO.PbSO_4$	
Lander (4)	$4PbO.PbSO_4$		$2PbO.PbSO_4$	$PbO.PbSO_4$

Table II

d, Å	8.0	4.00	3.00	2.00	1.500
±Δd, Å	0.1	0.05	0.02	0.01	0.005

min, the x-ray powder pattern observed being in agreement with that of Swanson and Fuyat (8).

Lead Oxide-Lead Sulfate System

Lead sulfate $PbSO_4$—Preparation.—Lead acetate was dissolved in water and dilute H_2SO_4 added to the solution. The mixture was allowed to stand until precipitation was complete; the precipitate was then filtered off, washed, and dried.

Chemical analysis of the material so prepared gave $PbO/SO_3 = 1.00$ in agreement with the formula $PbSO_4$.

X-ray data.—The x-ray powder pattern obtained from the lead sulfate so prepared is given in Table III.

Heating the lead sulfate at 600°C in air and then cooling to room temperature resulted in no change in the x-ray pattern, so that lead sulfate is stable under these conditions.

Lead oxide-lead sulfate compounds.—For the preparation of known composition lead oxide-lead sulfate materials the following general method was employed, values of x and y being chosen to give the required composition. x g of lead nitrate were dissolved in water, y g of ammonium sulfate added to the solution, and the mixture evaporated to dryness. The product was heated in air at 500°C for 30 min and, when cool, was ground and reheated in air at a temperature between 600° and 700°C for 60 min.

A series of such materials of different composition was prepared and the results of the x-ray analysis are given in Table IV. PbO(r) denotes the red (tetragonal) form of lead oxide.

Under the conditions of preparation employed, in addition to lead oxide and lead sulfate two other definite compounds which are stable at room temperature occur in the system. These compounds A and B occur at compositions corresponding to formulas $4PbO.PbSO_4$ and $PbO.PbSO_4$, respectively.

Lead tetroxysulfate $4PbO.PbSO_4$—Preparation.—General method with $x = 66.0$, $y = 5.2$. Chemical analysis of the material so prepared gave $PbO/SO_3 = 4.95$ (calc. for $4PbO.PbSO_4$, 5.00).

X-ray data.—The x-ray powder pattern obtained from the lead tetroxysulfate so prepared is given in Table V.

Table III

d	I	d	I	d	I
4.3	vs 90	2.40	m 25	1.88	w —
3.80	s 45	2.37	vw —	1.79	m 30
3.62	m 25	2.28	m 25	1.74	mw 15
3.47	m 30	2.24	vw —	1.70	m 25
3.32	vs 80	2.16	m 30	1.65	mw 20
3.21	s 60	2.12	vw —	1.61	m 30
3.00	vvs 100	2.07	vvs 100	1.57	w —
2.78	ms 40	2.02	vs 80	1.54	vw —
2.70	ms 40	1.97	m 30	1.49	m —
2.62	mw —	1.90	vw —		

Table IV

Composition molecular % $PbSO_4$	X-ray powder pattern corresponding to
0	PbO (r)
10.0	PbO(r) + Compound A
16.7	PbO (r) + Compound A
20.0	Compound A
25.0	Compound A + Compound B
33.3	Compound A + Compound B
50.0	Compound B
66.7	Compound B + $PbSO_4$
75.0	Compound B + $PbSO_4$
80.0	Compound B + $PbSO_4$
83.3	Compound B + $PbSO_4$
90.0	Compound B + $PbSO_4$
100	$PbSO_4$

Lead monoxysulfate $PbO.PbSO_4$—Preparation.—*(a)* General method with $x = 66.2$, $y = 13.2$; *(b)* 50 g of basic lead acetate.

$(CH_3COO)_2Pb.Pb(OH)_2$ were dissolved in water and the turbid solution poured into a warm solution of 200 g of sodium sulfate in water. The mixture was allowed to stand until precipitation was complete; the precipitate was then filtered off, washed, and dried.

Chemical analysis of the material prepared by method *(b)* gave a value of $PbO/SO_3 = 1.95$ (calc. for $PbOPbSO_4$, 2.00).

X-ray data.—The x-ray powder patterns obtained for the lead monoxysulfate prepared by the two methods were identical and the pattern is given in Table VI.

Table V. $4PbO\ PbSO_4$

d	I
8.3	m —
7.2	w —
6.3	w —
5.8	vw —
5.5	vw —
4.3	w —
3.23	vvs 100
3.10	ms —
3.06	ms —
2.97	w —
2.88	ms 35
2.68	S 65
2.60	vw —
2.45	vw —
2.35	vw —
2.20	vw —
2.14	vw —
2.06	vw —
1.97	ms 30
1.95	ms 40
1.86	w —
1.83	mw 15
1.72	m 20

Table VI. PbO $PbSO_4$

d	I
6.4	m 30
5.9	mw —
5.3	vw —
4.4	m 20
3.70	m 25
3.52	m 30
3.34	vvs 100
3.19	w —
2.96	vs 85
2.85	s 45
2.60	vw —
2.48	m 25
2.43	mw 15
2.35	mw —
2.28	m 20
2.24	vw —
2.17	vw —
2.12	vw —
2.05	m 25
1.96	w —
1.91	mw —
1.85	ms 35
1.76	w —
1.72	mw —

Table VII

d	I	d	I	d	I
5.5	w —	2.78	m 25	1.99	m 30
5.0	ms 35	2.61	m 30	1.97	mw 15
4.4	m 30	2.59	w —	1.93	w 10
3.74	m 25	2.49	w 10	1.86	ms 40
3.49	s 50	2.31	m 25	1.79	w 10
3.38	vw —	2.27	m 25	1.74	vw —
3.28	vvs 100	2.21	w —	1.72	w —
3.16	mw —	2.10	ms 40		
3.08	vvs 95	2.07	w —		

Lead Oxide-Lead Selenate System

Lead selenate $PbSeO_4$—Preparation.—38 g of lead acetate were dissolved in water and the solution added to a solution of 19 g of sodium selenate in water. The mixture was allowed to stand until precipitation was complete; the precipitate was then filtered off, washed, and dried. Chemical analysis of the material so prepared gave PbO/SeO_3 = 1.03 (calc. for $PbSeO_4$, 1.00).

X-ray data.—The x-ray powder pattern obtained from the lead selenate so prepared is given in Table VII.

Heating of the lead selenate at 600°C in air and then cooling to room temperature resulted in a change in the x-ray pattern indicating that the lead selenate is unstable under these conditions. The decomposition product is usually complicated; lead oxide and lead oxyselenates have been detected. When the heating was carried out below about 500°C for the periods used in practice (30-60 min) decomposition of the lead selenate did not occur to any appreciable extent.

Lead oxide-lead selenate compounds.—For the preparation of known composition lead oxide-lead selenate materials the following general method was employed, values of x and y being chosen to give the required composition. x g of lead nitrate were dissolved in water, y g of lead selenate (prepared as above) added to the solution and the mixture evaporated to dryness. The product was heated in air at 450°C for 30 min and when cool was ground and reheated in air at T °C for 60 min. The value of T was chosen so that decomposition of the lead selenate did not occur. It was found that in the range 0-50 molecular % lead selenate T = 600 was satisfactory, but in the region 50-100 molecular % lead selenate it was necessary to reduce T to 450.

Table VIII

Composition molecular % $PbSeO_4$	X-ray powder pattern corresponding to
0	PbO (r)
10.0	PbO(r) + Compound C
16.7	PbO(r) + Compound C
20.0	Compound C
25.0	Compound C + Compound D
33.3	Compound C + Compound D
50.0	Compound D
66.7	Compound D + $PbSeO_4$
75.0	Compound D + $PbSeO_4$
80.0	Compound D + $PbSeO_4$
83.3	Compound D + $PbSeO_4$
90.0	Compound D + $PbSeO_4$
100	$PbSeO_4$

A series of lead oxide-lead selenate materials of different composition were prepared and results of the x-ray analysis are given in Table VIII.

Under the conditions of preparation employed, in addition to lead oxide and lead selenate, two other definite compounds which are stable at room temperature occur in the system. These compounds C and D occur at compositions corresponding to formulas $4PbO.PbSeO_4$ and $PbO.PbSeO_4$, respectively.

Lead tetroxyselenate $4PbO.PbSeO_4$—Preparation.—General method with x = 33.00, y = 8.75, T = 600. Chemical analysis of the material so prepared

Table IX. 4PbO $PbSeO_4$

d	I
8.3	m —
7.5	w —
6.3	w —
5.9	w —
5.5	vw —
4.4	vw —
3.27	vvs 100
3.18	ms —
3.11	ms —
3.00	vw —
2.91	ms 40
2.71	S 60
2.62	vw —
2.49	vw —
2.39	vw —
2.35	vw —
2.28	vw —
2.22	vw —
2.16	vw —
2.07	vw —
2.00	ms 30
1.96	ms 40
1.86	m 20
1.75	m 20

Table X. $PbOPbSeO_4$

d	I	Indices
6.5	m 25	001
6.0	mw —	$20\bar{1}$
4.5	mw 15	$11\bar{1}$
3.79	w 10	111 201
3.57	vw —	$31\bar{1}$
3.41	vvs 100	310
3.27	mw 15	002
3.01	vs 80	$11\bar{2}$ $40\bar{2}$
2.89	s 40	020
2.62	vw —	220 $22\bar{1}$
2.50	m 20	202
2.39	w —	$51\bar{2}$ $20\bar{3}$
2.33	mw —	403
2.28	mw —	221 $60\bar{2}$
2.20	vw —	$31\bar{3}$
2.16	vw —	022 003
2.09	m 25	600
2.01	vw —	312
1.96	vw —	511
1.89	m 20	402 222
1.79	mw 15	$20\bar{4}$
1.75	m —	

gave $PbO/SeO_3 = 4.89$ (calc. for $4PbO.PbSeO_4$, 5.00).

X-ray data.—The x-ray powder pattern obtained from the lead tetroxyselenate so prepared is given in Table IX.

Lead monoxyselenate $PbO.PbSeO_4$—Preparation.—*(a)* General method with $x = 11.30$, $y = 12.00$, $T = 600$. *(b)* Two g of basic lead acetate were dissolved in water and the turbid solution poured into a solution of 12 g sodium selenate in water. The mixture was allowed to stand until precipitation was complete; the precipitate was then filtered off, washed, and dried. Chemical analysis of the material prepared by method *(b)* gave a value of $PbO/SeO_3 = 2.04$ (calc. for $PbO.PbSeO_4$, 2.00).

X-ray data.—The x-ray powder patterns obtained for the lead monoxyselenate prepared by the two methods were identical and the pattern is given in Table X.

Discussion

The work on the lead oxide-lead sulfate system confirms that of Lander (4) in that two lead oxysulfates, namely, lead monoxysulfate $PbO.PbSO_4$ and tetroxysulfate $4PbO.PbSO_4$, exist under the conditions employed. The lead dioxysulfate $2PbO.PbSO_4$ reported by Lander to be unstable below 450°C was not detected in the present work, but this is understandable since only compounds stable at room temperature would be detected.

The x-ray powder pattern given for lead sulfate $PbSO_4$ is in good agreement with that of Swanson, Fuyat, and Ugrinic (9), while the patterns of lead monoxysulfate $PbO.PbSO_4$ and lead tetroxysulfate $4PbO.PbSO_4$ are in reasonable agreement with those of Lander (4) and the Shell Petroleum Co. (5).

The lead oxide-lead selenate system is very similar to the lead oxide-lead sulfate system, two lead oxyselenates, namely, lead monoxyselenate $PbO.PbSeO_4$ and lead tetroxyselenate $4PbO.PbSeO_4$, being stable at room temperature. The x-ray patterns of these are very similar to the corresponding oxysulfates, and the lead oxyselenates are therefore isomorphous with the corresponding lead oxysulfates.

Binnie (7) found the unit cell of lead monoxysulfate to be monoclinic of dimensions, $a = 13.75$Å, $b = 5.68$Å, $c = 7.05$Å, $\beta = 116.2°$, and since the present work shows lead monoxyselenate to be isomorphous with lead monoxysulfate, the x-ray powder pattern of lead monoxyselenate can be indexed from that of lead monoxysulfate. The unit cell dimensions of lead monoxyselenate then become $a = 13.94$Å, $b = 5.78$Å, $c = 7.25$Å, $\beta = 115.9°$, that is the sides of the unit cell are all increased and the angle decreased from those of lead monoxysulfate.

Acknowledgments

Permission of the Directors of Mullards Research Laboratories to publish this work is gratefully acknowledged by the authors.

Manuscript received May 29, 1957. This paper was prepared for delivery before the New York Meeting, April 27–May 1, 1958.

Any discussion of this paper will appear in a Discussion Section to be published in the December 1958 JOURNAL.

REFERENCES

1. F. M. Jaeger and H. C. Germs, *Z. anorg. u. allgem. Chem.*, **119**, 145 (1921).
2. R. Schenck, *Metall. u. Erz*, **23**, 408 (1926).
3. G. L. Clark, J. N. Megudick, and N. C. Schieltz, *Z. anorg. u. allgem. Chem.*, **229**, 401 (1936).
4. J. J. Lander, *This Journal*, **95**, 174 (1949).
5. "X-ray Diffraction Patterns of Lead Compounds", pp. 47-51, The Shell Petroleum Co. Ltd., Chester (1954).
6. "Strukturbericht 1913-1928," Von P. P. Ewald and C. Herman, Editors, pp. 344, 384, Leipzig (1931) [Edward Brothers, Inc., Ann Arbor (1943)].
7. W. P. Binnie, *Acta Cryst.*, **4**, 471 (1951).
8. H. E. Swanson and R. K. Fuyat, "Standard X-ray Diffraction Powder Patterns," N.B.S. Circular 539, II, p. 30.
9. H. E. Swanson, R. K. Fuyat, and G. M. Ugrinic, "Standard X-ray Diffraction Powder Patterns," N.B.S. Circular, 539, III, p. 67.

Equilibria between Titanium Metal and Solutions of Titanium Dichloride in Fused Magnesium Chloride

K. Komarek and P. Herasymenko

Department of Metallurgical Engineering, Research Division, College of Engineering, New York University, New York, New York

ABSTRACT

A method has been developed for collecting vapors over solid $TiCl_2$ or over mixtures of $TiCl_2$ and $MgCl_2$ in a specially designed titanium pipette at elevated temperatures. The reaction of titanium tetra- and trichloride with Ti metal could not be prevented on cooling, but the analytical total content of chlorine could be used to determine the apparent total concentration of titanium in the vapor phase. The study indicated strong positive deviations from Raoult's Law for liquid $MgCl_2$-$TiCl_2$ solutions and limited solubility of $TiCl_2$ in liquid $MgCl_2$ in the range from 720° to 800°C. This was confirmed by thermal analyses of mixtures. The system $MgCl_2$-$TiCl_2$ is of the peritectic type. The peritectic point lies at about 0.3 wt % $TiCl_2$ and at 716°C. The melting point of $TiCl_2$ is 1025°C. Salt mixtures in equilibrium with Ti metal contain only $TiCl_2$, and no measurable quantities of $TiCl_4$ or $TiCl_3$.

In Kroll's method of Ti metal production, $TiCl_4$ reacts with Mg at temperatures above 700°C. Solutions of $TiCl_3$ and $TiCl_2$ in liquid $MgCl_2$ are likely to occur as intermediate stages of this reaction. The present work proposes to investigate the nature of such solutions in the presence of Ti metal. Two experimental methods were used: (*a*) a specially designed method of measuring the vapor pressure of volatile constituents over molten mixtures, and (*b*) thermal analysis of molten salts.

Measurements of the Apparent Vapor Pressure

The following method appeared to be promising in determining the composition of the gas phase over fused salt mixtures. If a known volume of vapor over the molten salt could be collected by means of a pipette without disturbing the vapor-liquid equilibrium, and the closed pipette were rapidly cooled, the salt vapors would condense on the inside walls of the pipette and could be analyzed for the different molecular species present in the vapor, and their relative amounts could be determined. The partial pressures could then be calculated, assuming ideal behavior of the gas phase. For practical reasons the volume of the pipette cannot be very large, and therefore an accurate microanalytical method is required to analyze the salts condensed from the vapor on the pipette walls. The analytical results will be correct only if no reaction between the vapors and the pipette material takes place during cooling. Here, the choice of the pipette material was limited to Ti metal, because any other material would affect the equilibrium between liquid and vapor. As shown below, the reaction between $TiCl_3$ or $TiCl_4$ and metal could not be prevented. This fact, and other difficulties inherent in the system under study, did not allow determination of the values of partial pressures of different titanium chlorides. However, the apparent values of the vapor pressure derived from the authors' measurements permitted drawing some conclusions on the nature of the $MgCl_2$-$TiCl_2$ mixtures.

The final design of the apparatus used for the study of the vapor phase is shown in Fig. 1. After assembly of the apparatus, the whole system is evacuated at room temperature, and then transferred into a furnace preheated to a temperature at which the vapor pressure

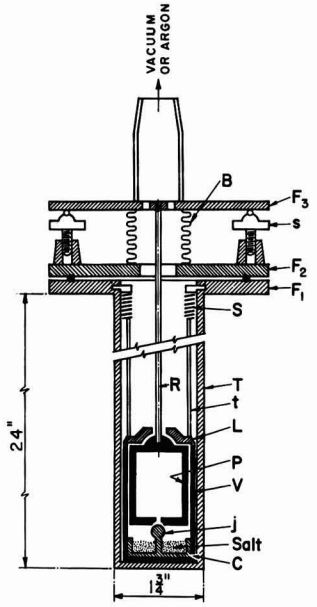

Fig. 1. Apparatus for collecting salt vapors. B, bellows; F_1, F_2, F_3, flanges; s, screw; S, spring; T, t, stainless steel tubes; R, Ti tube; L, Ti lid; P, pipette; J, Ti vessel; j, ground ball joint; C, salt container.

of the salts is negligible. The evacuation of the system is continued and the temperature slowly increased. When the temperature of the Ti vessel approaches the desired level, the pipette is raised to close the lid L. The vapors of the salts saturate the space inside vessel V, and pipette P. The closed vessel is then held for the desired time to equalize the temperature in the vessel and to attain equilibrium between salt, vapor, and metal parts. The temperature in the upper part of the vessel in which the pipette is located is maintained about 2° to 3°C above the temperature of the salt container. This was thought necessary to prevent condensation of salts in the pipette due to small fluctuations of temperature.

When the space inside the closed vessel V and pipette P had equilibrated with the vapor of salt in the salt container, the pipette was lowered until its opening was closed by the ball joint j attached to the salt container. Then the whole stainless steel tube was withdrawn from the furnace and cooled. After complete cooling, argon at atmospheric pressure was introduced into the apparatus so that it could be opened and the pipette removed from the tube for analysis.

The ball joint j sealed the pipette quite tightly. It was frequently observed that, when the pipette was carefully removed from the tube, the salt container, hanging on the ball joint, was also lifted from the tube. The difference in pressure—partial vacuum inside the pipette and atmospheric pressure outside it—could be preserved for at least 1 hr.

The polarographic method was used for microanalysis. The salts condensed on the inner walls of the pipette were dissolved in a small volume of 1*N* H_2SO_4. It was found that this acid does not dissolve Ti from the vessel at room temperature in a polarographically detectable amount. Only the total content of Ti, Mg, and Cl could be determined polarographically.

The convenient concentration range of Ti^{4+} and Cl' ions for polarographic analysis is from about 5×10^{-5} to 10^{-3} moles per liter. If the total pressure of titanium chlorides is about 1 mm Hg at 1000°K, the amount of Ti salt condensed on the inner walls of the pipette (22.4 ml) will be about 4×10^{-7} moles. In order to obtain the final concentration of Ti^{4+} in the analyzed solution of the order of 10^{-4} moles per liter, the required volume of the final solution is about 4 ml. For larger amounts of condensed titanium chlorides, correspondingly larger volumes of acid solution can be used for leaching.

This method was applied first to determine the composition of the vapor phase over solid $TiCl_2$ in equilibrium with metal. The dichloride was prepared by disproportionating solid $TiCl_3$ under vacuum at 450°C for about 30 hr. The reaction was carried out in the apparatus shown in Fig. 1 except that the pipette was not introduced. From 0.2 to 0.5 g of solid $TiCl_3$ was charged into the salt container. The trichloride was covered by a layer of iodide titanium chips to reduce the tetrachloride formed during the reaction to dichloride. After this treatment, the Ti pipette was introduced into the apparatus, and the vapor pressure determined as described above.

Denoting the number of moles of di-, tri- and tetrachloride in the gas phase over the salt at the temperature of the experiment as n_2, n_3, and n_4, respectively, the total content of Ti atoms is

$$n_2 + n_3 + n_4 = \Sigma n_{Ti} \qquad (I)$$

and the total content of chlorine atoms:

$$2n_2 + 3n_3 + 4n_4 = \Sigma n_{Cl} \qquad (II)$$

Assuming that the gas condensed in the pipette can be cooled and condensed so that the reaction of higher chlorides with the walls of the pipette can be neglected, the analysis will give the values of Σn_{Ti} and Σn_{Cl}. Equations (I) and (II) are not sufficient to determine all three unknown values, n_2, n_3, and n_4, unless one of them is negligibly small or unless one of them can be determined by an independent method.

The ratio Cl/Ti in the condensed salt was found to be equal to 2 within experimental error (±0.05). Two interpretations of this fact are possible: (*A*) the vapor consists predominantly of $TiCl_2$ molecules, the content of $TiCl_3$ and $TiCl_4$ being negligibly small; (*B*) tri- and tetrachloride react with metal of the pipette on cooling to form $TiCl_2$. The latter interpretation seemed more probable. In this case, the total number of Ti atoms, $\Sigma n'_{Ti}$, as determined analytically, will be given by the equation:

$$\Sigma n'_{Ti} = \tfrac{1}{2}\,\Sigma n_{Cl} = n_2 + 1.5n_3 + 2n_4 \qquad (III)$$

The "apparent" total pressure, i.e., $\Sigma P'_{Ti} = p_2 + 1.5\,p_3 + 2p_4$, calculated from the analysis of the condensed salt, will be higher than the equilibrium pressure $\Sigma P_{Ti} = p_2 + p_3 + p_4$. The values of the apparent pressure for the experiments reported in Table I are given in the third column.

The disproportionation of lower titanium chlorides was studied recently by Skinner and Ruehrwein (1). They measured the total pressure of vapors over solid dichloride and calculated the partial pressures of di- tri- and tetrachloride from other thermodynamic data and estimated entropies and specific heats. Their values for p_2, p_3, and p_4 are shown in Fig. 2. Sanderson and MacWood (2) measured the heats of formation of $TiCl_2$ and $TiCl_3$ and the disproportionation equilibria of trichloride. From these measurements and from the estimated entropies and specific heats they deduced a consistent set of thermodynamic data for titanium chlorides. The values of partial pressures of tri- and tetrachloride over solid $TiCl_2$ calculated from their data are also shown in Fig. 2. Uncertainties in the estimated thermodynamic data are responsible for considerable differences in the calculated values of the partial pressure derived from both investigations.

Table I. Disproportionation of $TiCl_2$

Temp, °C	G-atoms × 10^{-6} chlorine in 22.5 ml	$\Sigma P'_{Ti}$ mm Hg
652	3.64	5
670	6.04	8.5
682	6.3	9.0
687	8.9	12.5
695	10.4	15
703	14.5	21
704	9.7	14
730	20.8	31
733	26.1	39
735	22.0	33
737	32.0	48
762	45.6	70

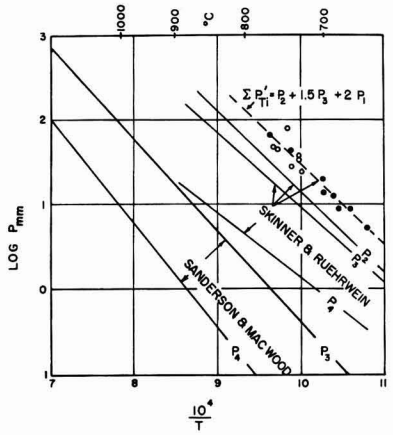

Fig. 2. Comparison of experimental $\Sigma P'_{Ti}$ values with the values derived from Skinner's and Sanderson's papers.

The broken line in the diagram, Fig. 2, represents the sum $\Sigma P'_{Ti} = p_2 + 1.5p_3 + 2p_4$, calculated from the data by Skinner and Ruehrwein to make a comparison with our experimentally found values, shown in the same figure as full circles. The agreement is good, but may be fortuitous. Sanderson and MacWood have not estimated the value of p_2 (the sublimation pressure of $TiCl_2$). If their values for p_3 and p_4 are taken to be more correct than those estimated by Skinner and Ruehrwein, then—in order to conform with present measurements—one has to assume that the sublimation pressure of $TiCl_2$ should be only slightly lower than the apparent pressures. Further experimental studies will be necessary to decide this matter.

Further measurements of the apparent total pressure $\Sigma P'_{Ti}$ were made over mixtures of $TiCl_2$ and molten $MgCl_2$. Results for mixtures containing more than 40 mole % $TiCl_2$ are shown in Table II. At the time when these experiments were carried out, a suitable dry box was not available to remove the salt from the reaction tube for analysis. When the salt container was removed from the argon-filled stainless steel tube the salt reacted violently with moist air with evolution of light. In only three cases was it possible to obtain approximate analyses of the salt by introducing an acid solution directly into the argon-filled titanium vessel. The accuracy was probably not greater than ±1% Ti by weight.

Table II. Values of the apparent vapor pressure of $TiCl_x$, $\Sigma P'_{Ti}$, over mixtures of $MgCl_2$ with over 40 mole % $TiCl_2$

Temp, °C	Approximate mole % $TiCl_2$	G-atoms × 10^{-6} Ti in 22.5 ml	$\Sigma P'_{Ti}$ mm Hg	P_{MgCl_2} mm Hg
720	42	8.1	24	—
726	—	14.0	42	0.5
730	—	11.7	35	0.4
737	63	15.4	46	0.5
740	—	9.6	29	—
742	—	25.8	78	—
751	45	13.8	42	0.6
757	—	15.0	46	1.2?
763	—	34.1	105	—

Since the salt mixtures were always prepared in similar proportions, one can conclude that the content of $TiCl_2$ varied within the limits found in three analyzed mixtures, i.e., from about 40 to 60% $TiCl_2$. The values of $\Sigma P'_{Ti}$ found by the analysis of vapors entrapped in the pipette are plotted in Fig. 2 as open circles. It is seen that within the limits of experimental accuracy, the points fall on the same line as for pure $TiCl_2$. This fact indicates that the activity of $TiCl_2$ in salt mixtures containing more than about 40 molar % of Ti is practically the same as that of pure $TiCl_2$. In other words, it can be safely stated that the solubility of $TiCl_2$ in molten $MgCl_2$ at about 750°C is less than 40 mole % $TiCl_2$.

Experiments with dilute solutions of $TiCl_2$ in molten $MgCl_2$ also pointed to the same conclusion. A few experiments carried out in the range up to about 2.4 mole % $TiCl_2$ are shown in Table III.

The activity of $TiCl_2$ in these dilute solutions can be taken as approximately equal to the ratio of the apparent pressure, $\Sigma P'_{Ti}$, for the given solution to the apparent pressure of the $MgCl_2$-free $TiCl_2$ at the same temperature (extrapolated from the data of Tables I and II and designated by P_o in Table III). The activity coefficient, γ, calculated in this manner is about 5, indicating a strong positive deviation from Raoult's Law.

Further determinations with the described method were not carried out. Although the accuracy of the method could be improved by further experimentation, measurements of the apparent total vapor pressure for the sole purpose of determining the solubility of $TiCl_2$ in $MgCl_2$ were not justified.

Thermal Analysis in the System $MgCl_2$-$TiCl_2$

Experimental procedure.—Materials used for this investigation were anhydrous $MgCl_2$ and $TiCl_2$. The $MgCl_2$ was obtained from the Bureau of Mines Experimental Station in Albany, Oregon, in a pure anhydrous form as received as a by-product from the production of zirconium metal by the Kroll process. The salt dissolved in water without any residue. Its melting point was determined to 715°C, which agreed well with the value of 714°C reported in the literature (3).

The $TiCl_3$ was obtained by reacting high purity $TiCl_4$ with Ti metal. The $TiCl_4$ was furnished in part by the Bureau of Standards and the rest was purchased from the Fisher Scientific Company. The former was 99.99% pure and the latter was purified according to NBS

Table III. Values of the apparent vapor pressure of $TiCl_x$ ($\Sigma P'_{Ti}$) over mixtures of $MgCl_2$ with small contents of $TiCl_x$

Temp, °C	Approximate mole % of $TiCl_2$*	G-atoms × 10^{-6} Ti in 22.5 ml	$\Sigma P'_{Ti}$ mm Hg	P_{Mg} mm Hg	P_o mm Hg	γ
760	1.8	2.3	7.0	—	75	5.2
791	1.4	3.2	10.3	—	142	5.2
800	2.4	5.5	17.5	1.7	170	4.3
839	1.3	7.6	25.0	—	390	4.9
846	—	8.0	26.5	3.3	450	—
857	1.2	9.3	31	3.4	550	4.7

* The molar percentage of $TiCl_2$ was calculated on the assumption that only this species is present in the molten salt.

Report 3874 by addition of Cl_2 to the refluxing liquid. The $TiCl_4$ was transferred by distillation to avoid exposure to humid air. The Ti metal used was either iodide-grade with 99.98% Ti or an electrolytic product (Bureau of Mines, Boulder City) with 99.53% Ti.

The reaction between the tetrachloride and the metal was carried out in a quartz apparatus. A quartz flask of 250 ml capacity served as a container for the tetrachloride. The neck of the flask was connected to a quartz tube 1 3/16 in. in diameter and approximately 15 in. long. The tube was constricted about 5 in. above the flask to keep the solid piece of Ti metal in place, and then tetrachloride was distilled into the flask in excess of the amount required to react with the metal to form $TiCl_3$. The tetrachloride was cooled to —70°C, the apparatus evacuated to about 1μ and the quartz tube was finally sealed close to the upper end. The flask had a thin sealed side tube through which the excess of $TiCl_4$ could be distilled off after the run. The quartz tube with the metal was then inserted in a furnace and the metal heated to 750°C, while the temperature of the liquid $TiCl_4$ was maintained at 80°-100°C. The reaction was allowed to proceed for about 14 days. Titanium trichloride condensed in the wider parts of the quartz tube above and below the metal in the form of dense, deep violet crystal masses which would gradually fill the whole diameter of the tube. When no decrease in the volume of tetrachloride was noticeable, the temperature of the furnace was slowly lowered to convert $TiCl_2$ to $TiCl_3$. The side tube of the flask was then broken, the excess of tetrachloride distilled off, and finally the $TiCl_3$ was heated to about 200°C and the whole apparatus evacuated to remove all tetrachloride. The quartz tube was then cut off from the flask in a dry box; the trichloride was removed and stored in glass bottles. One run produced about 110 g of very dense $TiCl_3$.

For the thermal analysis, mixtures of $MgCl_2$ and $TiCl_3$ were prepared in a dry box in argon atmosphere. The crucibles and the thermocouple protection tubes which were in direct contact with molten salt were made of commercial Ti. In one modification, the crucible was open at the top and a thin Ti tube closed at the lower end served as the thermocouple well. The latter carried also at its lower end a perforated Ti disk to make the stirring of the melt more efficient. The crucible was covered with a screwed-in lid provided with an opening for the thermocouple well. To prevent excessive evaporation of salt at temperatures above 950°C, an entirely closed crucible was employed. The cap of the crucible with the thermocouple well was machined from one piece of Ti. The cap could be tightly screwed on the top of the crucible, with a thin annealed Ti sheet serving as a gasket.

The crucibles were placed in a stainless steel tube of a design similar to that shown in Fig. 1. The Ti thermocouple protection tube was screwed to a thin stainless steel tube which served as an extension of the thermocouple well, and was connected with the upper brass flange. The brass bellows permitted raising or lowering of the thermocouple well to stir the melt in the open crucible or to shake the closed type crucible. The large stainless steel tube with two brass top flanges was connected with the argon purification train by a series of movable glass elbows with ground joints so that the tube could be inserted into the preheated vertical furnace and quenched in cold water after the run without disconnecting it. The chromel-alumel thermocouple wires were sealed, vacuum tight, into the glass part of the top of the stainless steel tube with black Apiezon wax. The wires were insulated by a double-bore, hard porcelain tube. This tube reacted at elevated temperatures with Ti parts: a shiny coating, presumably of titanium silicide, was formed on its surface which could further contaminate the thermocouple. Frequent calibrations of the thermocouple with pure NaCl (Baker, analytical grade) and pure $MgCl_2$ have shown that the change in the thermocouple readings amounted to only 1°-2°C after two or three runs.

Magnesium chloride and titanium trichloride were mixed in the desired proportions in a dry box filled with argon, and were charged in Ti crucibles. In some cases, a certain amount of Ti powder was added to avoid excessive corrosion of Ti crucibles, especially at higher contents of $TiCl_3$ in the charge. The amount of salt charged in the crucibles was always about 20 g. The crucibles were transferred into the stainless steel tube under argon. The tube was connected with the vacuum system, evacuated, filled with argon, and then put into the preheated furnace. The salt was heated well above the expected freezing point and the melt was stirred or shaken frequently to homogenize the melt during an hour, the time sufficient to attain equilibrium. The power input of the furnace was then gradually lowered by means of a Variac transformer to obtain a constant cooling rate of 1-2°C/min. Readings were taken at intervals of 1 min, and between the readings the melt was stirred. Since no thermal arrests were found below 700°C, the stainless steel tube was taken out of the furnace and quenched in a water tank. The crucibles were then opened in the dry box and samples taken for analysis.

For the determination of total soluble Ti a sample was dissolved in a titration flask which was continuously flushed with hydrogen to prevent oxidation of trivalent Ti. Then, 200 ml 0.5*N* HCl and 5 ml 85% H_3PO_3 were added, and the trivalent Ti was oxidized with 50 ml 0.1*N* ferric ammonium sulfate solution. Eight drops of a 0.2% aqueous barium diphenylamin sulfonate solution were added as an indicator and the ferrous ions were titrated with 0.1*N* potassium dichromate solution.

For the determination of $TiCl_2$ the following procedure is suggested in literature (4). Titanium dichloride on dissolving in dilute acid reacts according to the equation

$$TiCl_2 + HCl = TiCl_3 + \tfrac{1}{2} H_2$$

The content of dichloride can thus be obtained from the volume of hydrogen formed in this reaction. The resulting solution of $TiCl_3$ can be titrated for the total content of Ti, and the initial content of trivalent Ti in the analyzed salt is then obtained from the difference,

$$\%\ Ti_{total} - \%\ Ti_{TiCl_2} = \%\ Ti_{TiCl_3}$$

Most of the salt mixtures were analyzed for divalent and trivalent titanium according to this scheme. Titanium dichloride and trichloride were always found together, the ratio being about 7.5. The fair reproducibility of the analyses led the author to believe that the knowledge of the sum of di- and trichloride was sufficient to define completely the salt composition. Therefore, the content of $MgCl_2$ and total chlorine were not determined. However, the final experiments with $MgCl_2$-free titanium chloride cast considerable doubt on the accuracy of determinations of $TiCl_2$ from the volume of hydrogen. The $MgCl_2$-free salt which solidified at 1025°C gave

Table IV.

Position in the crucible	$TiCl_2$ %	$TiCl_3$ %	$TiCl_2 + TiCl_3$ %	Total soluble Ti %	$TiCl_2$ calculated from total soluble Ti %
Top	84.20	20.60	104.8	40.30	99.9
Bottom	88.25	16.57	104.8	40.75	101.2

the values shown in Table IV. The melt contained from 9.4 to 19.7% of finely dispersed Ti metal which was separated by filtration after dissolving the samples in dilute HCl, and after the volume of hydrogen had been measured. The percentages of $TiCl_2$ and $TiCl_3$ given in Table IV refer to the composition of the metal-free salt.

The above analyses show that the sum, ($TiCl_2 + TiCl_3$), was about 105%. This high result could be due to the fact that not all hydrogen formed during the dissolution of samples in HCl had been collected. This failure of the exact determination of divalent Ti from the volume of hydrogen can be explained by the formation of titanium hydride in the reaction between the nascent hydrogen and Ti metal dispersed in the solid salt.

When, in the case considered here, the total soluble Ti was assumed to be present exclusively in the divalent form, the calculated percentage of dichloride was found to be close to 100%, which is a more reasonable analytical result than the 105% obtained for the sum, ($TiCl_2 + TiCl_3$). In other words, it appeared probable that the salt did not contain $TiCl_3$. In order to prove this conclusion, two further preparations of the $MgCl_2$-free salt were made under widely different conditions of cooling from the liquid state, and were analyzed several times for total Ti and Cl. Sample N 15 was prepared by heating $TiCl_2$ at about 1050°C, cooling slowly in the furnace to about 675°C, and then rapidly cooling. Sample V 16 was heated to 1050°C in a closed Ti crucible inserted in a sealed quartz tube, and then quenched in water. Portions of the samples were dissolved in dilute (2.5%) H_2SO_4, the Ti particles removed by filtration, and the total soluble Ti content determined by precipitation with cupferron or with acetic acid. Both methods gave the same results. The chlorine content was determined as silver chloride.

Gravimetric analyses gave the results shown in Table V.

The results show that the solidified salt contained only $TiCl_2$. The content of trichloride, if it was at all present, must be negligibly small. There are no reasons to suppose that trivalent Ti would be more stable in $MgCl_2$-$TiCl_2$ mixtures which solidified as heterogenous mixtures of $MgCl_2$ and $TiCl_2$. Therefore, the total contents of soluble Ti as found by titration of samples dissolved in HCl were recalculated to $TiCl_2$. Table VI gives the summary of analytical results and of thermal analyses.

Table V.

	V 16			N 15		Theoretical composition of pure $TiCl_2$
Wt % Ti	40.2	40.3	40.2	40.3	40.9	40.32
Wt % Cl	—	59.5	57.8	58.3	59.1	59.68
Total %	—	99.8	98.0	98.6	100.0	100.00

These experiments show that measurements of the content of $TiCl_2$ from the volume of hydrogen evolved during dissolution in acids in the samples containing dispersed metal particles are not reliable. We suspect that errors similar to those experienced here could occur in the work of other investigators who reported analyses for di- and trichloride in melts containing dispersed metal particles.

The phase diagram of the system $TiCl_2$-$MgCl_2$ shown in Fig. 3 indicates that the system is of the peritectic type. The peritectic point lies close to the melting point of pure $MgCl_2$ at about 0.29 mole % (0.35 wt %) $TiCl_2$ and 716°C. The observed peritectic temperature shows a tendency to increase with increasing content of $TiCl_2$ reaching about 725°C near the $TiCl_2$-end of the diagram. The reason for this increase is not known.

The solubility of $TiCl_2$ in solid $MgCl_2$ is below 0.35 wt % $TiCl_2$ at 715°C; the solubility of $MgCl_2$ in solid $TiCl_2$ was not determined, but it is believed to be small.

The solidified salt low in $TiCl_2$ had an emerald green color which deepened to a dark green at about 50 wt % $TiCl_2$. Further increase of the concentration of the dichloride changed the color from a grayish dark green to black with a violet tinge. The salt also changed in physical appearance, and it was more and more difficult to remove it from the crucible. The magnesium-chloride-free salt was a graphite-like substance which had to be scraped out of the crucible and which "smeared" when it was crushed with a pestle in a mortar. It was not pyrophoric and not particularly sensitive to moisture when in compact form. Much longer time was required to dissolve a sample of pure $TiCl_2$ in acid solution than samples containing $MgCl_2$.

The Ti powder was mostly deposited as a spongy mass on the walls and on the thermocouple protection tube. At higher concentrations the top part of the salt contained more Ti powder than the bottom part, and sometimes a layer of pure salt was observed at the bottom with almost no metallic Ti.

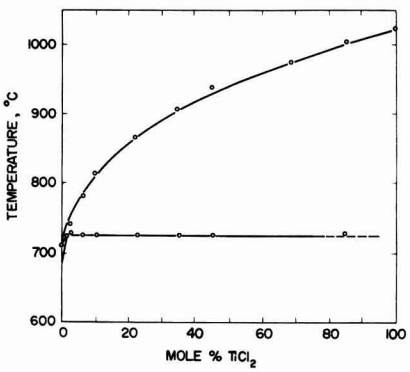

Fig. 3. Phase diagram of the $MgCl_2$-$TiCl_2$ system

Table VI. Summary of experimental results[1]

Run No.	Charge wt, g	Wt loss, g	Ti metal (insoluble residue) wt %	Total soluble Ti, wt %[2]	$TiCl_2$ Wt %[2]	$TiCl_2$ mole %	Thermal arrests, °C
			Open Crucibles				
1	—	—	—	0	0	0[3]	714
2	—	—	—	2.68	6.6	5.35	769 718
3	24.4	—	0.41	4.28	10.57	8.64	795 719
4	17.05	—	1.1	10.21	25.18	21.22	848.5 720
5	22.06	Apprec.	2.26	10.08	25.03	21.18	851 719
6	19.16	—	1.24	15.96	39.5	34.32	897 722
7	19.75	—	13.64	19.82	49.1	43.58	929 722
			Closed Crucibles				
12	—	—	—	0	0	0[3]	714
11	—	—	—	0.02	0.05		715.5
10	—	—	—	0.14	0.35	0.29	722 716
9	—	—	—	0.38	0.94	0.76	722 716
8	—	—	—	0.75	1.86	1.50	732 716
13	17.32	0.1	41.1	29.55	73.2	68.63	977 —
14 top			14.4	36.10	89.2		
14 middle	16.26	0.2	10.4	34.50	85.4	84.59	1001 726
14 bottom	[4]		0.15	35.10	87.2	[7]	
15 top			19.7	40.30	99.9		
	20.85	3.4				100.0	1025 —
15 bottom	[5]		11.8	40.75	101.2	[8]	
V 16	—[6]	—	5.2	40.25	98.9	100.0	
N 15	—[6]	—	4.0	40.55	99.3	100.0	

Remarks: [1] Determinations of $TiCl_2$ content from the volume of hydrogen collected after dissolving samples in dilute acid are not given here because they were found to be inaccurate.
[2] The percentages of total soluble Ti and of $TiCl_2$ were calculated from analyses after subtracting the insoluble (metallic) Ti dispersed in the salt.
[3] 100% $MgCl_2$.
[4] 1.15 g metallic Ti powder added to the charge.
[5] 3.9 g metallic Ti powder added to the charge.
[6] Average values.
[7] Average value.
[8] Accepted value.

It has to be pointed out that appreciable amounts of metallic Ti dispersed in the melts were found in all cases, whether Ti powder was added to the charge or not. As it is seen from Table VI, the percentage of dispersed metal generally increased with increasing content of soluble Ti. The origin of the dispersed metal was certainly the material of the crucible. The dispersions were formed through the corrosive action of $TiCl_3$ in the charge which strongly attacked the inner walls of the crucibles. Some metallic particles were coarse (up to 0.5 mm in cross section); they were probably metal crystals loosened from the crucible walls. Similar formation of metallic dispersions ("pyrosols") was observed by Straumanis (5) in the melts exposed to air or when the metal immersed in a halide melt contained oxygen. The material of our crucibles was commercial grade Ti with about 0.3% oxygen: it did not form Straumanis' "pyrosols" in pure magnesium or sodium chloride melts, under argon atmosphere, but could do so when exposed to the corrosive action of $TiCl_3$ in the charge.

The formation of metal dispersion by some disproportionation reaction on cooling, e.g.,

$$2TiCl \rightarrow Ti + TiCl_2$$

does not seem probable. Our data do not lend any tangible support for the assumption that titanium monochloride could form in the melts and disproportionate on cooling.

Acknowledgments

B. L. Dunicz participated in the early development stages of the vapor pressure measurements method. Arnold Veinbachs did most of the analytical work. The study was supported by the Office of Naval Research Contract No. Nonr 285(13) as a part of the research program on the Extraction Metallurgy of Titanium.

Manuscript received April 15, 1957. This paper was prepared for delivery before the Cleveland Meeting, Sept. 30-Oct. 4, 1956.

Any discussion of this paper will appear in a Discussion Section to be published in the December 1958 JOURNAL.

REFERENCES

1. G. B. Skinner and R. B. Ruehrwein, *J. Phys. Chem.*, **59**, 113 (1955).
2. B. S. Sanderson and G. E. MacWood, *ibid.*, **60**, 314 (1956).
3. O. Kubaschewski and E. Ll. Evans, "Metallurgical Thermochemistry," p. 255, Pergamon Press, New York, 2nd ed. (1956).
4. W. C. Kreye, C. J. B. Fincham, L. Nanis, M. Jaworsky, and H. Kellogg, Final Report, Nonr 266(24), Columbia University, June, 1956.
5. S. T. Shih, M. E. Straumanis, and A. W. Schlechten, *This Journal*, **103**, 395 (1956).

Equilibria between Titanium Metal and Solutions of Titanium Dichloride in Fused Sodium Chloride

K. Komarek and P. Herasymenko

Department of Metallurgical Engineering, New York University, New York, New York

ABSTRACT

Thermal analyses of $TiCl_2$ and NaCl in closed titanium metal crucibles were made in the range from 0 to 100 wt % $TiCl_2$. The melting point of $TiCl_2$ was confirmed to be 1025°C. The phase diagram of the system has two compounds and one eutectic. The eutectic point lies at 50.0 wt % $TiCl_2$ and 605°C. One compound, $NaCl \cdot TiCl_2$, is formed by a peritectic reaction at 628°C; the other one, $2NaCl \cdot TiCl_2$, decomposes in the solid state at 548°C.

The free energy curves derived from the phase diagram indicate that liquid $NaCl$-$TiCl_2$ melts have the highest stability at temperatures up to about 800°C at the composition 2Na + 1 Ti + 4Cl, thus making probable the existence of $[TiCl_4]^{2-}$ complex ions. At higher temperatures or in the presence of large cations, more complex ionic clusters are likely to exist.

Results of an investigation of the $MgCl_2$-$TiCl_2$ system were reported in a previous paper (1). Information on other salt systems containing titanium tri- and di-chloride is rather scarce. Mixtures of NaCl and $TiCl_3$ or $TiCl_2$ are of special interest because they are formed transitionally in the Na reduction process, and may also be used in the electrolytic production of Ti metal.

Thermal Analysis in the System NaCl-$TiCl_2$

This paper gives the results of an investigation of the phase diagram in the system NaCl-$TiCl_2$ by thermal analysis. The charge consisted of NaCl and $TiCl_3$. The NaCl was of the AR grade and was dried by heating *in vacuo* at 500°C. Titanium trichloride was prepared in this laboratory. The materials were charged under argon into Ti crucibles made of commercial Ti. The crucibles were provided with lids which permitted them to be closed tightly. The lid carried a thermocouple-well tube made of Ti, which projected into the salt mixture. The experimental procedure and the analysis of salt mixtures have been already described (1). On heating, $TiCl_3$ reacted with the metal of the crucible, giving $TiCl_2$. The weight of the mixture was about 20 g. It was rather difficult to attain complete tightness of the crucible lid, so that in most cases some loss due to evaporation was observed. The average amount lost from mixtures containing NaCl was 0.5 g or about 2.5% of the charge. The mixtures were heated about 100°C above the expected melting point, and thermal arrests were determined on cooling. Chemical analyses of solidified salts presented similar difficulties as were observed in the case of $MgCl_2$-$TiCl_2$ mixtures. The salts contained dispersed Ti metal powder in varying amounts (from 1 to 5 g/melt). There was no correlation between the amount of dispersed Ti metal and the chemical analysis of the salt soluble in dilute HCl. The most probable origin of this metallic dispersion was the crucible material. The crucibles were made of commercial grade Ti which contained about 0.3% oxygen. Straumanis and co-workers have shown recently (2) that oxygen-bearing Ti tends to form fine dispersions of metal ("pyrosols") in molten halides. In the present case, the formation of such dispersions was assisted by corrosive action of $TiCl_3$ in the charge which strongly attacked the inner walls of the crucible. Some metallic particles were rather coarse, up to 0.5 mm in cross section; they were most probably metal crystals loosened from the inner surface of the crucibles by the corrosive action of $TiCl_3$.

The solidified salt was scraped out of the crucible in a dry box under argon. The mixture was then dissolved in HCl and the total analyzed content of soluble Ti was calculated as $TiCl_2$. It was shown previously (1) that $TiCl_2$ solidifying at 1025°C in closed Ti crucibles contained titanium and chlorine atoms in the ratio 1:2. This ratio was found in several preparations of the salt made under different conditions of cooling from the molten state and containing different amounts of suspended metal. In the present work it was assumed that fused mixtures of NaCl and TiCl obtained in contact with Ti metal also contained only divalent Ti. A direct determination of divalent Ti from the volume of hydrogen evolved during the dissolution of salts in acids was found to be unreliable in the presence of fine metallic particles. As already mentioned (1), part of the hydrogen reduced by $TiCl_2$ from dilute acid reacts with finely dispersed Ti metal to form solid titanium hydride. Therefore, the measured volume of hydrogen gas is lower than would correspond to the content of $TiCl_2$.

Values of $TiCl_2$ as found by titration are given in Table I and were used in construction of the phase diagram shown in Fig. 1.

Table I. Summary of results

Charge weight in g	Weight loss in g	$TiCl_2$ wt %	$TiCl_2$ mole %	Thermal arrests in °C			
22.0	—	0	0*	801	—	—	—
21.1	0.6	15.84	8.46	762.5	—	605.5	—
19.1	0.8	21.75	12.02	740	—	611.5	—
24.3	0.0	30.32	17.62	709.5	—	612.5	566.5
24.5	0.3	40.3	24.92	656.5	—	611	549
16.5	0.9	46.2	29.68	621	—	603	547.5
21.7	0.2	49.9	32.9	—	—	608	552
21.2	0.2	52.7	35.3	680	629	605	548
19.7	0.2	61.25	43.75	822	628	605	546
20.8	1.3	76.8	61.9	938.5	625	(597.5)†	(548)†
18.9	0.1	83.15	70.8	969	626.5	(598)†	(543)†
19.0	3.6	100	100	1025	—	—	—

* 100% NaCl; † Faint arrests.

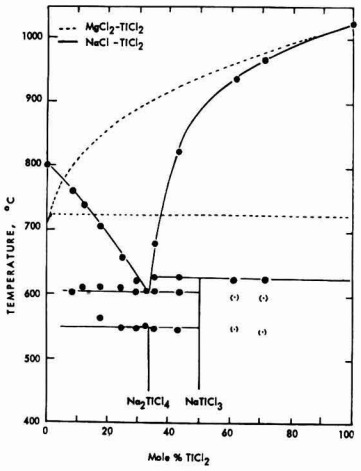

Fig. 1. Phase diagrams of the NaCl-$TiCl_2$ and $MgCl_2$-$TiCl_2$ systems.

Discussion

The phase diagram of the system has one eutectic at 605°C and at 50.0 wt % (33.3 mole %) $TiCl_2$.

The solid phase in equilibrium with the melt on the NaCl-rich side of the diagram is a solid solution of $TiCl_2$ in NaCl. The extent of this solid solution was not determined. The curve of primary crystallization rises steeply on the side of higher concentrations of $TiCl_2$ to the melting point of $TiCl_2$. The melting point of $TiCl_2$ was redetermined twice and was found to be, respectively, 1027° and 1023°C which is in good agreement with the previously reported value of 1025°C. The composition of the solid phase in equilibrium with the liquid on the $TiCl_2$-rich side was not investigated, but the formation of extensive solid solutions of NaCl in $TiCl_2$ seems to be improbable.

At 628°C, a peritectic reaction takes place; the melt reacts here on cooling to form a compound. The composition of this compound was not determined. A tentative formula of NaCl·$TiCl_2$ was assigned to this compound.

On further cooling below the eutectic temperature another reaction takes place at 548°C. This can be interpreted as a peritectoid reaction: a compound, probably $2NaCl \cdot TiCl_2$, disproportionates at 548°C into two solid phases, the solid solution of $TiCl_2$ in NaCl and the above mentioned compound NaCl·$TiCl_2$. The formula $2NaCl \cdot TiCl_2$ is very probable, since the arrests are strongest around 33.3 mole % $TiCl_2$. Analogous compounds, $2KCl \cdot TiCl_2$ and $KCl \cdot TiCl_2$, have been found in the KCl-$TiCl_2$ system by Ehrlich (3). The existence of these compounds was confirmed by x-ray studies.

The solidified salt low in $TiCl_2$ had a bluish-green color which deepened with increasing content of $TiCl_2$. At about 50 wt % the salt was gray-green. At higher contents of $TiCl_2$ the color changed to a black-violet and the physical appearance became like that described previously for $TiCl_2$.

Figure 1 shows a comparison of the phase diagrams for the two systems—$MgCl_2$-$TiCl_2$ and NaCl-$TiCl_2$—on the molar concentration basis. A qualitative discussion of thermodynamic properties of these systems will be helpful for a general explanation of the behavior of $TiCl_2$ in molten salts.

Figure 2 shows schematic curves of the free energy of formation of liquid NaCl-$TiCl_2$ solutions from solid NaCl and solid $TiCl_2$ at three temperatures: just above the eutectic temperature, just above the decomposition temperature of NaCl·$TiCl_2$,

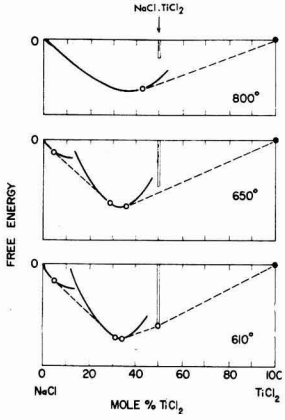

Fig. 2. Free energy curves for NaCl-$TiCl_2$ system at 610°, 650°, and 800°C. Open circles correspond to two-phase boundaries.

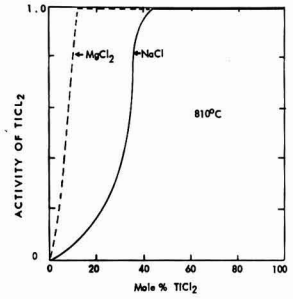

Fig. 3. Activities of $TiCl_2$ in NaCl-$TiCl_2$ and $MgCl_2$-$TiCl_2$ mixtures at 810°C.

and at 800°C. It is seen that the free energy of liquid NaCl-$TiCl_2$ solutions is the lowest near the eutectic composition, i.e., at 33.3 mole % $TiCl_2$. It is evident also that this conclusion is not affected by the existence of the compound $NaCl \cdot TiCl_2$ at temperatures below 650°C, because the free energy of formation of this compound should be more positive than that of the liquid at temperatures above the eutectic point.

Figure 3 shows a qualitative comparison of $TiCl_2$ activities in both systems at 810°C, i.e., above the melting points of NaCl and $MgCl_2$ but below the melting point of $TiCl_2$. An appreciable solid solubility of either $MgCl_2$ or NaCl in $TiCl_2$ is improbable. Therefore, the activity of $TiCl_2$ in the two-phase regions, liquid + $TiCl_2$, should be very close to unity. In the liquid phase, the activity should decrease with decreasing content of $TiCl_2$. It is evident that the activity of $TiCl_2$ in liquid NaCl-$TiCl_2$ solution will be considerably lower at all concentrations below about 42 mole % $TiCl_2$ at 810°C than in $MgCl_2$-$TiCl_2$ mixtures. Thus, $TiCl_2$ is more strongly bound in NaCl liquid solutions than in $MgCl_2$ melts. The fact that the free energy of formation of NaCl-$TiCl_2$ melts has a minimum at the composition of $2NaCl \cdot TiCl_2$ was used in construction of the activity curve in Fig. 3 to indicate that the activity of $TiCl_2$ in NaCl melts should have an inflection point at this composition.

The highest stability of the liquid at the composition $2Na + 1Ti + 4Cl$ makes the assumption of stable complex ions $[TiCl_4]^{2-}$ very probable. Thus the main structural units of the melt on the NaCl-rich side of the phase diagram appear to be Na^+, Cl^-, and $[TiCl_4]^{2-}$ ions.

The liquidus on the $TiCl_2$ side of the NaCl-$TiCl_2$ system rises steeply above the eutectic temperature and begins to deflect toward the temperature axis at a perceptibly accelerated rate only above 800°C. Thus, it can be concluded that NaCl-$TiCl_2$ melts can dissolve $TiCl_2$ in excess of 33.3 mole % only at the expense of an increase of the free energy in the system. The dichloride dissolving in the melt in excess of 33.3 mole % should be present in a form different from that of the complex ions, $[TiCl_4]^{2-}$; it may be either undissociated molecules of $TiCl_2$ or large ionic clusters composed of $Cl\text{-}\overset{|}{\underset{|}{Ti}}\text{-}Cl$ sub-units with direct bonds between Ti atoms. The existence of undissociated molecules in ionic melts is rather improbable. On the other hand, by postulating the existence of large ionic clusters, the general behavior of $TiCl_2$ can be explained and partly predicted on the basis of the electrostatic theory of bonding in molten electrolytes.

For clarity of further discussion, the term "complex ion" is reserved here for units containing only one metallic ion in the center, e.g., $[TiCl_4]^{2-}$, $[MgCl_4]^{2-}$, and the like. The bonding between the central atom and chlorine atoms is largely ionic. The "ionic clusters" are defined as structural units containing more than one metallic atom per unit, e.g.,

$$\begin{array}{c} Cl\ Cl \\ | \quad | \\ Cl\text{-}Ti\text{-}Ti\text{-}Cl, \\ | \quad | \\ Cl\ Cl \end{array} \qquad \begin{array}{c} Cl\ Cl\ Cl \\ | \quad | \quad | \\ Cl\text{-}Ti\text{-}Ti\text{-}Ti\text{-}Cl \text{ etc.} \\ | \quad | \quad | \\ Cl\ Cl\ Cl \end{array}$$

The bonding between Ti ions is nonionic.

The large clusters represent a transition to solid $TiCl_2$ which is known to possess a layer structure with direct bonds between Ti atoms. The activity of $TiCl_2$ in melts containing such large clusters should be higher than in melts containing only $[TiCl_4]^{2-}$ ions; it approaches the value of unity on approaching the phase boundary between the liquid solution and solid titanium dichloride. The structural units of the $MgCl_2$-$TiCl_2$ melts are mainly large clusters composed of $Cl\text{-}\overset{|}{\underset{|}{Ti}}\text{-}Cl$ and $Cl\text{-}\overset{|}{\underset{|}{Mg}}\text{-}Cl$ sub units.

(Solid $MgCl_2$ has also a layer structure, and it is reasonable to suppose that the structure of liquid $MgCl_2$ at not very high temperatures does not differ substantially from that of the solid.) Since divalent Mg and Ti atoms have approximately the same ionic radii, Cl ions are attracted to them roughly to the same degree: neither Ti nor Mg cations possess a marked tendency to form preferentially complex ions, $[TiCl_4]^{2-}$ or $[MgCl_4]^{2-}$. On the other hand, the electrostatic field of force of Na ions, which have a larger size and a smaller charge than Mg ions, is weaker than that of divalent ions. Therefore, chloride ions in the NaCl-$TiCl_2$ melts are more strongly attracted by bivalent Ti ions than by Na ions with the formation of complex ions of the type $[TiCl_4]^{2-}$. The stability of these complex ions is strongly influenced by the charge and size of the solvent cations. Thus, the activity of divalent Ti in molten chlorides should decrease when Mg ions are replaced by larger divalent cations (Ca^{2+}, Sr^{2+}, or Ba^{2+}); this decrease should be even more pronounced when Mg ions are replaced by monovalent cations (Na^+, K^+, Rb^+, or Cs^+).

A similar effect of different cations on the activity of AgBr in molten alkali bromides was observed by Salstrom and Hildebrand (4). They found that Li and Na cations which have a smaller size than Ag ions increased the activity of AgBr, whereas K and Rb cations having larger diameters decreased it. Analogous effects of the solvent cation size are observed in molten basic steelmaking slags. The activity of P, which is present in the slags in form of

$[PO_4]^{3-}$ complex ions decreases by several orders of magnitude when small Fe^{2+} or Mg^{2+} ions are replaced by large Ca^{2+} ions (5, 6).

Large clusters composed of two or more Cl-Ti-Cl sub-units can be held in solution when the structure of the melt is sufficiently open. (An increased openness of the melt structure can be attained either by expansion due to temperature increase or in the presence of large cations.) Sodium ions are evidently not large enough to make the structure of NaCl-$TiCl_2$ melts sufficiently open to permit the dissolution of $TiCl_2$ much in excess of 33.3 mole % at temperatures below about 800°C, i.e., the melt cannot accommodate much of the large cluster ions. The solubility of $TiCl_2$ in these melts increases rapidly at temperatures above 800°C; thermal expansion becomes a predominant factor here. Monovalent cations of larger size than Na ions should permit the accommodation of more of such clusters in the melt; in other words, they should extend the range of liquid solutions to the $TiCl_2$ side more than is observed in the NaCl-$TiCl_2$ system. This conclusion is in agreement with observation. The solubility of $TiCl_2$ in NaCl melts at 800°C is 42 mole % (present work), and in KCl melts it is 67 mole % [Ehrlich's work (3)]. One can safely predict that this solubility will be considerably lower in LiCl-$TiCl_2$ melts and appreciably higher in RbCl-$TiCl_2$ and CsCl-$TiCl_2$ melts. In the binary systems with alkaline earth chlorides the solubility of $TiCl_2$ will increase with increasing radius of solvent cation in the sequence Mg, Ca, Sr, Ba.

Analogous conditions are found in other binary systems where one of the components has a layer structure in the solid state. Thus, the solubility of solid $CdCl_2$ (or of $MgCl_2$) in binary melts with alkali chlorides increases when Na ions are replaced by K ions. Similarly, the solubility of solid silica in silicate melts (7) increases in binary oxide systems in the direction of the increasing size of alkali or alkaline-earth cations:

Cs>Rb>K>Na>Li>Ba>Sr>Ca>Mg

(Silica dissolved in silicate melts forms large ionic units, i.e., chains, networks and even more complex spacial structures, in which some oxygen atoms are shared by two Si atoms and which require an open structure for their accommodation in the melt.)

Acknowledgments

This study was supported by the Office of Naval Research, Contract No. Nonr 285(13), as part of the Research Program on the Extractive Metallurgy of Titanium. The authors gratefully acknowledge the assistance of A. Veinbachs in carrying out chemical analyses.

Manuscript received May 22, 1957.

Any discussion of this paper will appear in a Discussion Section to be published in the December 1958 JOURNAL.

REFERENCES

1. K. Komarek and P. Herasymenko, Submitted for publication.
2. M. E. Straumanis, et al., *This Journal*, **103**, 395 (1956).
3. P. Ehrlich, *Z. anorg. u. allgem. chem.*, **292**, 146 (1957).
4. E. J. Salstrom and J. H. Hildebrand, *J. Am. Chem. Soc.*, **54**, 4252 (1932).
5. P. Herasymenko, *J. Iron and Steel Inst.*, **166**, 169 (1950).
6. H. Flood and K. Grjotheim, *ibid.*, **171**, 64 (1952).
7. F. C. Kracek, *J. Am. Chem. Soc.*, **52**, 1436 (1930).

Equilibria in the Niobium-Hydrogen System

W. M. Albrecht, M. W. Mallett, and W. D. Goode

Battelle Memorial Institute, Columbus, Ohio

ABSTRACT

Equilibria in the niobium-hydrogen system were determined in the range 100°-900°C, 10-1000 mm of mercury hydrogen pressure, and atomic ratios of hydrogen to niobium of 0.01-0.85. A single phase solid solution of hydrogen in niobium was produced throughout most of the system. In no region did the equilibrium solubility exactly follow a simple pressure dependency. The heat of solution increased with hydrogen content, which behavior may be related to an expansion in the niobium lattice.

Until recently, the chief interest in niobium was its use as an alloying constituent of steels. Now in the nuclear reactor field, Nb *per se* is attractive because of its potential high temperature properties. In order to evaluate these properties, a knowledge of the behavior of Nb in various environments is essential. In the present study the equilibria in the Nb-H system were determined.

An early study of the solubility of hydrogen in rather impure Nb was reported by Hagen and Sieverts (1). Later, Sieverts and Moritz (2) determined the solubility at 1 atm pressure using a purer (98.5%) metal. The major impurity was Ta. It is considered that the later study is more reliable. McKinley (3) recently presented an equilibrium-solubility study for low hydrogen compositions.

Gulbransen and Andrew (4) investigated the reaction of hydrogen with Nb in the range 200°-900°C at pressures up to 5.7 cm Hg. These investigators stated that there were probably two hydrides of Nb which formed at low hydrogen pressures. In a few kinetic experiments performed at this laboratory no

Table I. Summary of room temperature x-ray studies of the Nb-H system

Composition, H/Nb	Body-centered cubic lattice parameter, kX		Reference
	Alpha	Beta	
0.39	3.300 to 3.306	3.416 to 3.420	(5)
0	3.302 ± 0.004	—	(6)
0.11	3.327 ± 0.003	—	(6)
0.49	3.323 ± 0.003	Complex*	(6)
0	3.295	—	(7)
0.11	3.307	—	(7)
0.11 to 0.41	3.303	Orthorhombic†	(7)
>0.41	—	Orthorhombic†	(7)
0.091	3.297 ± 0.005	3.420 ± 0.005	(8)
0.098	3.302 ± 0.005	3.410 ± 0.010	(8)
0.63	—	3.410 ± 0.005	(8)
0.82	—	3.440 ± 0.005	(8)
0.09	3.301 ± 0.002	—	This work
0.20	3.305 ± 0.002	3.43	This work
0.68	3.301 ± 0.002	3.41	This work

* Close packed hexagonal structure believed by Brauer and Hermann (7) to be nitride.
† a = 4.718, b = 4.768, c = 3.421. This structure was also considered to be a distended BCC structure, a_o = 3.44 kX.

surface product was formed at 400°-700°C at 1 atm of hydrogen pressure.

Several limited, room temperature x-ray studies have been reported for the Nb-H system. Umanski (5) found a two-phase structure in Nb containing H at an atomic ratio of H to Nb of 0.39. Both phases were given as body-centered cubic having different lattice constants. Horn and Ziegler (6) studied the system at concentrations up to 0.49 atomic ratio and reported a single phase (alpha phase) and a two-phase (alpha plus gamma prime) region. Brauer and Hermann (7) report two single-phase regions with a two-phase region in between 10 and 41 a/o hydrogen (0.11 to 0.70 H/Nb ratio). Knowles (8), likewise, reports two single phases and a two-phased region over the range of atomic ratios of H to Nb of 0.091-0.83. The results of the various room temperature x-ray investigations are summarized in Table I. In general, these studies show that there is a lattice expansion in each single-phase region as the H content increases.

Material

Bar niobium having a Vicker's hardness of 113 was fabricated into rod approximately 0.3 cm in diameter and into a 0.03 cm sheet. Analysis of the fabricated Nb, shown in Table II, was obtained by spectrographic, chemical, and vacuum-fashion techniques.

Pure hydrogen was obtained from the thermal decomposition of uranium hydride prepared from dry, tank hydrogen and degreased uranium chips.

Method

A micro-Sieverts' apparatus, shown in Fig. 1, having a double-walled reaction tube was used for the pressure-temperature-composition equilibria determinations. The total volumes of the reaction section at room temperature and at several selected elevated temperatures were measured with helium. From these, the effective volumes of the hot zone (at furnace temperature) and cold zone (at room temperature) were calculated for each furnace temperature. Reference curves were plotted of the variation of the volumes of the hot and cold zones over the temperature range of the study.

Table II. Analysis of Nb

Element	PPM by weight
Ta	1500
Fe	200
Sn	200
Mo	50
Si	50
V	50
Cr	20
Al	20
Ti	20
C	120
O_2	430
N_2	120
H_2	<3*

* After degassing.

Specimens consisted of 3-4 g of sheet Nb in pieces 1-2 cm long, 0.6 cm wide, and 0.03 cm thick. Also, small pieces of 0.3 cm diameter rod were used in one experiment. Samples were dry abraded with 240-grit silicon carbide paper and placed in the calibrated inner chamber of the reaction tube. A Pt-Pt + 10% Rh thermocouple was inserted into the reaction tube so that the bead was in close proximity with the specimen. The reaction tube was then evacuated and the specimen degassed for 1 hr at 800°C and 0.02μ of Hg.

Equilibrium data were obtained in the following manner. An initial measured quantity of H was added to the inner reaction tube at the desired temperature. The system was allowed to come to a constant pressure as measured on a Hg manometer. This pressure was considered to be the equilibrium pressure. The equilibrium composition was calculated from the equilibrium pressure, specimen weight, the gas addition, and volume of the reaction system. The temperature was increased and equilibrium points determined at various temperatures. Another gas addition was then made and the process repeated by decreasing temperature. This was continued until the entire ranges of pressure, tempera-

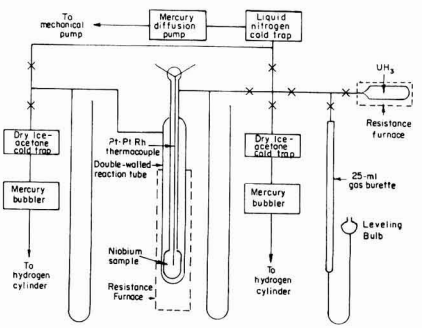

Fig. 1. Schematic diagram of micro-Sieverts apparatus

ture, and composition were covered. Equilibrium data were obtained in a comparable manner by making gas extractions from the system. Also, H additions and extractions were made isothermally at 400°, 450°, and 500°C to note whether hysteresis occurs. No hysteresis was noted.

Throughout the experiments, a pressure close to that in the system was maintained in the outer chamber of the furnace tube with dry, tank H. This was done to prevent diffusion of H out of the reaction system.

Vacuum-fusion analysis of the Nb specimens after the runs showed that there was little or no change in the oxygen content of the metal. The Nb that originally contained 430 ppm oxygen by weight analyzed 460 ppm by weight, after an equilibrium experiment. This is within the normal reproducibility limit for oxygen analyses.

Results

The pressure-temperature-composition equilibria of the Nb-H system were determined in the range 100°-900°C, 10-1000 mm Hg, and atomic ratios of H to Nb of 0.01-0.85. Determinations were made with three different samples of 0.03 cm Nb sheet and one of 0.3 cm diameter rod. Figures 2 and 3 show isotherms for all the equilibrium data. Figure 2 is a plot of equilibrium pressure against the H/Nb ratio, while Fig. 3 is a logarithmic plot of the same variables. The 300°C isotherm (Fig. 2) is invariant at about 8 mm Hg, indicating the presence of a two-phase region. No other invariant pressures were obtained for any of the isotherms at 350°C and above. Therefore, the results show that nearly all of the equilibrium data were obtained in a single-phase region. This is also shown in Fig. 4, in which the equilibrium temperature is plotted against the H/Nb ratio to show isobars at 10, 100, and 1000 mm Hg. It is seen that only a small portion of the 10 mm isobar is invariant in the range of H/Nb ratios of 0.21-0.42.

To determine room-temperature structures, x-ray diffraction patterns were obtained and metallographic examinations were made on several Nb specimens having compositions of H/Nb of 0.09, 0.20, and 0.68. These samples were water quenched from equilibrium at 700°, 500°, and 400°C, respectively. The sample containing 0.09 H/Nb showed primarily a body-centered cubic Nb structure, alpha phase, with lattice parameter, $a_o = 3.301 \pm 0.002$ kX. A very small amount of a second phase was also detected. This phase can be seen as needles in the photomicrograph of the material shown in Fig. 5. The alpha matrix phase of the microstructure appears the same as that of the original hydrogen-free Nb. Two phases were found in the specimen containing 0.20 H/Nb, an alpha niobium phase ($a_o = 3.305 \pm 0.002$ kX) and another body-centered cubic structure, beta phase, with $a_o = 3.43$ kX. The two-phase structure of this material can be seen in Fig. 6. The specimen containing 0.68 H/Nb contained primarily the beta phase, $a_o = 3.41$ kX, and a small amount of alpha phase, $a_o = 3.301 \pm 0.002$ kX. This structure is shown in Fig. 7. These data are in agreement with the published results

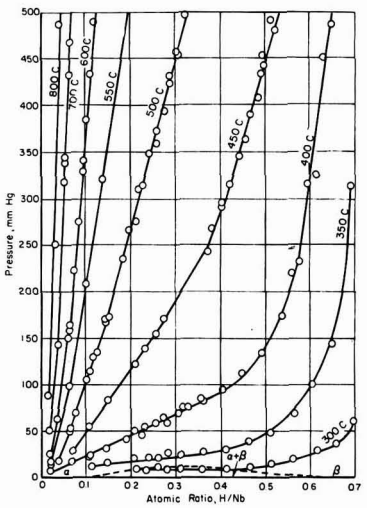

Fig. 2. Isotherms in the Nb-H system

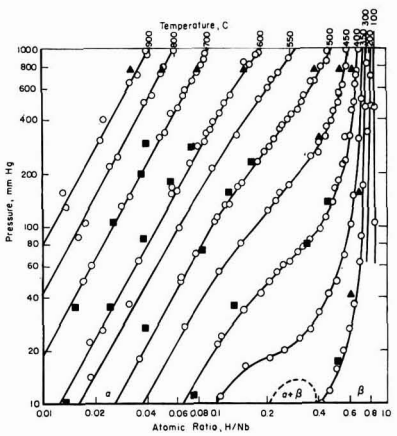

Fig. 3. Logarithmic plot of isotherms in the Nb-H system. Open circle, present study; solid square, McKinley (3); solid triangle, Sieverts and Moritz (2).

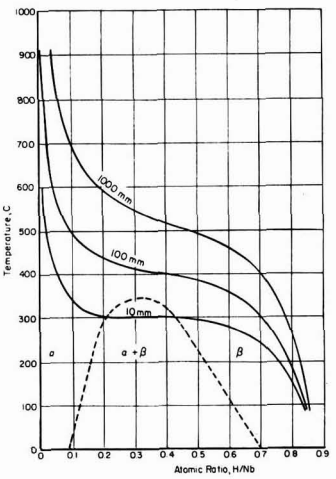

Fig. 4. Representative isobars for the Nb-H system

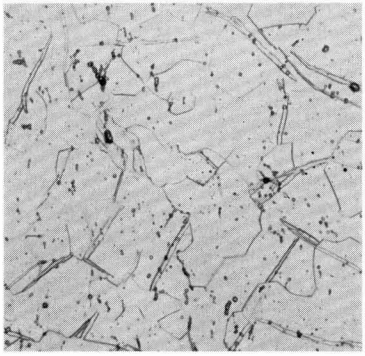

Fig. 5. Niobium containing 0.09 H/Nb quenched from equilibrium at 700°C. Magnification, 250X before reduction for publication.

from room temperature x-ray investigations (5-8) shown in Table I. If all the x-ray data are considered, the two-phase region extends from about 0.09 to 0.7 H/Nb at room temperature. These limits were used with those obtained at 300°C in the present equilibria study to outline the probable two-phase boundary in the Nb-H system shown in Fig. 4. Apparently, the temperature of the critical point where the two phases, alpha and beta, become identical lies somewhere between 300° and 350°C. Above the critical temperature, S-shaped isobars were obtained. This is also indicated in the experimental isotherms in Fig. 2 and Fig. 3. In equilibrium diagrams S-shaped isotherms are usual in single-phase regions immediately above the critical point. Similar curves have been shown in the palladium-deuterium system reported by Gillespie and Downs (9).

Figure 3 shows that the isotherms from a logarithmic pressure-composition plot were straight at concentrations up to 0.1 H/Nb. At higher hydrogen contents the S-shaped curvature of the isotherms is quite evident. Similar curves fit the limited data for the Nb-H equilibrium reported by Sieverts and Moritz (2) and McKinley (3). As shown in Fig. 3, their data corroborate those of the present study. However, at high H/Nb ratios Sieverts and Moritz show a lower equilibrium hydrogen concentration at the same temperature and pressure than the present work. Since they used Nb that was less pure (98.5%) this would be expected. Impurities in the metal would probably decrease the hydrogen solubility. This effect would be more pronounced in the high hydrogen concentration range. McKinley reports that at concentrations up to H/Nb of 0.055 the equilibrium solubility follows the square root of pressure or Sieverts law and a heat of solution of 18.5 kcal/mole was obtained. In the present study, a plot of square root of equilibrium pressure against composition deviated from Sieverts law. Deviations were observed at lower compositions than expected. However, a heat of solution estimated from a Sieverts type plot for compositions below about 0.085 H/Nb agrees very well with that of McKinley. It would not be expected that the equilibrium solubilities at higher compositions necessarily follow a square root of pressure dependency since the published x-ray investigations show lattice expansions

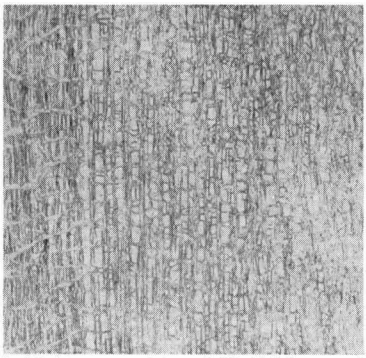

Fig. 6. Niobium containing 0.20 H/Nb quenched from equilibrium at 500°C. Magnification, 250X before reduction for publication.

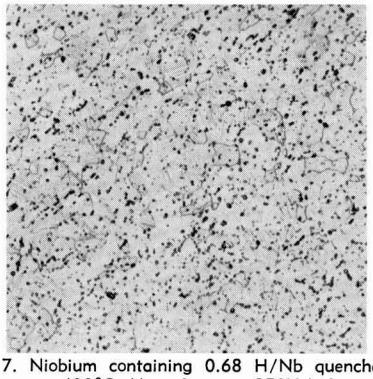

Fig. 7. Niobium containing 0.68 H/Nb quenched from equilibrium at 400°C. Magnification, 250X before reduction for publication.

in Nb as the hydrogen content increases. This constitutes another variable which may affect equilibrium solubility.

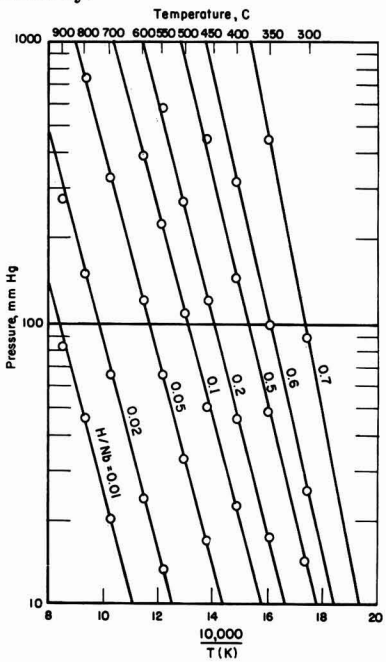

Fig. 8. Representative isopleths for the Nb-H system

Table III. Thermodynamic data for various Nb-H compositions

Composition H/Nb	Constants in $\log_{10}P_{mm} = -A/T + B$ A	B	ΔH, cal/mole
0.01	3509	4.92	16,050 ± 380
0.02	3628	5.54	16,600 ± 170
0.05	3674	6.30	16,810 ± 170
0.10	3693	6.83	16,900 ± 190
0.20	3908	7.49	17,880 ± 240
0.50	4131	8.33	18,900 ± 450
0.60	4503	9.21	20,610 ± 190
0.70	5093	10.80	23,300*

* Calculated from two points.

To put the equilibrium in the Nb-H system on a sound basis, it is necessary to consider the equilibrium of formation of various products (solid solutions) having definite H/Nb ratios. Therefore, various isopleths were plotted, logarithm of equilibrium pressure against reciprocal temperature, in Fig. 8. It is seen that a series of straight lines were obtained which increase in slope with hydrogen content. The equation for these lines is

$$\log_{10}P_{mm} = -\frac{A}{T\,(K)} + B$$

The values of the constants, A and B, in this equation and the heats of solution for the various compositions are given in Table III. It is seen that the heat of solution increases with hydrogen content.

Conclusions

The Nb-H system has been investigated in the ranges 100°-900°C, 10-1000 mm Hg, and H/Nb ratios of 0.01-0.85. The absorption of hydrogen resulted in the formation of a single-phase solid solution throughout most of the system. However, at about 300°C and a pressure of 8 mm Hg, the presence of a two-phase region was indicated between H/Nb ratios of 0.21-0.42. In the equilibrium diagram, the critical point where the two phases become identical probably lies just within the ranges of this work.

At low hydrogen compositions the equilibrium solubility follows approximately a square root of pressure relationship. This indicates that hydrogen is absorbed as atoms. At the higher hydrogen compositions, no simple pressure dependency was evident. Lattice expansion of the niobium causes deviations from a strict square root of pressure dependency. Both lattice parameter and heat of solution increase with hydrogen concentration.

Manuscript received Sept. 10, 1957. Work performed under AEC Contract W-7405-eng-92.

Any discussion of this paper will appear in a Discussion Section to be published in the December 1958 JOURNAL.

REFERENCES

1. H. Hagen and A. Sieverts, *Z. anorg. u. allgem. Chem.*, **185**, 225 (1930).
2. A. Sieverts and H. Moritz, *ibid.*, **247**, 124 (1941).
3. T. D. McKinley, Paper presented before the Regional AIME Meeting, Cleveland, Ohio (April 1957).
4. E. A. Gulbransen and K. F. Andrew, *J. Metals*, **188**, 586 (1950).
5. Y. S. Umanski, *J. Phys. Chem. U.S.S.R.*, **14**, 332 (1940).
6. F. H. Horn and W. S. Ziegler, *J. Am. Chem. Soc.*, **69**, 2762 (1947).
7. G. Brauer and R. Hermann, *Z. anorg. u. allgem. Chem.*, **274**, 11 (1953).
8. D. R. Knowles, Report No. IGR-R/C-190, United Kingdom Atomic Energy Authority (March, 1957).
9. L. J. Gillespie and W. R. Downs, *J. Am. Chem. Soc.*, **61**, 2496 (1939).

Electromotive Force Measurements in Cerium-Cerium Chloride Liquid Systems

Seymour Senderoff and G. W. Mellors

National Carbon Research Laboratories, National Carbon Company, A Division of Union Carbide Corporation, Cleveland, Ohio

ABSTRACT

The emf of the cell $Ce|CeCl_3(1-x)Ce(x)||CeCl_3|Cl_2$ (graphite) has been measured over a temperature range from the melting point of $CeCl_3$ to about 950°C. Preliminary conductance measurements indicate that the saturated solution of cerium in cerium chloride is an ionic conductor. The potential results indicate the presence of a subhalide, $Ce^+[CeCl_4]^-$, in which both monovalent and trivalent cerium exist. Further, it is suggested that cerium chloride may exist in a highly associated state in which the following formula may represent the dominant species, viz., $[CeCl_2]^+ [CeCl_4]^-$. The addition of cerium to this system may result in the reduction of the less highly complexed cation as follows:

$$[Ce^{3+}Cl_2]^+ [Ce^{3+}Cl_4]^- + Ce \rightarrow\rightarrow \frac{3}{2} Ce^+[Ce^{3+}Cl_4]^-$$

In the course of the work a reversible chlorine electrode, satisfactory at temperatures up to 950°C, has been developed and will be reported elsewhere.

Few investigations of metal-metal halide liquid systems have been reported. Some information exists in the form of phase diagrams by Cubicciotti and co-workers (1, 2, 3). Conductance work in alkali metal-alkali halide melts has been reported by Bronstein and Bredig (4); phase equilibria have been studied in these systems by Bredig, *et al.* (5, 6). Corbett and Winbush (7) have reported the solubility of some metals in their molten halides, while Grjotheim, Grönwold, and Krogh-Moe (8) studied cryoscopy in Cd-$CdCl_2$ melts.

Various theories have been presented regarding the structure of the molten metal-metal halide systems; the first was that of Lorenz (9), who called them "pyrosols" and considered them to be emulsions or colloidal dispersions of the metal in the metal halide. Cubicciotti (1-3) showed that this could not be true in the systems he studied, since definite freezing point depressions were observed, which could only be ascribed to true solution formation. The nature of these solutions, however, has been a matter of controversy and three approaches have been used to describe them:

(*A*) The metal dissolves by entering the liquid as atoms which occupy vacancies or interstitial sites in the liquid.

(*B*) The metal dissolves as cations occupying normal cationic sites. The electrons are considered either to occupy anionic vacancies or to be more or less free electrons in a postulated band structure in the liquid analogous to the conditions in a nonstoichiometric crystal.

(*C*) The metal reduces the salt to a lower halide. The system may then be considered as the solution of a subhalide in the normal halide.

Emf studies of metal-metal halide systems appear to be a promising method of distinguishing among these alternatives, since each would produce distinctly different effects on the emf of a reversible metal electrode immersed in the molten salt solution. The first model would be equivalent to simple dilution and the change in emf on the addition of metal to the salt should be of the order of magnitude predicted by the Nernst equation for the appropriate changes in activity of the components of the system. The second model should result in considerable electronic conductivity in the system which should cause changes in the emf which depend on the degree of electronic conductivity as discussed by Wagner (10). Wagner showed that when electronic conductance is small $\Delta E/E_o = t_e$, where E_o is the emf of the system in the absence of electronic conductance, ΔE the difference between the observed emf and E_o, and t_e the "transference number" for electrons. The third model would introduce a new ionic species, which may produce a widely different emf from that of the higher valence ion. If both the higher and lower valence ions exist, they should also exhibit a characteristic redox potential.

The system selected for study was cerium metal dissolved in cerium trichloride, the phase diagram for which has been reported by Cubicciotti (3), who found a rather large solubility of cerium, up to a maximum of 33 mole %. There are no reports in the literature of previous emf measurements in this system.

Experimental

Materials

$CeCl_3$ was prepared from Ce_2S_3 as follows: Pellets of Ce_2S_3 were charged into a previously chlorinated graphite crucible; the crucible was tightly closed with a fitted graphite cover containing graphite tubes for gas inlet and outlet and thermowell. This

was placed in a quartz tube and the entire assembly put into a pot furnace. The outer quartz tube was fitted with a "Transite" cover. Purified argon was continually passed through the quartz tube and a mixture of argon and chlorine through the graphite crucible containing the Ce_2S_3. On heating the charge, the reaction started at about 300°C with the evolution of sulfur chlorides and sulfur. The temperature rose rapidly to about 700°C and was controlled by varying the ratio of Cl_2 to argon in the feed gas. When, after several hours, the evolution of sulfur compounds almost stopped, the temperature of the charge was raised to 900°C. When the charge melted (at about 820°C) sulfur compounds again appeared in the exit gases and the reaction was continued until these were eliminated. Finally, the apparatus and contents were cooled slowly in an argon atmosphere. The material was stored in a dry box. Analysis indicated the theoretical Ce:Cl ratio and over-all purity of 99.2%. No foreign metals were observed by spectrographic analysis and no water-insoluble material (i.e., CeOCl) was noted.

Creium metal was prepared by electrolysis of a LiCl-KCl eutectic mixture containing 40 wt % $CeCl_3$ by a method based on that described by Eastman, *et al.* (11). Analysis indicated that the cerium was 99.6% pure. All weighings and transfers were performed in a dry box.

Chlorine electrodes were prepared by inserting the end of a 2-ft length of high-density graphite base tubing, 10.4 mm O.D., 5.4 mm I.D., to the bottom of a porous graphite cylinder (National Carbon Company, Grade 60), 4 in. high and 15 mm O.D., a seal being made with F-cement (National Carbon Company). The base of the porous cylinder was about 3-4 mm thick. The electrodes were purified by treatment with chlorine at 2300°C for 2 hr. In use chlorine was passed into the tube and allowed to emerge through the porous cylinder into the electrolyte. The electrode, its reversibility, and its other properties are described more fully elsewhere (12).

Argon was purified by passage through titanium chips at 900°C. Chlorine was dried by passage through a column of "Drierite" desiccant. Spectroscopic examination of chlorine showed no significant traces of impurities, water, CO, and CO_2 being absent.

Furnace and cell.—The furnace was a tensile test type made by Marshall Products. The bore was 3½ in. and an iron tube 3¼ in. O.D. ¼ in. wall thickness served as a baffle between the furnace windings and the "Vycor" glass tube containing the cell and electrodes. The cell envelope was a 51 mm O.D. "Vycor" glass tube, 30 in. in length, closed at each end with a 10½ rubber stopper. Each stopper was protected by an Alundum thermal radiation shield. Through the lower stopper passed a 9 mm "Pyrex" glass tube, which served as entry tube for argon and as guide for the pedestal, the latter being a ¼ in. diameter iron rod. A short piece of molybdenum rod (⅛ in. diameter) threaded 6/32 screwed into the top of the iron rod and was secured by a Mo collar (inner) and a stainless nut (outer) through the base of a "Morganite" ΔRR XN100 recrystallized alumina crucible. A liquid-tight seal was always obtained by

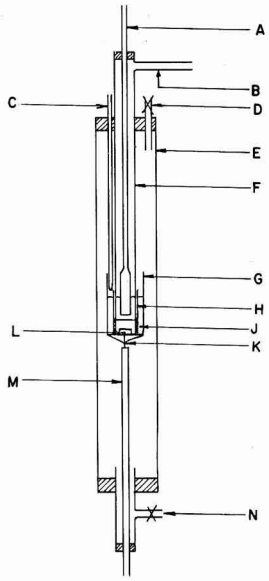

Fig. 1. Cell envelope and contents. A, chlorine electrode; B, chlorine exit; C, thermocouple sheath; D, argon exit; E, 51 mm O.D. Vycor glass envelope; F, 25 mm O.D. Vycor glass sheath; G, XN100 alumina crucible; H, XN20 alumina crucible; J, ΔRR alumina pedestal; K, molybdenum rod, threaded 6/32; L, molybdenum collar; M, iron pedestal; N, argon entry tube.

this method. Inside the XN100 crucible an XN20 crucible was mounted on a ΔRR alumina collar. Communication between the melts in the two crucibles was established through a 1/32 in. diameter hole, drilled through the base of the XN20 crucible, packed with asbestos and prefired. Through the upper 10½ rubber stopper, passed an argon exit tube, (provided with a tap), a "Vycor" thermocouple sheath and a 25 mm O.D. "Vycor" glass tube, provided with a side arm for exit of chlorine. This tube fitted snugly inside the XN20 crucible and, with the apparatus charged with molten salts, a good "liquid seal" between the Cl_2 and A atmospheres was maintained. The Cl_2 electrode passed through a No. 4 stopper in the top of the 25-mm tube. The upper part of the electrode was protected from atmospheric oxidation as follows: chlorine passed through a glass entry tube, the O.D. of which was equal to the I.D. of the graphite tube, and a pressure tubing sleeve gripped both members. Electrical contact was maintained by a copper band, tightened into a groove around the graphite: the whole was coated with "Unichrome" stop-off (Metal and Thermit Corporation) and no portion of the electrode was exposed to the atmosphere. A schematic diagram and a photograph of the apparatus are shown in Fig. 1 and 2.

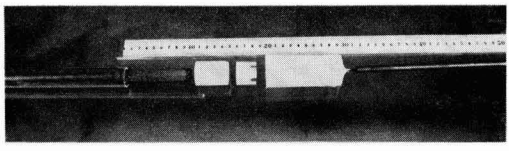

Fig. 2. Cell and electrodes

Temperature.—Chromel-alumel thermocouples were used, protected by 6 mm "Vycor" glass sheaths, closed at the lower end. The thermocouple was positioned at the top of the XN20 crucible, ¼ in. above the melt in the outer (XN100) crucible. It was shown that there was less than 1° difference in temperature between this portion and a point immediately beneath the base of the outer (XN100) crucible. An L&N potentiometer was used to measure thermocouple output. The temperature of the furnace was controlled by a "Wheelco" controller with an independent thermocouple adjacent to the furnace winding.

Measurement of potential.—A "Rubicon" galvanometer and potentiometer were used, the latter reading from 0 to 1.6 v in steps of 0.05 mv. Since the potential to be measured was of the order of 2.2 v, it was necessary to include a source of "bucking" potential in the circuit. An "Eveready" "Air Cell" (National Carbon Company) battery was employed, shunted permanently across a 200 ohm resistor; the potential was ascertained accurately each time a measurement was made.

General procedure.—The apparatus was charged with an amount of $CeCl_3$ previously calculated to give a satisfactory depth of melt in the crucibles. A large excess of cerium metal was used, since it was necessary for there to be sufficient (*a*) to saturate the $CeCl_3$ in the outer crucible and (*b*) to cover completely the molybdenum collar in the base of the XN100 crucible. (This was usually of the order of 40 g.) All joints in the apparatus were sealed with a "Unichrome" stop-off prior to commencement of a run. The apparatus was flushed with argon for several hours and then heated slowly overnight to about 900°C. The Cl_2 was then bubbled slowly (¼ c.f.h.) through the melt. After two to three hours a steady, reproducible value of potential was obtained and measurements were made, cooling and heating, between 810° and about 950°C. The argon supply was stopped during potential measurements, since the flow cooled the lower electrode, leading to inaccurate results.

Results

Potential values as a function of temperature for the cell $Ce|CeCl_3$ (saturated with Ce)$||CeCl_3|Cl_2$ (graphite) (I) are shown in Fig. 3. The chlorine electrode was the + electrode in all the measurements.

Over the temperature range 820°-920°C, dE/dT has the value −0.68 mv/°C. The curve of Fig. 3 represents the average of three runs, the maximum deviation being 2 mv at low temperatures (820°C) and 3 mv at high temperatures (920°C and above). It will be observed that the values obtained here are about 0.7 v less than those calculated from thermal data by Hamer, *et al.* (13). Since the departure of 0.7 v (equivalent to approx. 48 kcal) from the theoretical decomposition potential of $CeCl_3$ suggests that the reaction $2Ce + 3Cl_2 \rightarrow\rightarrow 2CeCl_3$ is not the one which is responsible for the observed potential, a series of experiments was performed to determine whether a lower valence state of cerium may be the potential-determining species. In this case the solution of cerium in cerium chloride would form a redox system and its potential could be studied by

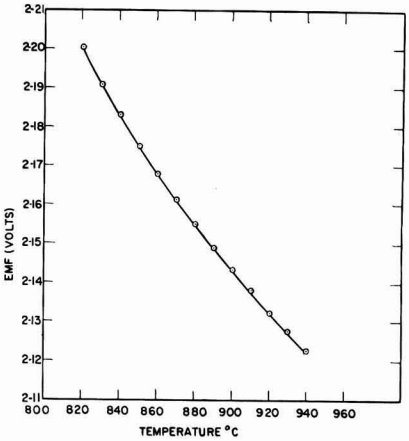

Fig. 3. Emf as a function of temperature in saturated solution.

varying the concentration of added cerium metal and observing the potential on an inert electrode in a cell which can be written as follows:

Mo, Ce^{3+}, $Ce^{(3-x)+}||CeCl_3|Cl_2$ (graphite) Cell (II)

In most experiments, molybdenum electrodes were used, but in two cases identical potentials were obtained using tungsten electrodes, thus establishing the inert character of both of these elements in the system.

In Table I, the weight of Ce and $CeCl_3$ in the outer crucible are shown, together with Ce^{3+}/Ce^{2+} and Ce^{3+}/Ce^{1+} [1] hypothetical ratios calculated on the assumption that such are the valence states exhibited by the Ce ions in these systems. The last column gives the value of the observed emf of Cell II at a number of compositions.

Discussion

The first important result to consider is the departure of 0.7 v in the observed potential of Cell (I) from the calculated value of Hamer, *et al.* (13). The uncertainty in the thermal data of Brewer (14) may be of the order of 150 mv. A measurement of the Cell $Ce|KCl$ (0.95) $CeCl_3$ (0.05)$||KCl$ (0.95) $CeCl_3$ (0.05)$|Cl_2$ (graphite) (III) gave a potential of 2.8 v

[1] $Ce^{3+}/Ce^{2+} = [0.189\ y/x - 0.667]$
$Ce^{3+}/Ce^{1+} = [0.379\ y/x - 0.333]$
where x = wt of Ce in grams and y = wt of $CeCl_3$ in grams.

Table I.

Wt Ce (g)	Wt $CeCl_3$ (g)	Mole ratio Ce/$CeCl_3$	Ce^{3+}/Ce^{2+}	Ce^{3+}/Ce^{1+}	E (880°C)
Excess	—	—	0	1.	2.1550
12.56	72.00	0.307	0.446	1.84	2.1583
12.55	72.00	0.307	0.446	1.84	2.1586
11.30*	83.90	0.237	0.736	2.48	2.1562
9.00*	83.90	0.189	1.098	3.20	2.1580
6.95	83.90	0.146	1.620	4.25	2.1571
4.13	83.90	0.0867	3.160	7.36	2.1540
2.91	83.90	0.0611	4.790	10.61	2.1478
1.48	72.00	0.0362	8.550	18.12	2.1024
1.18	72.00	0.0289	10.890	22.77	2.0904
0.871	83.90	0.0183	17.57	36.09	2.0372
0.8557	83.90	0.0180	17.94	36.87	2.0882

* Tungsten electrodes.

at 922°C. The solubility of cerium in the electrolyte of Cell (III) is very small (probably of the order of 0.1%), so in this case it is the Ce^0/Ce^{3+} couple that is being measured. Using concentration instead of activity in the Nernst equation to correct for the dilution of $CeCl_3$ in Cell (III), the potential of Cell (III) with pure $CeCl_3$ as the electrolyte would be about 2.7 v, in fair agreement with the value of 2.87 v calculated from the approximate thermal data. The departure then is real and not ascribable to the uncertainty in the literature value.

An obvious source of error in the potential measurement is the liquid junction potential in Cell (I) between the cerium-saturated $CeCl_3$ and the pure cerium chloride. The liquid junction potential between silver chloride and cerium chloride has been found by the authors to be less than 60 mv over the temperature range 820°-920°C. Since the cerium-saturated solution of $CeCl_3$ has a lower conductance than that of silver chloride, the liquid junction potential in Cell (I) should be substantially less than this value and must be considered as not significant. A formal calculation of the activity of $CeCl_3$ in the cerium-saturated solution based on the observed potential value and the E_o of Hamer (14) gives a value of 10^{-6} for the activity at a mole fraction of 0.67. This indicates the essential absence of $CeCl_3$ in its usual state.

Ascribing the deviation to electronic conductance is impossible on two grounds. First, the interposition of pure $CeCl_3$, generally considered to be a pure ionic conductor, as an electrolyte in Cell (I) "filters out" any electronic current which may be supported by the cerium-containing electrolyte on the other side of the cell, and thus eliminates any effect on the cell potential of electronic conduction (15). Second, preliminary conductance measurements which the authors have made indicate that the almost saturated solution of cerium in cerium chloride is a typical ionic conductor having a conductance of 3.76 mhos at 840°C and 3.57 mhos at 810°C, a positive temperature coefficient of conductance, which is also a property of ionic conductance. The conductance of $CeCl_3$ at 840°C is about 0.92 mhos and no evidence for electronic conductance may be deduced from this comparatively small change in conductance on adding 32 mole % cerium, especially in view of the results of Bronstein and Bredig (4), who showed that addition of 20 mole % K to KCl increased the conductance by a factor of 70. To explain the deviation of 0.7 v on the basis of Wagner's (10) equation would require about 24% electronic conductance.

Another alternative would be to consider the $Ce\text{-}CeCl_3$ mixture not as an electrolyte with either ionic or mixed conduction, but as a semiconducting electrode. In this case, however, the cell would be essentially $Ce|CeCl_3|Cl_2$ and, in the case of the saturated solution of Ce in $CeCl_3$, the potential would be expected to approximate the calculated value for this cell. As noted above, it is actually found to be 0.7 v lower. The assumption of semiconduction of the $Ce\text{-}CeCl_3$ system is apparently not in accord with the observed emf.

There remains, then, the formation of subhalides by reduction of $CeCl_3$ with cerium to explain the observed result. The stoichiometric reduction of $CeCl_3$ to the "dichloride" may be expressed by either of the following equations:

$$2CeCl_3 + Ce \rightarrow\rightarrow 3CeCl_2 \qquad (a)$$

$$4CeCl_3 + 2Ce \rightarrow\rightarrow 3Ce^+ [CeCl_4]^- \qquad (b)$$

The "dichloride" of equation (*a*) is written to indicate the cerium is present as Ce^{2+} and the "dichloride" of equation (*b*) indicates the cerium is present in two valence states, Ce^{1+} and Ce^{3+}. The existence of Ce^{+1} in the absence of Ce^{3+} (i.e., a net valence state less than +2) may be disregarded because of insufficient "solubility" of cerium in cerium chloride.[2]

The preponderance of evidence derived from the emf measurements suggests equation (*b*) as the description of the "solution" of cerium in $CeCl_3$. It was noted in Table I that no appreciable change in potential was observed on changing the concentration of cerium metal in the system from that containing excess cerium (in which a pool of cerium formed the electrode) to one containing only 8.7 mole % cerium (in which molybdenum or tungsten rods were the electrodes). This indicates that in these solutions a redox potential between two valence states in solution was being measured in which the cerium, molybdenum, or tungsten electrodes were inert electrodes. If reaction (*a*) described the 33 mole % cerium solution, then a rapid decrease of potential with decreasing cerium content should have been observed, with the initial increments of Ce^{3+} resulting from cerium concentrations just below this value. However, if reaction (*b*) describes the 33 mole % cerium solution, then the ratio of oxidant to reductant in this solution is unity and increments of either oxidant or reductant at this concentration would have only a small effect on the potential. In Fig. 4 the observed potentials are plot-

[2] The phase diagram for the system published by Cubiciotti (3) indicates the maximum solubility of cerium as 33 mole %, with a temperature coefficient close to zero over a range of at least 100°C. This would correspond exactly to the stoichiometry of equations (*a*) and (*b*). Work now in progress in this laboratory indicates some modification of the phase diagram may be necessary, but the "solubility" of cerium certainly is not greater than this value.

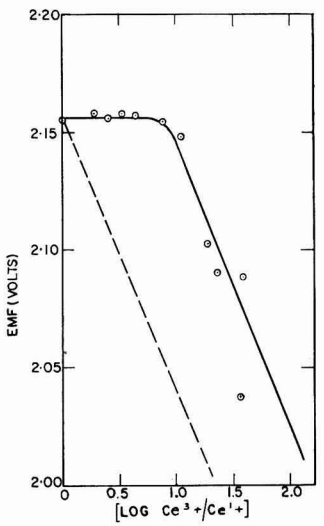

Fig. 4. Emf as a function of cerium metal concentration, 880°C (Cell II). Dotted circles, experimental results; dashed line, theoretical Nernst plot for n = 2.

ted against the logarithm of the concentration ratios using Ce^{3+}/Ce^{1+} as the potential-determining couple. Also indicated on the curve is the ideal Nernst plot using $n = 2$, the slope of which at 880°C is 0.115 v. It will be noted that, in the region of dilute Ce^{+}, the slope approaches the Nernst value for $n = 2$.

It seems reasonable, then, to conclude that the cerium "dichloride" present in solutions of Ce in $CeCl_3$ is actually $Ce^{+}[CeCl_4]^{-}$, in the temperature range between 820° and 920°C. Consistent with this is the work of Woodward, *et al.* (16), who showed by Raman Spectra studies that liquid gallium dichloride is $Ga^{+}[GaCl_4]^{-}$ and the work of Garton, *et al.* (17), who showed by x-ray studies that solid gallium dichloride has the structure $Ga^{+}[GaCl_4]^{-}$ in the crystal. Further subsidiary evidence is the fact that cerium metal cannot be obtained by electrolysis of pure cerium chloride from a cell without a diaphragm, while it is easily obtained from a solution of $CeCl_3$ in alkali halides. If $CeCl_3$ is an associated liquid which may be described by a formula such as $[CeCl_2]^{+}[CeCl_4]^{-}$ then electrolysis will produce initially $Ce^{+}[CeCl_4]^{-}$, probably by reduction of the less completely coordinated cations, and not cerium, since the $Ce^{3+} \rightarrow\rightarrow Ce^{1+}$ potential is noble by about 0.7 v to that of $Ce^{3+} \rightarrow\rightarrow Ce^{0}$. However, dilution with alkali halides (i.e., KCl) would probably give a liquid which may be formulated $K^{+}[CeCl_4]^{-}$ and allow the direct reduction of $[CeCl_4]^{-}$ to Ce^{0}. Taking the literature value (13) for the potential of the Ce^{3+}/Ce^{0} half-cell (−2.9 v)[3] and the authors' value for the Ce^{3+}/Ce^{1+} half-cell (−2.2 v), then the potential for the Ce^{1+}/Ce^{0} half-cell should be −4.3 v, a value much less noble than either of the other two reactions. This indicates that where oxidation-reduction cycling of $Ce^{1+} \rightarrow\rightarrow Ce^{3+}$ in a cell is possible, cerium metal cannot be expected to be formed by reduction of either the monovalent or trivalent ion.

The formulation of $CeCl_3$ as $[CeCl_2]^{+}[CeCl_4]^{-}$ while purely speculative at this time is in line with suggestions by Yaffe and Van Artsdalen (18) regarding other rare earth halides, and also consistent with the increase in conductance to approximately that of NaCl, which is observed on adding cerium to the trihalide.

The flattening of the curve in Fig. 4 at high concentrations of monovalent cerium in the solution is apparently a buffering effect which the authors have not yet been able to explain. A suitable explanation would involve the postulation of a reservoir for Ce^{1+} in a complex ion in an un-ionized particle or as suggested by Flood and Hill (19) for Fe_2O_3-FeO systems in vacancies in the structure. Alternatively, the buffering effect may merely result from the variation of activity of the potential-determining ions with concentration, so that at high concentrations the ratio of the activities of the oxidized and reduced ions remains constant. The buffering would also be found if the system in this region were not actually a single phase as is indicated by the published phase diagram. Studies of the phase diagram, of conductance, and of density now in progress may assist in accounting for the behavior in this buffered region.

[3] If one considers the chlorine electrode as a reference zero in metal/metal chloride/chlorine, graphite cells, then the measured emf or the calculated decomposition potential for the chloride is numerically equal to the potential of the half-cell appropriate to the metal electrode.

Summary

The emf of the cell $Ce|CeCl_3(1-x)Ce(x)||CeCl_3|Cl_2$ (graphite) has been measured over the temperature range 820°-940°C from a mole ratio of cerium to cerium chloride of 0.018-0.333. The potential of the saturated cell is 2.2005 v at 820°C and 2.1225 v at 940°C, the temperature coefficient of emf being −0.68 mv/°C over this temperature range. Over a concentration range from 33.3 molar % to 8.67 molar % Ce, the emf of the cell remains constant, while with less cerium a decrease in potential in agreement with a Nernst slope for a 2-electron change is observed. It is concluded that the solution of Ce in $CeCl_3$ contains a subhalide consisting of monovalent and trivalent cerium ions, the probable formula of which is $Ce^{+}[CeCl_4]^{-}$. Preliminary measurements indicate that the saturated solution is a typical ionic conductor with a conductance of 3.76 $ohms^{-1}$ cm^{-1} at 840°C.

Acknowledgments

The authors wish to express their thanks to E. R. Van Artsdalen, R. Didchenko, and L. M. Litz for many enlightening discussions, and to B. Flashman for considerable experimental assistance during the course of the work.

Manuscript received Sept. 3, 1957. This paper was prepared for delivery before the New York Meeting, April 27-May 1, 1958.

Any discussion of this paper will appear in a Discussion Section to be published in the December 1958 JOURNAL.

REFERENCES

1. D. D. Cubicciotti, *J. Metals*, **5**, 1106 (1953).
2. D. D. Cubicciotti and C. D. Thurmond, *J. Am. Chem. Soc.*, **71**, 2149 (1949).
3. D. D. Cubicciotti, *ibid.*, **71**, 4119 (1949).
4. H. R. Bronstein and M. A. Bredig, Abstract of paper presented at AIME Convention, New Orleans, Feb. 1957.
5. M. A. Bredig, J. W. Johnson, and W. T. Smith, *J. Am. Chem. Soc.*, **77**, 307 (1955).
6. M. A. Bredig, H. R. Bronstein, and W. T. Smith, *ibid.*, **77**, 1454 (1955).
7. J. D. Corbett and S. Von Winbush, *ibid.*, **77**, 3964 (1955).
8. K. Grjotheim, F. Grönwold, and J. Krogh-Moe, *ibid.*, **77**, 5824 (1955).
9. R. Lorenz. "Die Electrolyse Geschmolzener Salze," W. Knapp-Halle A-S (1906).
10. C. Wagner, *Z. Physik. Chem.*, **21B**, 36 (1933).
11. E. D. Eastman, B. S. Fontana, *et al.*, USAEC TID-5212 14-24 (1955).
12. S. Senderoff and G. W. Mellors, To be published.
13. W. J. Hamer, M. S. Malmberg, and B. Rubin, *This Journal*, **103**, 8 (1956).
14. L. Brewer, *et al.*, Paper 6, page 76 et seq. "Chemistry and Metallurgy of Miscellaneous Materials: Thermodynamics," L. L. Quill, Editor, National Nuclear Energy Series.
15. K. Kiukkola and C. Wagner, *This Journal*, **104**, 308 (1957).
16. L. A. Woodward, G. Garton, and H. L. Roberts, *J. Chem. Soc.*, **1956** 3723.
17. G. Garton and H. M. Powell, *J. Inorg. and Nucl. Chem.*, **4**, 84 (1957).
18. I. S. Yaffe and E. R. Van Artsdalen, To be published.
19. H. Flood and S. G. Hill, *Z. Elektrochem.*, **61**, 18 (1957).

Kinetics of the Thiosulfate-Bromoacetate Reaction in the Presence of Electrolytes

Gerald Corsaro and Ronald W. Smith

Department of Chemistry, The University of Akron, Akron, Ohio

and

Howard L. Stephens

Institute of Rubber Research, The University of Akron, Akron, Ohio

ABSTRACT

The reaction between thiosulfate and bromoacetate ions in solvent mixtures of different dielectric constant and in the presence of added salts fails to give results conforming to the predictions of the Brönsted primary salt effect. The deviation from theory is particularly high in solvents of low dielectric constant and in the presence of higher valence type electrolytes. A mechanism for the over-all reaction is proposed to account for the apparent abnormalities. New experimental data are added to those previously obtained and are correlated with the Brönsted-Christiansen-Scatchard theoretical expressions which relate the log of the molar reaction rate constants to the dielectric constant of the solvent mixture in which reaction takes place, the ionic strength of the solutions making up the reaction mixture, and the size and charge of the intermediate complex assumed to be formed in ionic reactions. The essential condition in the postulated mechanism is that the reaction proceeds through the formation of a complex or ion pair between the added cation and thiosulfate ion, followed by reaction of this complex with bromoacetate ion.

The reaction between bromoacetate and thiosulfate ions in several solvent systems has been investigated extensively (3-10). The conclusions reached by Ciapetta and Tomilinson (10) are pertinent to the remarks to be made in the present discussion. They may be summarized as follows.

(*A*) Specific solvent effects are minor. Observed rate constant data obtained with different isodielectric constant solvents, but with identical concentrations of reactants and added salt, are of the same order of magnitude.

(*B*) Strontium and calcium nitrate mixed with reactants produce high rate constants. Rate constants level off to almost constant values when these salts are present in excess of the reactants.

(*C*) When lanthanum nitrate is the added salt, reaction rate constants are as high as one hundredfold times those anticipated from the Brönsted-Christiansen-Scatchard theoretical expressions (1,2). When the reaction is allowed to take place in solvents of low dielectric constant, the rate constants increase in value with increase in the added salt concentration, reaching a maximum when the added salt concentration equals that of reactants, then fall off with further increases in added salt.

(*D*) LaMer and Davis (3) have shown that when solvents range in dielectric constant from 20 to 35 so that constant DT values are obtained, the observed energies of activation for the reactions with added salt are the same as those in which salt addition is absent. They concluded that abnormal rate constants were the result of certain electrostatic attractions leading to possible ion pair formations. Ciapetta and Tomilinson postulated an ion pair $(LaS_2O_3BrAc)^o$ since they observed that the maximum in the rate constant value was usually obtained when the salt concentration added with reactants was equal to that of the reactants. They concluded further that rate constants were lower in the presence of greater concentrations of added salt because lanthanum ions would compete with each other for the formation of this complex.

If electrostatic attractions influence the course and rate of reaction, it is also reasonable to assume that a complex or ion pair could form between the added cation of the salt and thiosulfate ion, and this in turn would react with bromoacetate ion. Furthermore, the complex postulated by Ciapetta and Tomilinson would be specific for those reaction studies involving only lanthanum nitrate additions, and thus would provide no over-all explanation for the effect of other valence type salts which also produce deviation from predicted results.

A reaction mechanism can be written:

$$M^{+n} + S_2O_3^{=} \rightarrow (M\,S_2O_3^{=})^{n-2} \qquad \text{(I)}$$

$$(M\,S_2O_3^{=})^{n-2} + BrA\bar{c} \rightarrow [\text{Complex}]^{Z_a+Z_b} \qquad \text{(II)}$$

$$[\text{Complex}]^{Z_a+Z_b} \rightarrow \bar{Br} + CH_2COOS_2O_3^{-} + M^{+n} \qquad \text{(III)}$$

M^{+n} is the cation of the added salt with valence charge $+n$, and Z_a, Z_b the valence charge of the ion pair and bromoacetate ion, respectively. Since, according to this mechanism, the cation is regenerated

in the slow step of the over-all reaction, a rate expression can be written:

$$\frac{-d[S_2O_3^{=}]}{dt} = Kf(M) \cdot [\text{Reactant}]^2 = k[\text{reactant}]^2 \quad \text{(IV)}$$

In this expression the term [reactant] represents equimolar concentration of thiosulfate and bromoacetate ions, k the observed second order rate constant, and $f(M)$ a function of the added salt concentration. This function should represent [M] raised to a fractional power $1/X$, representing the extent to which the added cation concentration takes part in ion pair formation with thiosulfate ion concentration. Then K equals $k/[M]^{1/x}$.

If one assumes that [M] in the above expressions is limited to salt concentrations less or equal to that of reactants, then the constancy represented by $k/f(M)$ will be limited to added salt concentrations equal to that of reactants, or less. There is no specific way of predicting the actual fraction of salt which enters into ion pair formation, but this fraction may be approximately deduced from the rate constant data.

The discussion in this paper includes some of the data reported by Ciapetta and Tomilinson whose work involved the use of solvent mixtures containing 72.2% by weight isopropyl alcohol with water which corresponds to a dielectric constant value of 30. The present reported results involve mixtures of 10 and 40% ethyl alcohol by weight with water and dielectric constant values of 72 and 55, respectively. To avoid repetition of solvent description, only the dielectric constant value is designated hereafter.

Experimental

The reaction rate between thiosulfate and bromoacetate was followed by titration of residual thiosulfate with 0.01N iodine solution. The reaction mixture was prepared by mixing weighed amounts of bromoacetic acid in the chosen solvent mixture, equilibrating this with previously standardized NaOH solution, also prepared in the same solvent mixture, and then diluting the solution to twice the molar concentration for the bromoacetate ion concentration used in the run. The sodium thiosulfate was prepared from a standard thiosulfate solution and mixed with the appropriate concentration of the salt investigated. After bringing the two separate solutions to thermal equilibrium, they were mixed and the reaction rate was followed by taking samples at specified intervals of time. The latter procedure involved tripping the stop watch at the instant of mixing the two prepared solutions. About one minute before a specified interval of time, a sample analysis was withdrawn from the reaction vessel. At the instant the time interval was completed excess 0.01N iodine solution was run into the sample. Back titration with 0.01N thiosulfate was then carried out. Blank runs with iodine on samples of solvent were made to make corrections for end point detection using the starch indicator. Volume ratios between thiosulfate and iodine solutions were made at the beginning of each separate run. Rate constants were calculated using the expression:

$$k = \frac{x}{at[a-x]}$$

where a is the initial reactant concentration of thiosulfate ion and x is the amount reacted in time t.

For thorium nitrate additions, it was observed that only plots of $1/[S_2O_3^{=}]^2$ vs. time, where $[S_2O_3^{=}]$ is the residual thiosulfate concentration, gave linear plots. Rate constants were calculated by the expression for third order reactions:

$$k = \frac{x}{2at[a-x]^2}$$

The average values of second and third order calculated rate constants were compared with the values of $1/[S_2O_3^{=}]$ vs. time and $1/[S_2O_3^{=}]$ vs. time plots from whose slopes the rate constants can be evaluated. Typical rate data with lanthanum and thorium nitrate are summarized in Tables I and II. Al-

Table I. Typical rate data with lanthanum nitrate additions (D=72)

$[BrA\bar{c}] = [S_2O_3^{=}] = 0.002M$ $[La] = 0.0015M$

t Min	I_2 ml	$S_2O_3^{=}$ ml	I_2 ml net	$[S_2O_3^{=}]$	k Liter/moles × sec
5	12.67	3.66	9.23	0.001957	3.25
15	12.77	4.33	8.70	0.001844	3.22
30	11.41	3.65	7.78	0.001678	3.19
45	9.56	2.30	7.40	0.001569	3.05
60	9.41	2.70	6.87	0.001456	3.12

Blank with 0.01N I_2 = 0.14 ml. Results above corrected.

Table II. Typical rate data with thorium nitrate additions (D=72)

$[BrA\bar{c}] = [S_2O_3^{=}] = 0.002M$ [Thorium] = 0.0015M

t Min	I_2 ml	$S_2O_3^{=}$ ml	I_2 ml net	$[S_2O_3^{=}]$	$k \times 10^{-4}$
5	6.85	1.30	5.55	0.001187	2.90
15	4.82	1.18	3.72	0.000796	3.19
30	4.76	2.20	2.71	0.000579	3.50
45	3.35	1.15	2.27	0.000466	3.52
60	3.26	1.21	2.13	0.000456	3.09

Table III. Data from Ciapetta and Tomilinson. Calcium and strontium nitrate additions (D=30)

	$[S_2O_3^{=}] = [BrA\bar{c}] = 0.005M$		0.003M Reactants		
M (C_a)	k Liter/moles × sec	M (S_r)	k Liter/moles × sec	M (C_a)	k Liter/moles × sec
0.00236	1.98	0.00204	1.62	0.00293	2.76
0.00580	3.17	0.01206	3.04	0.00597	3.60
0.01452	3.82	0.01917	3.77	0.01019	3.70
0.01885	4.01	0.02893	4.09	0.01451	3.89
0.02320	3.85	0.03624	3.82	0.02327	3.54
0.04352	3.85	0.04826	3.92	0.03480	3.48

though times up to 60 min are shown in these tables, in some cases times of reaction up to 1300 min were taken. A titration error of 0.05 cc 0.01*N* iodine is equivalent to the average deviation shown.

Data in Tables III-VII represent results of the present investigation and those taken in part from the work of Ciapetta and Tomilinson (10). Data summarized in the remaining tables are those used for the plots in Fig. 1-8.

Discussion of Results

According to Brönsted-Christiansen-Scatchard (1, 2) the molar rate constant for an ionic reaction in dilute solution for reaction between ions of Z_a and Z_b charges is given by:

$$\log k = \log k'_o - \frac{Z_a Z_b E^2 N}{DRT} \cdot \frac{1}{r_a + r_b} + \frac{Z_a Z_b E^2 N}{DRT} \cdot \frac{\kappa}{1 + ai\kappa} \qquad \text{(V)}$$

where κ is the Debye-Hückel constant given by:

$$\kappa = \left[\frac{8\pi \ E^2 u}{DRT \cdot 1000} \right]^{1/2} \qquad \text{(VI)}$$

and the remaining terms have their usual significance. According to Amis (13) the Debye first approximation parameter ai, and the term $r_a + r_b$, the distance of closest approach for ions before they react, may be taken as equal in magnitude.

The term, log k'_o represents the reaction rate constant at infinite dielectric constant. The Brönsted salt effect is included in this expression since log k vs. $u^{1/2}$ should give a linear relation according to expression (V). The Brönsted equation for primary salt effect alone may be written in its limiting form as:

$$\log k = \log k_o + 2A \cdot Z_a \cdot Z_b (u)^{1/2} \qquad \text{(VII)}$$

where A is the Debye-Huckel constant obtained from

$$A = \frac{1.824 \times 10^6}{(DT)^{3/2}} \qquad \text{(VIII)}$$

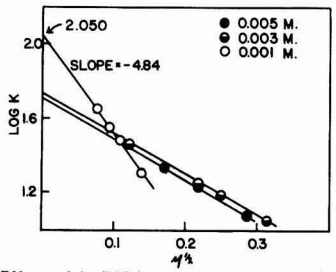

Fig. 1. Effect of $La(NO_3)_3$ on rate constant values in solvents, D = 30. [La] equal and in excess of [reactants]. Data from Table VIII.

Table IV. Data from Ciapetta and Tomilinson. Effect of lanthanum nitrate additions (*D*=30)

M (La)	$[BrAc^-] = [S_2O_3^=] = 0.005M$ k	$k/M \times 10^{-3}$
0.00180	9.78 ± 0.04	5.43
0.00299	17.4 ± 0.4	5.67
0.00354	19.7 ± 0.1	5.56
0.00474	23.3 ± 0.2	5.00
0.00596	22.7 ± 0.3	—
0.00956	17.7 ± 0.2	—
0.01194	15.4 ± 0.1	—
0.01792	11.1 ± 0.1	—
	$[BrAc^-] = [S_2O_3^=] = 0.003M$	
M (La)	k	$k/M \times 10^{-3}$
0.00095	9.34 ± 0.01	9.83
0.00237	24.8 ± 0.1	10.40
0.00343	29.9 ± 0.1	9.00
0.00473	22.6 ± 0.1	—
0.00593	21.9 ± 0.3	—
0.00953	14.8 ± 0.2	—
0.01480	12.1 ± 0.3	—
0.02621	9.19 ± 0.05	—

Table V. Effect of lanthanum nitrate additions on the bromoacetate-thiosulfate reaction in 10% ethyl alcohol (*D*=72)

M (La)	$u^{1/2}$	$(BrAc^-) = (S_2O_3^=) = 0.002M$ k	log k	$k/M^{1/2}$
0.0005	0.097	1.51 ± 0.04	0.179	67.4 ± 1.8
0.00075	0.101	2.24 ± 0.06	0.350	81.7 ± 2.2
0.0010	0.104	2.56 ± 0.05	0.408	84.1 ± 1.6
0.0015	0.111	3.28 ± 0.06	0.516	84.8 ± 1.7
0.00175	0.115	3.69 ± 0.22	0.567	88.3 ± 5.2
0.002	0.119	3.78 ± 0.18	0.577	84.6± 4.0

Table VI. Effect of lanthanum nitrate additions on the bromoacetate-thiosulfate reaction in 40% ethyl alcohol (*D*=55)

M (La)	$u^{1/2}$	$(BrAc^-) = (S_2O_3^=) = 0.002M$ k	log k	$k/M^{1/2}$
0.0005	0.097	6.32 ± 0.19	0.801	282 ± 8.4
0.00075	0.101	9.70 ± 0.06	0.987	354 ± 2.1
0.0010	0.104	11.19 ± 0.04	1.049	354 ± 1.2
0.00125	0.108	12.65 ± 0.11	1.102	357 ± 3.1
0.00175	0.115	14.49 ± 0.23	1.161	352 ± 5.5
0.0019	0.117	15.48 ± 0.31	1.499	355 ± 2.1
0.004	0.161	13.51 ± 0.27	1.131	213 ± 4.2
0.006	0.194	11.87 ± 0.06	1.074	153 ± 0.9
0.008	0.223	10.47 ± 0.21	1.029	117 ± 2.3

Table VII. Effect of thorium nitrate additions on the bromoacetate-thiosulfate reaction in 10% ethyl alcohol (*D*=72)

M (Th)	$[BrAc^-] = [S_2O_3^=] = 0.0005M$ k, $\frac{\text{Liter}^2}{\text{mole} \times \text{min}}$	log k	$k/M \times 10^{-7}$
0.0005	1,150,000	6.060	—
0.001	1,030,000	6.012	—
0.002	660,000	5.819	—
	$[BrAc^-] = [S_2O_3^=] = 0.001M$		
0.0005	16,000	4.204	32.0
0.0001	34,000	4.532	34.0
0.0002	65,000	4.813	32.5
0.0005	152,000	5.185	30.4
0.001	318,000	5.502	31.8
0.002	303,000	5.482	15.1
0.006	148,000	5.170	2.8
	$[BrAc^-] = [S_2O_3^=] = 0.002M$		
0.0005	9,300	3.968	18.6
0.001	21,100	4.324	21.1
0.0015	31,000	4.491	20.6
0.00175	36,800	4.566	21.0
0.002	41,500	4.618	20.7
0.004	27,700	4.443	6.9
0.006	18,000	4.255	3.0
0.008	15,400	4.215	2.0

The term log k_o in the Brönsted equation represents the log of the reaction rate constant at zero ionic strength and therefore zero κ. The log k_o may be obtained from the experimental data by extrapolating the linear plots of log k vs. $u^{1/2}$ to zero ionic strength. According to expression (V) a plot of these extrapolated log k_o values for solvents of different dielectric constant plotted against $1/D$ should give linear curves.

By the new mechanism described in expressions (I), (II), and (III), reaction rates should increase when the ion pair concentration increases. The portion of a plot involving the log of the molar reaction rate constant vs. the square root of the ionic strength up to ionic strengths equivalent to added salt concentrations equal to that of reactants cannot then be interpreted as the influence of ionic strength increase on the thiosulfate-bromoacetate ion reaction. This portion of the plot reflects only the increase in rate as a function of increase in reactant concentration represented by increasing amounts of ion pair formed as more and more salt is added. Once the maximum concentration of ion pair has formed, further increases in salt addition then provide the increase in ionic strength which may influence the reaction taking place between ion pair and bromoacetate ion. The Brönsted salt effect manifests itself by reduction in rate constants if the ion pair is opposite in charge from that of the bromoacetate ion, or rate constant values should remain constant with increase in ionic strength if the ion pair has a zero net charge. Hence, the slopes of the portion of the log k vs. $u^{1/2}$ plots, starting with reactants and added salt at equal concentrations, should be given by expression (VII), namely $2A \cdot Z_a \cdot Z_b$.

Ionic strength values associated with all of the plotted data described in this paper have been calculated by assuming that the ion pair is a distinct ion species. For solvents of D equal to 30, the concentration of the ion pair was assumed equal to that of the added lanthanum nitrate. Thus, for example, when 0.0005M lanthanum nitrate is mixed with 0.001M reactants, it is assumed that 0.0005M ion pair has been formed leaving 0.0005M thiosulfate and the remaining ions. With solvents D equal to 55 and 72, for reasons which will be given, it is assumed that only half the added lanthanum participates in ion pair formation. In these cases a 0.001M addition of salt with 0.001M reactant concentration would produce 0.0005M ion pair leaving 0.0005M lanthanum ion, 0.0005M thiosulfate ion, and the remaining ionic concentrations.

Figure 3 drawn with the data taken from Table VI shows a typical plot of log k vs. $u^{1/2}$ when solvents with D equal to 55 are used with lanthanum nitrate salt additions.

The extent to which added cation takes part in ion pair formation should be greater the lower the dielectric constant of the solvent, the smaller the cation size, and the greater the valence charge of the cation (11, 12).

The fraction, $1/x$, of the added cation concentration which participates in ion pair formation may be determined approximately by noting the fractional power of (M) which gives constant values of $k/(\mathrm{M})^{1/x}$.

With solvent mixtures (D equal to 30), the limited data available in the low salt concentration range from the results of Ciapetta and Tomilinson indicate that almost all the added cation concentration is involved in ion pair formation. Table IV shows that $k/(\mathrm{M})$ values are almost constant. Again it should be emphasized that $k/(\mathrm{M})$ does not give constant values when cation concentration is in excess of reactant concentration. The regeneration of the cation in the slow step of the reaction process provides the means of continuing the reaction so as to give $k/(\mathrm{M})$ constant values.

Tables V and VI show data which indicate that about one-half the added cation concentration takes part in ion pair formation. The first result in each of these tables is low, suggesting that some minimum salt concentration must be present to form the ion pair to its maximum extent.

It has already been stated that, when thorium nitrate is added with reactants, a third order reaction process is apparent. The over-all reaction may be written:

$$2(\mathrm{Th\,S_2O_3})^{++} + \mathrm{BrA\bar{c}} \rightarrow (\mathrm{Complex}) \rightarrow \mathrm{Products} \quad (\mathrm{IX})$$

Plots of the log of the third order rate constants vs. $u^{1/2}$ also produce maxima as illustrated by Fig. 4. The data in Table VII show that, although the solvent mixture represented by these data is that for D equal to 72, $k/[\mathrm{M}]$ values are constant. The effect of high valence charge and small cation size for the Th ion is probably a strong factor in ion pair formation and in changing the over-all reaction process from second to third order. The intermediate complex formed in this reaction may be quite different from that produced with the other salt additions. The size factor is also manifest in the results obtained with strontium or calcium nitrate additions with reactants. First, although the solvent mixture corresponds to D = 30, the rate constants are not as high as when lanthanum nitrate is used. Further, Table III shows that 0.00580M concentration of the smaller calcium ion produces reaction rates which give almost the same rate constant as 0.01206M strontium ion, although both salts eventually give about the same rate constant values at higher concentrations. When log k values are plotted against $u^{1/2}$, therefore, one obtains slopes which are almost zero in value in the region of ionic strengths equiva-

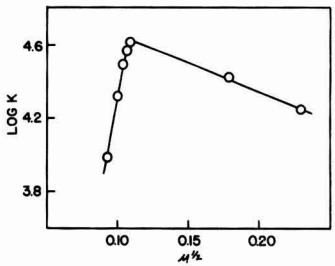

Fig. 4. Effect of $Th(NO_3)_4$ on third order reaction rate constants in solvents, D = 72. Data from Table VII.

lent to concentration in excess of reactants. This result conforms to the views postulated in this paper since the ion pair between Sr or Ca and thiosulfate ion should have a zero net charge. The slight maximum noted from Table III suggests that the reaction between thiosulfate and bromoacetate ions alone, as well as that between ion pair and bromoacetate, contributes to the over-all rate, because of the small fraction of salt participating in ion pair formation.

The preceding discussion should make it apparent that the Brönsted salt effect must be limited to reaction rates obtained when the added salt is equal to or in excess of the reactant concentration. Consider, for instance, the data of Table VIII and Fig. 1. The ionic strengths used are those calculated in the manner described and are for concentrations of added lanthanum nitrate, equal and in excess to that of the reactants. The log k vs. $u^{1/2}$ plots are linear with negative slopes. Values of these slopes are not too different from those calculated by the expression $2A \cdot Z_a \cdot Z_b$.

Figure 2, on the other hand, employs data (Table IX) for the reaction rates obtained when using only those concentrations of added lanthanum nitrate equal to reactants at 0.001, 0.003, and 0.005M concentration. In this case the plot of log k vs. $u^{1/2}$ gives a slope of −4.31 which happens to be identical with that calculated in the manner given.

Following a procedure similar to that employed in making the plot of Fig. 2, the data of Tables X

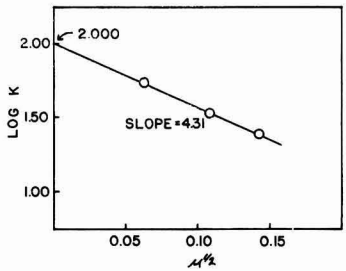

Fig. 2. Effect of $La(NO_3)_3$ on rate constant values in solvents, D = 30. [La] = [reactants] = 0.001, 0.003, and 0.005M. Data from Table IX.

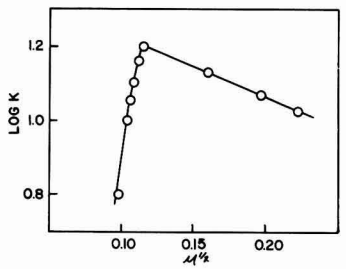

Fig. 3. Effect of $La(NO_3)_3$ on rate constant values in solvents, D = 55. Data from Table VI.

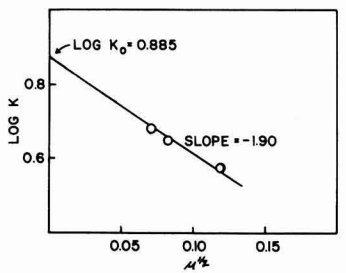

Fig. 5. Effect of $La(NO_3)_3$ on rate constant values in solvents, D = 72. [La] = [reactants] = 0.0005, 0.001, and 0.002M. Data from Table X.

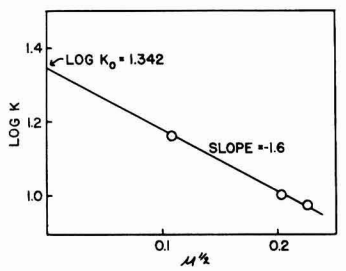

Fig. 6. Effect of $La(NO_3)_3$ on rate constant values in solvents, D = 55. [La] = [reactants] = 0.002, 0.006, 0.008M. Data from Table XI.

Table VIII. Data for Fig. 1. Effect of lanthanum nitrate on the bromoacetate-thiosulfate reaction (D=30) La in excess of reactants.

Reactants [.005M]		Reactants [.003M]		Reactants [.001M]	
$u^{1/2}$	log k	$u^{1/2}$	log k	$u^{1/2}$	log k
0.1207	1.476				
0.1496	1.352	0.1605	1.356	0.0773	1.656
0.1720	1.340	0.2176	1.248	0.0932	1.552
0.2262	1.170	0.2483	1.188	0.1100	1.480
0.2878	1.083	0.3120	1.049	0.1385	1.350
0.3889	0.964				

Table IX. Data for Fig. 2. Effect of lanthanum nitrate on the bromoacetate-thiosulfate reaction (D=30); [La] = [$\overline{BrAc}$] = [S_2O_3]

$u^{1/2}$	log k	[La] = [Reactants]
0.141	1.396	0.005
0.109	1.520	0.003
0.063	1.730	0.001

Extrapolated value of log k_o = 2.000, slope = −4.31

Table X. Data for Fig. 5. Effect of lanthanum nitrate on the bromoacetate-thiosulfate (D=72), [La] = [Reactants]

M (La) (Reactant)	$u^{1/2}$	log k
0.0005	0.0598	0.680
0.0010	0.083	0.645
0.0020	0.119	0.577

Extrapolated value of log k_o = 0.885, slope = −1.90

Table XI. Data for Fig. 6. Effect of lanthanum nitrate on the bromoacetate-thiosulfate reaction (D=55). [La] = [Reactants]

M (La) (Reactant)	$u^{1/2}$	log k
0.002	0.119	1.161
0.006	0.205	1.012
0.008	0.237	0.973

Extrapolated value of log k_o = 1.342, slope = −1.60

Table XII. Data for Fig. 7. Effect of thorium nitrate on the bromoacetate-thiosulfate reaction (D=72). [Th] = [Reactants]

M (Th) (Reactant)	$u^{1/2}$	log k
0.0005	0.054	6.060
0.0010	0.077	5.500
0.0020	0.109	4.060

Slope = −11.7

Table XIII. Data for Fig. 8. Log k_o vs. $1/D$

log k_o	D	$1/D$	Solvent
0.885	72	0.0137	10% EtOH-H_2O
1.342	55	0.0182	40% EtOH-H_2O
2.000	30	0.0333	72% Isopropanol-H_2O

Per cent compositions are by weight.

and XI are plotted in Fig. 5 and 6. The linear plots of log k vs. $u^{1/2}$ have slopes of −1.90 and −1.60 compared to calculated values of −1.14 and −1.74. These data correspond to solvents of D equal to 72 and 55, respectively. Although these values do not coincide with theory, the signs of the slopes are significant, and deviation from theory may be accounted for by the fact that, in solvents of high dielectric constant, the ion pair participation is not as complete as with cases of low solvent dielectric constant values. Similar data taken for reactions carried out with thorium nitrate additions as given in Table XII and plotted in Fig. 7 show that log of the third order rate constants vs. $u^{1/2}$ also give negative slopes, but of much higher magnitude than the others. However, the present Brönsted theoretical effect is derived on the basis of a bimolecular mechanism and cannot be applied to third order reactions. The similarity of results between lanthanum and thorium nitrate additions is striking, and suggests that similar rate expressions can be derived for reactions, described by expression (IX).

Expression (V) indicates that for log k_o vs. $1/D$, linear plots with slopes equal to

$$S = \frac{-Z_a \cdot Z_b \cdot E^2 N}{2.303 \cdot r \cdot RT} \qquad (X)$$

should be obtained. The values of log k_o are those obtained by extrapolating the plots of log k vs. $u^{1/2}$ to zero ionic strength. These values are listed with the tabulated data already described and are also shown in the Fig. 2, 5, and 6. Since as stated, the value of a_i and $r_a + r_b$ may be taken equal, the value of r in expression (X) is equal to the size of the intermediate complex assumed to be formed in ionic reactions. E is the electronic charge, Z_a and Z_b the valence charge of the ion pair and bromoacetate ion, respectively, and the remaining symbols have their usual significance.

The plot of the log k_o values vs. $1/D$ is shown in Fig. 8. This is not strictly linear because of the character of the deviations mentioned above, but the average slope is positive at a value of 75. The value of r using this slope is 3.3×10^{-8} cm. This value compares with values of r calculated for the ammonium ion-cyanate ion reaction carried out in solvent mixtures of methyl and ethyl alcohol with water. Results reported by Svirbely and Schramm and Lander and Svirbely (14, 15) are 2.2×10^{-8} and 2.5×10^{-8} cm for the two solvent mixtures, respectively. The effect of univalent cations on the reaction has been investigated by several workers and is included in most of the reference work already cited. The general conclusions seem to indicate that the order of departure from theory is Li > Na > K > Cs. Results, particularly with solvents of low dielectric constant, show that the largest unsolvated ion size gives results which best approach theory. If solvation of the smaller alkali ion is diminished in solvents of low dielectric constant, then ion pair participation would have the effect of reducing the net negative charge of the thiosulfate ion. The larger ions, K and Cs, should produce more closely the theoretical effect of ionic strength increases on the thiosulfate-bromoacetate reaction without ion pair formation. Results obtained by the present authors with tetramethyl ammonium salts and ammonium chloride do show that the values of slopes predicted by the Brönsted expression (V) are approached. This work is incomplete however, and will be reported in a later publication.

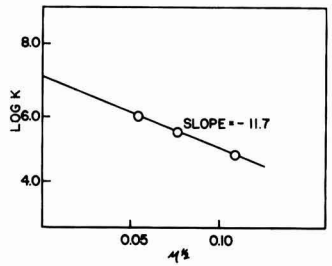

Fig. 7. Effect of $Th(NO_3)_4$ on third order reaction rate constant values in solvents, D = 72. [Th] = [reactants] = 0.0005, 0.001, and 0.002M. Data from Table XII.

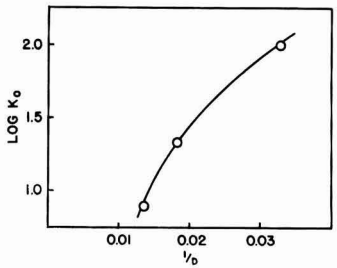

Fig. 8. Log k_o vs. 1/D. Log k_o values obtained by extrapolation to u = o. See Fig. 2, 5, and 6.

Conclusions and Summary

The high rate constants observed for the reaction between bromoacetate and thiosulfate ions in the presence of higher valence electrolytes may be attributed to the fact that the actual reaction is between a complex, formed by the addition of cation with thiosulfate ion, and bromoacetate ion. Since the cation is regenerated during the slow step of the reaction, the rate of the reaction is proportional to concentrations of added cation, or some function of

concentration of cation, until the latter concentration is equal to that of equimolar reactants. Increases in cation concentration beyond this value then cause the reaction rate to decrease in conformity with the Brönsted effect since the reactant species are oppositely charged. All of the observed rate constants and plots of log k vs. $u^{1/2}$ give slopes of the proper sign when the reaction mechanism is viewed in this manner; the values of slopes obtained are, in some cases at least, very close to the theoretical values. It is emphasized however, that these slopes show good agreement with theory only when the ionic strength is increased by equimolar increases in reactants and added salt. This suggests that the ionic strength principle, when mixed electrolytes are involved, may be inadequate to express the true ionic strength of such mixtures.

The observed data also demonstrate that ion pair formation, complex formation, or the increase in covalent nature of the bond between cation and anion, is favored by low dielectric constant of the solvent, small cation size, and high charge on the cation. The over-all mechanism outlined in this paper explains the previously observed conclusions of several investigators that deviations from theory were always greater, the lower the dielectric constant of the solvent in which reaction takes place.

The use of ionic reaction rates of this type may be used as a tool to detect possible ion association, although this obviously would be limited to ionic species capable of undergoing measurable reaction rates.

Manuscript received May 8, 1957. This paper was prepared for delivery before the Washington Meeting, May 12-16, 1957.

Any discussion of this paper will appear in a Discussion Section to be published in the December 1958 JOURNAL.

REFERENCES

1. G. Scatchard, *J. Am. Chem. Soc.*, **52**, page 52 (1930), *Chem. Revs.* **10**, 229 (1932).
2. J. A. Christiansen, *Z. Physik. Chem.*, **113**, 35 (1924).
3. H. G. Davis and V. K. LaMer, *J. Chem. Phys.*, **10**, 585 (1942).
4. A. N. Kappana, *J. Indian Chem. Soc.*, **51**, 3341 (1929).
5. V. K. LaMer, *J. Franklin Inst.*, **225**, 709 (1938).
6. V. K. LaMer and R. W. Fresden, *J. Am. Chem. Soc.*, **54**, 2351 (1932).
7. V. K. LaMer and N. E. Kammer, *ibid.*, **57**, 2669 (1935).
8. J. Slator, *J. Chem. Soc.*, **87**, 481 (1905).
9. H. M. Tomilinson and F. G. Ciapetta, *Ind. Eng. Chem. Anal. Ed.*, **13**, 539 (1941).
10. F. G. Ciapetta and H. M. Tomilinson, *J. Phys. Chem.*, **55**, 429 (1951).
11. K. Fajans, *Naturenissenschafren*, **11**, 165 (1923).
12. G. H. Cartledge, *J. Am. Chem. Soc.*, **50**, 2855 (1928).
13. E. S. Amis, "The Kinetics of Chemical Change in Solution," Chap. IV, MacMillan, New York (1949).
14. W. J. Svirbely and A. Schramm, *J. Am. Chem. Soc.*, **60**, 330 (1938).
15. J. Lander and W. J. Svirbely, *ibid.*, **60**, 1613 (1938).

Technical Note

Analysis of Manganese Dioxide with Special Reference to Electrodeposited Oxide on Graphite

Akiya Kozawa and W. C. Vosburgh

Department of Chemistry, Duke University, Durham, North Carolina

There is reason for questioning the analytical data in previous investigations (1, 2) for electrodes of electrodeposited MnO_2 on graphite. The analyses have led to the formula $MnO_{1.9}$ for freshly prepared and well washed electrodes. This is poorer in available oxygen than expected for electrolytic MnO_2 (3, 4). Also, the available oxygen as determined by the H_3AsO_3 method varies with the concentration of the reagent. The data obtained with 0.1N H_3AsO_3 were accepted because the results were reproducible, and the $FeSO_4$ method gave similar results, and because a sample of MnO_2 from the National Bureau of Standards was correctly analyzed.

The preparation of the electrodes has been described elsewhere (5). Briefly, they consisted of a graphite rod of 4 mm diameter covered for 51 cm of its length with about 0.2 mmole of electrodeposited MnO_2. Most of the rod above the seal was covered with a glass tube sealed to the graphite by glyptal cement, with only the top portion exposed for contacts. The area covered by MnO_2 was 8 cm^2.

Evidence of error—That the previous analyses of electrodes were in error was indicated when some MnO_2 which had been electrodeposited on Karbate rods gave $MnO_{2.0}$ on analysis. This pointed to the graphite rods as the source of the error. The significant difference between the two kinds of rod seems to be that graphite is porous, while Karbate is not.

The volume of the pores in the graphite rods used was estimated by determining the Cl^- retained from a chloride solution of known concentration after superficial washing. The volumes ranged from 12 to 20% of the volumes of the rods, and the presence of electrodeposited MnO_2 made no measurable difference.

Another indication of error in the previous results is that when the available oxygen is determined in MnO_2 on graphite by treatment with an

Table I. Analysis of electrodeposited MnO_2 on graphite rods after standing 15 hr in solutions of various salts

Solution in pores	No. of samples	x in MnO_x
4M NH_4Cl	2	1.81 ± 0.02
0.2 to 1M NH_4Cl	3	1.95 ± 0.01
4M NaCl	1	2.00
2M $(NH_4)_2SO_4$ or 1M Na_2SO_4	2	2.00
1M KOH	1	1.67
4M NH_4Cl or 1M KOH, washed	2	1.96 ± 0.01

excess of standard $FeSO_4$ at room temperature instead of at boiling temperature the results are higher. This is illustrated in Table I. Electrodes that had been immersed in various salt solutions for 15 hr were analyzed, because certain salts lead to very low results when the MnO_2 is dissolved by a hot reducing agent unless washed out previous to analysis (2). After titration of the excess $FeSO_4$ by $KMnO_4$, the total Mn was determined by the bismuthate method, with correction for the $KMnO_4$.

In the available oxygen determination the MnO_2 was dissolved by 10 ml of 0.1*N* $FeSO_4$ and 1.8M H_2SO_4 at room temperature (about 25°C) with no protection from air. The electrodes were allowed to stand in test tubes with the $FeSO_4$ solution for 1 or 2 hr, without stirring. Under these conditions the surface has the appearance of bare graphite after 40 min. One minor source of error for which no correction was made at this time was the $FeSO_4$ and $MnSO_4$ retained by the graphite rod after ordinary washing. This would lead to high values of x.

Table I shows that this procedure gives reasonable results for electrodes containing NaCl, $(NH_4)_2SO_4$, and Na_2SO_4 when an estimated 0.03 is allowed for the above error, but NH_4Cl and KOH cause low results. When the NH_4Cl and KOH are washed out, the results are much better, in agreement with previous experience (2). Apparently the combination of NH_4^+ and Cl^- is more harmful than either alone.

Similar experiments using hot $FeSO_4$ (80°-90°C) for the dissolving of the MnO_2 gave lower results varying from 1.57 to 1.98 for x, and $(NH_4)_2SO_4$ gave a considerably lower result than Na_2SO_4 and NaCl. An increase in temperature increases the error from some of the salts, and gives lower results for all.

It may be postulated that a solution of relatively high *p*H is trapped in the pores of the graphite while the exterior of the MnO_2 is in contact with a strongly acid solution. A local-action cell is formed with a high potential cathode. Reduction of the MnO_2 takes place if anything in the pores is oxidizable. Increase in temperature should decrease the overpotentials and favor the local action. If hot 0.025M arsenious acid is the reagent, the local-action cell seems to be able to oxidize considerable water before the MnO_2 is dissolved.

In the analyses of Table I it was observed that 0.4 to 2 ml of gas was evolved when electrodes that had been kept in either NH_4Cl or KOH solution were put into the acid $FeSO_4$ solution. The gas was considered to be the product of the anodic reaction of the local-action cell. Analysis showed that from NH_4Cl the gas was predominantly N_2 and from KOH it contained more O_2 than N_2.

Analysis of MnO_2 *on graphite.*—The accuracy of the analysis with cold $FeSO_4$ solution when applied to MnO_2 on graphite was tested. The available oxygen was determined as for the data of Table I except that following the dissolution of the MnO_2 the graphite rod was kept in 1M H_2SO_4 for an hour for the recovery of Fe^{++} and Mn^{++} in the pores. The two solutions were combined for the titration. Then the total Mn was determined by potentiometric titration (6, 7) and a correction made for the Mn added as $KMnO_4$ in the first titration.

In preparing a solution containing Fe for potentiometric titration of Mn it is best if neutralization of any acid present is done by $Na_4P_2O_7$ alone. However, if there is much acid, it may be partially neutralized by NaOH before addition of $Na_4P_2O_7$. Addition of NaOH after the $Na_4P_2O_7$ is likely to introduce an error.

The result for x in MnO_x for 5 electrodes was 1.955 ± 0.005. The MnO_2 was scraped from seven similar electrodes and analyzed by the same method giving $x = 1.947 \pm 0.005$. The two results are not significantly different and, since the graphite rod could not have affected the second, it is probable that the first is correct.

A third set of analyses was made of MnO_2 deposited on a Pt surface of the same size and shape as the graphite surface. Three samples gave $x = 1.976 \pm 0.002$. This may represent a real difference since the true Pt surface area was less than that of the graphite and the true current density higher, at least initially.

Analysis of precipitated MnO_2 *and ores.*—It would be expected that the use of $FeSO_4$ at room temperature for reduction of MnO_2 would require excessive time. However, if the $FeSO_4$ solution and sample are stirred vigorously, the time for dissolution is less than with a hot solution not stirred. Five different samples of precipitated MnO_2 of 200 mg each were treated with 25 ml of a solution of 0.25M $FeSO_4$ and 1.8M H_2SO_4 at 28°C with stirring by a magnetic stirrer until the last visible particles disappeared. The times required varied from 2 to 10 min.

To test the accuracy of the method, Standard Sample No. 25b, battery grade MnO_2 from the National Bureau of Standards, was analyzed. Seven samples of about 200 mg each were dissolved by 25 ml portions of a solution of 0.25M $FeSO_4$ and 1.8M H_2SO_4 at room temperature. The excess $FeSO_4$ was titrated with 0.02M $KMnO_4$. The solution was then brought to *p*H 6 to 7 either by about 35 g of $Na_4P_2O_7 \cdot 10H_2O$ or partly by KOH and then $Na_4P_2O_7$ and titrated potentiometrically with 0.02M $KMnO_4$. The available oxygen was found to be $16.66 \pm 0.015\%$ and the total manganese $58.40 \pm 0.07\%$ as compared with the certified values 16.67 and 58.35%.

To test the effect of NH_4Cl on the analysis in the absence of graphite, three samples of 25b were treated with 2 ml each of 1M, 2M, and 4M NH_4Cl for 24 hr. Then, without removal of any of the NH_4Cl solution, the $FeSO_4$ reagent was added and the analysis carried out as before, except that $HgSO_4$ was added before titration of the excess $FeSO_4$ to mask the Cl^-. It had been shown that Hg_2SO_4 has

no effect on the potentiometric titration of Mn^{++}. The results of the three analyses showed no effect of the NH_4Cl, the average being $16.64 \pm 0.003\%$ available O and $58.45 \pm 0.08\%$ Mn.

Acknowledgment

This work was supported in part by the Office of Naval Research.

Manuscript received Aug. 12, 1957.

Any discussion of this paper will appear in a Discussion Section to be published in the December 1958 JOURNAL.

REFERENCES

1. W. C. Vosburgh, R. S. Johnson, J. S. Reiser, and D. R. Allenson, *This Journal*, **102**, 151 (1955).
2. S. Hills and W. C. Vosburgh, *ibid.*, **104**, 5 (1957).
3. G. W. Nichols, *Trans. Electrochem. Soc.*, **62**, 400 (1932).
4. W. Buser and P. Graf, *Helv. chim. Acta*, **38**, 828 (1955).
5. A. M. Chreitzberg, Jr., and W. C. Vosburgh, *This Journal*, **104**, 1 (1957).
6. J. J. Lingane and R. Karplus, *Ind. Eng. Chem., Anal. Ed.*, **18**, 191 (1946).
7. R. F. Stalzer and W. C. Vosburgh, *Anal. Chem.*, **23**, 1880 (1951).

FUTURE MEETINGS OF
The Electrochemical Society

New York, N. Y., April 27, 28, 29, 30, and May 1, 1958

Headquarters at the Statler Hotel

Sessions will be scheduled on
Electric Insulation, Electronics (Luminescence and Semiconductors), Electrothermics and Metallurgy, Electrothermics and Metallurgy—Semiconductors Joint Symposium, Electrothermics and Metallurgy—Corrosion Joint Symposium, Industrial Electrolytics, and Theoretical Electrochemistry (including a symposium on "Electrokinetic and Membrane Phenomena")

★ ★ ★

Ottawa, Canada, September 28, 29, 30, October 1, and 2, 1958

Headquarters at the Chateau Laurier

Sessions probably will be scheduled on
Batteries, Corrosion, Electrodeposition (including symposia on "Electrodeposition on Uncommon Metals" and "Chemical and Electropolishing"), Electronics (Semiconductors), Electro-Organics, Electrothermics and Metallurgy, and a symposium on "Films Formed in Contact with Liquids" sponsored by Theoretical Electrochemistry, Battery, and Corrosion Divisions

★ ★ ★

Philadelphia, Pa., May 3, 4, 5, 6, and 7, 1959

Headquarters at the Sheraton Hotel

★ ★ ★

Columbus, Ohio, October 18, 19, 20, 21, and 22, 1959

Headquarters at the Deshler-Hilton Hotel

★ ★ ★

Chicago, Ill., May 1, 2, 3, 4, and 5, 1960

Headquarters at the Lasalle Hotel

★ ★ ★

Houston, Texas, October 9, 10, 11, 12, and 13, 1960

Headquarters at the Shamrock Hotel

★ ★ ★

Papers are now being solicited for the meeting to be held in Ottawa, Canada, September 28-October 2, 1958. Triplicate copies of each abstract (*not exceeding 75 words in length*) are due at the Secretary's Office, 1860 Broadway, New York 23, N. Y., *not later than June 2, 1958* in order to be included in the program. *Please indicate on abstract for which Division's symposium the paper is to be scheduled.* Complete manuscripts should be sent in triplicate to the Managing Editor of the JOURNAL at 1860 Broadway, New York 23, N. Y.

The Electrochemical Society

INSTRUCTIONS TO AUTHORS OF PAPERS

Address all correspondence to the Editor, JOURNAL OF THE ELECTROCHEMICAL SOCIETY, 1860 BROADWAY, NEW YORK 23, N. Y.

FORM

Manuscripts submitted for publication should be in triplicate to expedite review. They should be typewritten, double-spaced, with 2½-4 cm (1-1½ in.) margins.

Title should be brief, followed by the author's name and his business or university connection.

Abstract of about 100 words should state the scope of the paper and give a brief summary of results.

ILLUSTRATIONS

Drawings will be reduced to column width, 8.3 cm (3¼ in.), after reduction should have lettering at least 0.15 cm (1/16 in.) high. Original drawings in India ink on tracing cloth or white paper are preferred. Curves may be drawn on coordinate paper only if the paper is ruled in blue. All lettering must be of lettering-guide quality. See sample drawing on reverse page.

Photographs must be glossy prints and mounted flat.

Captions for all figures must be included on a separate sheet. Captions and figure numbers should not appear in the body of the figure.

General—Figures should be used only when necessary. Omit drawings or photographs of familiar equipment. Figures from other publications are to be used only when the publication is not readily available, and should always be accompanied with written permission for reprinting.

REFERENCES

Literature and patent references should be listed at the end of the paper on a separate sheet, in the order in which they are cited. They should be given in the style adopted by *Chemical Abstracts*. For example:

R. Freas, *Trans. Electrochem. Soc.*, **40**, 109 (1921).

H. T. S. Britton, "Hydrogen Ions," Vol. **1**, p. 309, D. Van Nostrand Co., New York (1943).

H. F. Weiss (To Wood Conversion Co.), U. S. Pat. 1,695,445, Dec. 18, 1928.

UNITS OF MEASUREMENT

Metric units should be used throughout but, where desirable, English units may be given in parentheses.

Corrosion rates in the metric system should preferably be expressed as milligrams per square decimeter per day (mdd), and in the English system as inches penetration per year (ipy).

As regards algebraic signs of potentials, the standard electrode potential for $Zn \rightarrow Zn^{++} + 2e$ is negative; for $Cu \rightarrow Cu^{++} + 2e$, positive.

ABBREVIATIONS

Abbreviations should conform with the American Standards Association's list of "Abbreviations for Scientific and Engineering Terms."

GENERAL

Authors should be as brief as is consistent with clarity, and must omit all material which can be regarded as familiar to specialists in the particular field.

The use of proprietary names, trade-marks, and trade names should be avoided if possible. If used, these should be capitalized so that the owner's legal rights are not jeopardized.

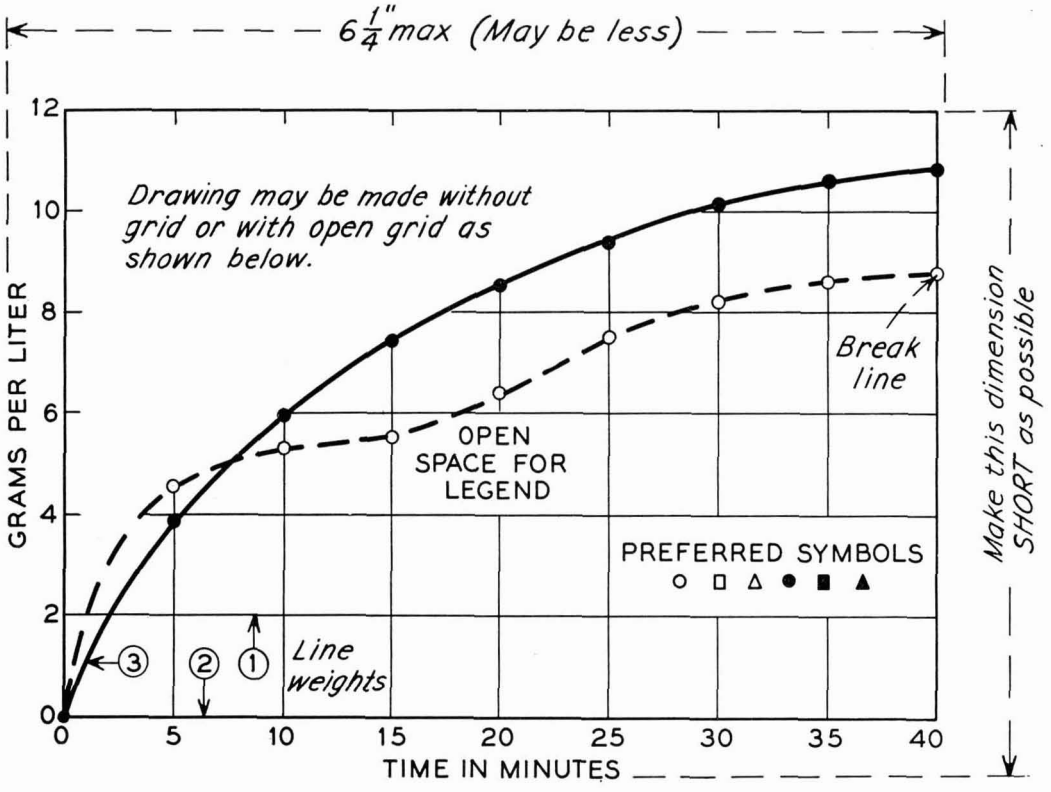

Remarks: Line weight ② is used for borders and zero lines. When several curves are shown, each may be numbered and described in the caption. Lettering is approx. 1/8".

SAMPLE CURVE DRAWING FOR REDUCTION TO $\frac{1}{2}$ SIZE

Karl Friedrich Bonhoeffer[1]

Paul Harteck[2]

I would like to express my appreciation for the great honor of being permitted to accept the Palladium Medal for my deceased friend, K. F. Bonhoeffer. This occasion is very unique since the Palladium Medal, which is perhaps the highest honor which can be bestowed in the field of electrochemistry, is being given to him posthumously. Professor Bonhoeffer himself was regarded in Germany as the most outstanding man in the field of physical chemistry, and his dignity and pleasant personality were likewise esteemed at home and abroad.

I had the privilege of being associated with him for 30 years, first as a pupil and then as a colleague and friend. Born in Breslau in 1899, he grew up in Berlin as a member of a distinguished family of a high cultural level. His father, Geheimrat Bonhoeffer, was Professor of Psychiatry at the University of Berlin.

After World War I, Berlin was one of the leading centers for physics and physical chemistry in the world. Bonhoeffer became influenced by men such as Walter Nernst, Max Planck, and Albert Einstein, but the man who influenced him most was Fritz Haber. In Haber's Institute, Bonhoeffer as a young man in the years 1923-1930 did perhaps his most beautiful work. I have only to mention the titles of his works to recall them to your memory: "Preparations of Hydrogen Atoms and Their Chemical Reactions," "Explanation of the Predissociation Phenomenon," "Investigation of Radicals," especially the "OH Radical in Chemical Equilibrium with Water Vapor at High Temperatures," and "Ortho and Para Hydrogen."

He was full of brilliant ideas and I know that he had to let many of them go simply because he had no time to follow them up. For example, I think he was one of the first people to whom it was clear that, due to the data from band spectroscopy, the gas equilibria could be calculated exactly by means of the Nernst Theorem.

In 1930 Bonhoeffer accepted the Chair in Physical Chemistry at the University of Frankfurt. From this time until his death he was a very hard-working man because the Director of the Institute of Physical Chemistry in Germany carried not only the burden of administration, teaching, and examination, but also practically was responsible for all the research carried on in the institute. I would like to mention that during this period in Frankfurt he did pioneer work in labeling, with heavy hydrogen, organic chemical reactions which led him to problems in physiological chemistry and biological physical problems which became more and more his dominant interest in research. In 1934 he was given the Chair in Physical Chemistry in Leipzig which was a Chair founded by Wilhelm Ostwald who is regarded in Germany as the founder of physical chemistry as a special field in science. Professor Bonhoeffer followed M. LeBlanc, who is, as you know, one of the classicists in electrochemistry. But the decision to go to Leipzig proved to be unfortunate. Wartime in Leipzig was very hard and, as you know, Leipzig is now in the Eastern Zone of Germany. From Leipzig he managed to go to the University of Berlin where he succeeded to the Chair of Nernst and Bodenstein in 1947. From there it was possible for him to return to pure research because he became the Director of the newly founded Institute of Physical Chemistry of the Max Planck Society in Göttingen. This institute was regarded as the legal successor to Haber's Institute in Berlin-Dahlem.

Bonhoeffer had to start with practically nothing in Göttingen and in a few years brought the institute to the forefront of electrochemistry. What he accomplished in these years he told The Electrochemical Society (Spring 1956 San Francisco Meeting) and other groups in the United States just one year ago.

All who saw him one year ago would not have expected such an abrupt end to his life. Obviously, his intensive work and the strain of war and post-war hardships had been too much for him.

Bonhoeffer was married to Greta von Cohananyi. He is survived by three sons and one daughter who brought him much joy. His father-in-law is the famous composer and conductor who lives in this country. However, the entire Bonhoeffer family passed through difficult times and lost several members to the Third Reich after the 20th of July, 1944.

The Electrochemical Society may be interested to know how the Medal will be forwarded to Bonhoeffer's family. Since the German Ambassador in Washington, Dr. Krekeler, was acquainted with Bonhoeffer, also having studied physical chemistry in Bodenstein's Institute 30 years ago, I will personally transfer the medal into his custody. Dr. Krekeler has promised that he will take care that the Medal is presented to Bonhoeffer's family with all the consideration commensurate to such an honor.

[1] Banquet Address at the Buffalo Meeting, October 8, 1957, following presentation of the Palladium Medal to Dr. Paul Harteck who accepted it for the Medalist, Professor Karl F. Bonhoeffer, who died in May 1957.

[2] Dept. of Chemistry, Rensselaer Polytechnic Institute, Troy, N. Y.

Swann, Linford, and Gilbertson to Take Office In New York

As a result of the recent annual election, in which the voting is by mail ballot, Sherlock Swann, Jr., has been elected the new President of the Society; Henry B. Linford, third Vice-President; and Lyle I. Gilbertson has been re-elected Treasurer. They will take office at 8:00 A.M. on Thursday, May 1, 1958, in New York City at the Spring Annual Meeting of the Society.

Dr. Swann, research professor of chemical engineering at the University of Illinois, Urbana, Ill., replaces Norman Hackerman, professor of chemistry, chairman of the department, and director of the Corrosion Research Lab., University of Texas, Austin, Texas. Dr. Hackerman, as Past President, will continue as a member of the Board of Directors.

Henry B. Linford, professor of chemical engineering, Columbia University, New York City, will start the first year of his three-year term as Society Vice-President, and will serve with the two previously elected Vice-Presidents, William C. Gardiner and Ralph A. Schaefer. When he takes office as Society Vice-President, Dr. Linford ends his term as Secretary of the Society, a post which he has held since the spring of 1949.

Lyle I. Gilbertson, director of the Murray Hill Labs. of Air Reduction Co., Inc., Murray Hill, N. J., will begin his second three-year term as Treasurer.

Sherlock Swann, Jr.

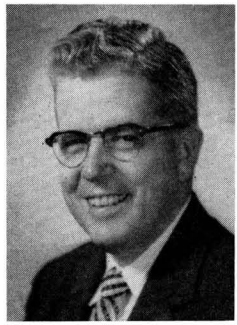

H. B. Linford

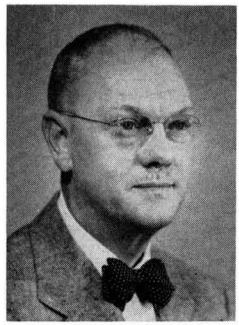

L. I. Gilbertson

New York Convention

As it has done every five years or so, the New York Metropolitan Section of the Society is preparing to welcome members, guests, and their ladies to a busy, interesting, and stimulating convention. As you already know, the headquarters hotel is the Statler, in midtown Manhattan, a thoroughly modern hotel having complete facilities and staff to ensure a smoothly running meeting. If you have not already made your reservation it is suggested that you do so immediately, preferably using the reservation card mailed to members some time ago; be sure to mention The Electrochemical Society Meeting.

The full technical and social program was published in the March issue, and, as usual, reprints in handy pocket size will be available when you register. This program details the many symposia and round-table discussions which constitute the technical aspect of the meeting, as well as the social features and the interesting series of events which have been planned for the ladies.

Richards Memorial Lecture

Dr. J. W. Richards was one of the founders and the first President of The Electrochemical Society. From 1904 to 1921 he was its Secretary and Editor of the TRANSACTIONS.

In 1929 a group of friends and admirers of Dr. Richards established the Joseph W. Richards Memorial Lectureship, the income from which is from time to time used to meet the expenses incurred by "inviting and entertaining" distinguished scientists to address the Society on the results of their work.

At 5 P.M. on Monday, April 28, the 13th Richards Memorial Lecture will be delivered by Dr. Abner Brenner. Dr. Brenner received his B.A. degree from the University of Missouri in 1929, an M.S. from the University of Wisconsin in 1930, and the Ph.D. from the University of Maryland in 1939. Since 1930 he has been on the staff of the National Bureau of Standards where he is now chief of the Electrodeposition Section. One of the country's outstanding younger electrochemists, he has made notable contributions to the study of alloy deposition, the physical properties of electrodeposits, "electroless" plating,

Abner Brenner

electrodeposition of metals from nonaqueous media, and cathode diffusion layers; he has developed several instruments used in testing electrodeposits, notably the widely used "Magne-gage."

Dr. Brenner's subject will be "Electrolysis of Nonaqueous Solutions, with Reference to Metal Deposition." The lecture is scheduled so

that no other sessions conflict with it, because it is felt that all registrants, regardless of their special interests, will want to hear it.

Monday Evening Mixer

The social side of the convention gets under way on Monday evening, April 28, at about 8 P.M., with an informal get-together of a type which has come to be called a "mixer"; whether the word refers to the people or the liquid refreshment is not known. Whatever the connotation, the Committee hopes that all registrants and their ladies will take advantage of the opportunity to meet their friends in congenial surroundings; your registration badge is your ticket.

Tuesday Society Luncheon and Business Meeting

The annual business meeting of the Society will take place on Tuesday, April 29, preceded by luncheon and followed by a talk which should prove of interest to all. The speaker will be Mr. Edwin Diamond, who is editor of the Science and Space and the Atom departments of *Newsweek* magazine. Mr. Diamond is an outstanding interpreter of science to the public, having won several awards for his efforts in this field; he will speak on "Science, the Press, and the Public."

Tuesday Evening Reception and Banquet

All registrants will want to welcome the newly elected officers of the Society and hear the address by the retiring President, Dr. Norman Hackerman, who has served the Society well during his tenure of office. Cocktails at 6:30 P.M. will be followed by dinner at 7:30. Dress is optional. The New York Committee has planned an unusual menu for this affair—guaranteed not to be conventional "banquet" fare. You'll be glad you came, we think.

In addition to these general functions, there are three Divisional luncheons and the Electronics Division Cocktail Mixer. For details consult the full program in the March JOURNAL. We believe we can assure you a lively week in New York.

Frederick A. Lowenheim,
General Chairman

1958 Gordon Research Conferences

The Gordon Research Conferences for 1958 will be held from June 9 to August 29 at Colby Junior College, New London, N. H.; New Hampton School, New Hampton, N. H.; and Kimball Union Academy, Meriden, N. H.

The Conferences were established to stimulate research in universities, research foundations, and industrial laboratories. This purpose is achieved by an informal type of meeting consisting of scheduled lectures and free discussion groups. Sufficient time is available to stimulate informal discussions among the members of a Conference. Meetings are held in the morning and in the evening, Monday through Friday, with the exception of Friday evening. The afternoons are available for participation in discussion groups as the individual desires. This type of meeting is a valuable means of disseminating information and ideas which otherwise would not be realized through the normal channels of publication and scientific meetings. In addition, scientists in related fields become acquainted and valuable associations are formed which result in collaboration and cooperative effort between different laboratories.

It is hoped that each Conference will extend the frontiers of science by fostering a free and informal exchange of ideas between persons actively interested in the subjects under discussion. The purpose of the program is not to review the known fields of chemistry but primarily to bring experts up to date as to the latest developments, analyze the significance of these developments, and to provoke suggestions as to underlying theories and profitable methods of approach for making new progress. In order to protect individual rights and to promote discussion, it is an established rule of each Conference that all information presented is not to be used without specific authorization of the individual making the contribution, whether in formal presentation or in discussion. No publications are prepared as emanating from the Conferences.

Individuals interested in attending a Conference are requested to send their applications to the Director. Each applicant must state the institution or company with which he is connected and the type of work in which he is most interested. Attendance at each Conference is limited to 100.

The complete program of the Conferences was published in *Science* for February 28.

Requests for attendance at the Conferences, or for any additional information, should be addressed to W. George Parks, Director, Dept. of Chemistry, University of Rhode Island, Kingston, R. I. From June 9 to August 29, 1958, mail should be addressed to Colby Junior College, New London, N. H.

Chemistry and Physics of Metals

Kimball Union Academy
Meriden, N. H.

J. A. Krumhansl, *Chairman*
E. I. Salkovitz and J. W. McClure, *Vice-Chairmen*

August 11

Electronic Structure—General

J. C. Slater—Electron Energy Bands in Metals
A. F. Kip—Cyclotron Resonance
D. H. Tomboulian—Soft X-Ray Valence Band Emission Studies

August 12

Specific Band Determinations

G. Lehman—Band Structure of Uranium and Thorium
J. R. Reitz—Band Structure of Selenium and Tellurium
J. W. McClure—Band Structure of Graphite

Liquid Metals

S. Strauss—Size Effects in Liquid Alloys

August 13

Transport Properties

E. I. Salkovitz—Transport Properties in Dilute Alloys
T. G. Berlincourt—Hall Effect in Metals and Alloys
A. I. Schindler—Band Dependent Properties in Transition Metal Alloys

Elastic Properties of Metals and Alloys

J. R. Reitz—Elastic Constants of Metals and Alloys and Electronic Structure

August 14

Point Defects and Electronic Properties

T. J. Rowland—Nuclear Magnetic Resonance in Copper and Silver Alloys
W. Harrison—Influence of Lattice Disturbances on Point Defect Scattering
L. Roth—Scattering of Bloch Waves
F. J. Blatt—Thermoelectric Power of Noble Metal Alloys

August 15

Special Topics

L. Apker—Recent Progress in Photoelectric Emission

Recapitulation—H. Brooks

Corrosion

Colby Junior College

New London, N. H.

J. E. Draley, *Chairman*

P. M. Aziz, *Vice-Chairman*

July 14-18

The Nature of Metal Surfaces

H. Juretschke—The Atomic Nature of Metal Surfaces

C. S. Smith—Metallography and Corrosion

Adsorption on Metals

J. T. Law—The Adsorption Process on Semiconductors

L. S. Bartell—Optical Studies of Adsorption from Solution

R. T. Gomer—Field and Ion Emission Microscopy

P. W. Selwood—Magnetization and Surface Chemistry

Oxides on Metals

J. V. Cathcart—The Microtopography of Oxide Films on Metals

Jerome Kruger—The Growth of Oxide Films on Copper in Water Containing Oxygen

W. D. Feitknecht—Chemistry of the Corrosion Products Formed on Cu, Cd, Zr, and Fe in Aqueous Solutions

E. A. Gulbransen—Crystal Habits in Localized Corrosion and Oxidation Processes in Relation to Metal Structure

Passivity

Review of Darmstadt Passivity Colloquium and General Discussion on Passivity Mechanisms

Physical Metallurgy

New Hampton School

New Hampton, N. H.

John Frye, Jr., *Chairman*

W. R. Hibbard, Jr., *Vice-Chairman*

Microstructures: Their Origin and Influence on Properties

June 9-13

Special Techniques

H. Wilsdorf—Electron Microscopy

R. M. Fisher—Electron Probe Analyzer

R. Gomer—Emission Microscopy

A. V. Baez—X-Ray Microscopy

Dislocations Studies

W. G. Johnston—Etch Pits

S. A. Kulin—X-ray Techniques

D. C. Robinson—Electron Microscopy

A. R. Lang—Berg-Barrett Techniques

Precipitation and 2nd Phases

J. Cahn—Quantitative Metallographic Techniques

Jack Washburn—Precipitation on Dislocations

John Hilliard—Kinetics of Precipitate Nucleation and Growth

A. J. Kelly—Deformation of Single Crystals of Age Hardened Aluminum Alloy

A. J. Cochart—Role of Second Phases in Creep

Deformation and Fracture

J. R. Low and R. W. Guard—Slip in Iron Alloys

Morris Cohen—Brittle Behavior in Steel

Looking Back at Buffalo

Photographs by Stratton

Top row—left, W. C. Gardiner, C. C. Furnas, and A. T. Hinckley; **center,** G. W. Heise, W. D. Sherrow, R. B. MacMullin, and P. P. Beno; **right,** M. J. Allen and H. B. Linford. **Center row—left,** Dr. and Mrs. W. C. Moore and H. J. Read; **center,** President Norman Hackerman presenting the Palladium Medal to Paul Harteck who accepted it for the late Professor Karl F. Bonhoeffer; **right,** C. A. Hampel, Dr. and Mrs. C. C. Furnas, and Mr. and Mrs. M. E. Bretschger. **Bottom row—left,** Mr. and Mrs. C. G. W. Carlsson; **center,** entertainers; **right,** Mrs. C. L. Faust, Mrs. Lottie Fink, and Mr. and Mrs. Axel Heilborn.

Peter Gibbs—Brittle Fracture of Crystals
Jack Gilman—Dislocations and Fracture

Oxidation and Corrosion

W. D. Forgeng and W. W. Webb—Crystal Growth During Oxidation
Ralph Condit —Sulfurization of Iron
D. Van Rooyen—Oxidation Nucleation
V. J. Albano—Metallic Films
D. Vermilyea—Oxidation Kinetics

Division News

Electro-Organic Division

The Nominating Committee of the Electro-Organic Division of the Society has met and nominated the following for Division officers to be elected in the Fall of 1958:

Chairman—Garrett Thiessen
Vice-Chairman—Milton Allen
Secretary-Treasurer—
Philip J. Elving

H. M. Scholberg, *Chairman*
Nominating Committee

E & M Division High Purity Metals Symposium Scheduled

The Electrothermics and Metallurgy Division of The Electrochemical Society has organized a symposium, entitled "The Preparation, Evaluation, and Uses of High Purity Metals," to be held in conjunction with the Annual Spring Meeting of the Society at the Statler Hotel, New York City, from April 27 through May 1, 1958.

The Electrothermics and Metallurgy Committee, in preparation for the 1958 Spring Meeting has chosen a subject for a symposium that will be of widespread interest to a large number of scientists and engineers engaged in the preparation and utilization of high purity metals for a variety of uses in the electronic, chemical, metallurgical, and associated fields.

Key discoveries in chemical and metallurgical technology, as well as widespread advances in engineering, have increased the need and utilization of high purity materials in many fields.

It was therefore the opinion of the committee that such a symposium covering the rapidly advancing technology of high purity metal preparation, the methods for the determination of purities obtainable, and the potential uses of such high purity materials would be timely and of high scientific interest.

The symposium consists of five sessions: (*a*) Zone Refining Methods for the Preparation of High Purity Metals, (*b*) Iodide Type Processes for the Preparation of High Purity Metals, (*c*) Electrorefining and Electrowinning Methods, (*d*) Chemical Purification Methods for Compound Preparation in Production of High Purity Metals, and (*e*) Criteria of Purity in Preparation of High Purity Metals. A total of approximately 28 papers have been scheduled for this meeting. Some of the subjects to be covered include boat and floating zone refining techniques for some metals, semiconductors, floating zone refining of tungsten by electron beam melting, continuous multistage zone refining of silicon tetraiodide. A number of papers on the preparation of silicon and refractory metals by iodide processes are also included.

Electrowinning and electrorefining using fused salt methods for the preparation of high purity hafnium, boron, columbium, uranium, and titanium are included in the papers.

Reduction methods for the preparation of tungsten, rhenium, and methods for preparation of high purity scandium and boron are also being covered.

A number of analytical techniques utilized for the determination of impurity levels in high purity metals will be described.

E & M—Corrosion Joint Symposium

A symposium entitled "Stress Corrosion Cracking of Stainless Steel" will be presented at the Annual Meeting of the Society, to be held in New York, April 27 to May 1. The program, under the joint sponsorship of the Electrothermics and Metallurgy and the Corrosion Divisions, has been formulated by W. E. Tragert and will consist of six papers in one session.

The symposium will be keynoted by J. J. Harwood who will review recent progress in this research area. Critical experiments directed toward obtaining a better understanding of the failure mechanism in austenitic stainless steel will be described by H. L. Logan, while the effect of composition will be the subject of a paper by H. R. Copson. The influence of corrosive environment will be presented in two papers: M. G. Fontana will discuss failure in high temperature water, and G. Wheeler will evaluate performance in caustic solutions. The stress corrosion of martensitic stainless steels comprises the third element of the program and a paper by F. Brown will be presented on this subject.

Brief prepared discussions have been solicited from several investigators who are active in the field and will be presented as time permits.

Theoretical Division Extended Abstracts

The Theoretical Electrochemistry Division is making available a booklet of extended abstracts of the papers to be presented at the Annual Spring Meeting of the Society in New York, April 27 to May 1. Extended abstracts of general papers and the papers of the Symposium on Electrokinetic and Membrane Phenomena are included. Copies will be available at the meeting, or they can be obtained, at $3.00 each, from:

Dr. Ralph Roberts
3309 Camalier Drive
Washington 15, D. C.

Section News

Boston Section

The tenth meeting of the Boston Section was held in the M.I.T. Graduate House. Professor Carl Wagner was guest of honor at the dinner. Professor Andre de Bethune, as official representative of The Electrochemical Society, Inc., reviewed Professor Wagner's experiences and researches, and expressed to him the Society's best wishes for him in his new position as head of the Max Planck Institut für Physikalische Chemie. Professor de Bethune, and others later, expressed personal appreciation and warm regards to Professor Wagner. In his response, Professor Wagner expressed his affection for New England, and his enjoyment in his experiences in this country, particularly in his work and associations at M.I.T.

For the technical program, Professor Manson Benedict, head of the Nuclear Energy Division at M.I.T., and professor of nuclear engineering, discussed "The M.I.T. Nuclear Reactor." Starting from fundamentals of nuclear reactions, Dr. Benedict sketched the construction of the reactor from the fuel elements out to the protecting building, pointing out a number of ingenious arrangements which facilitate the use of the reactor as a research and training instrument, and also maintain a high

level of safety. He briefly described some uses of the reactor in medical studies as well as in metallurgy, physics, and chemistry, and suggested the usefulness of the high neutron flux and great gamma-ray intensity in a variety of projects. After his discussion, the audience greatly enjoyed a tour of the reactor, whose construction was nearing completion.

W. Waring,
Secretary-Treasurer

India Section Symposium on Electrodeposition and Metal Finishing

The Symposium on "Electrodeposition and Metal Finishing" was held at the Central Electrochemical Research Institute, Karaikudi, on December 27 and 28, 1957. After a welcome speech by Dr. T. L. Rama Char and the reading of a special message from Dr. M. S. Thacker, Chairman of the Section, Dr. K. S. G. Doss, deputy director-in-charge, CECRI, delivered the inaugural address on "Some Fundamental Aspects of Electrodeposition and Metal Finishing." Beginning with an introduction he covered the mechanism of electrolytic conduction, kinetics of the discharge process, and the "redoxokinetic effect."

The papers were then presented. Dr. A. N. Kappanna, assistant director-in-charge, Central Salt Research Institute, Bhavnagar, presided over the session on December 27, and Dr. A. Joga Rao, assistant director, CECRI, presided on the next day. There were 35 papers covering the theoretical and industrial aspects of the following topics: electroplating, electrorefining, electrowinning, metal powders, anode phenomena, electropolishing, anodizing, and protective coatings.

The titles of the papers were: 1—Current Distribution on Microprofiles; 2—Electrochemistry of Fluorides, Part 4. Electrolysis of Cadmium Fluoride; 3—Hard Chromium Plating; 4—Nickel Plating from the Pyrophosphate Bath; 5—Bright Nickel Plating; 6—Electrodeposition of Aluminum on Steel Wire from a Fused Bath; 7—Brass Plating from the Pyrophosphate Bath; 8—Codeposition of Cobalt and Tungsten from an Aqueous Ammoniacal Citrate Bath, Part 2; 9—Electrodeposition of Iron-Zinc Alloys at Rotating Cathode; 10—Electrodeposition of Nickel Alloys from the Pyrophosphate Bath; 11—Tin-Copper Alloy Plating from the Pyrophosphate Bath; 12—Tin-Zinc Alloy Plating from the Pyrophosphate Bath; 13—Plating of Uncommon Metals; 14—Electron-Microscopic Examination of Anodic Layers of Tin; 15—Electrometallurgy in Japan; 16—Electrolytic Iron from Latenite; 17—Separation of Iron from Zinc Chloride Solution by Electrodeposition at Controlled Potential; 18—Electrodeposition of Lead from Chloride Solutions with Special Reference to Utilisation of Zawar Lead Sulphide Concentrates; 19—Electrowinning of Manganese from Chloride Bath; 20—Electrowinning of Zinc from Zawar Zinc Sulphide Concentrates; 21—Electrowinning of Zinc from the Lead-Zinc Ores of Zawar Mines; 22—Electrodeposition of Copper and Zinc Powders; 23—Electrolytic Nickel Powder; 24—Electrolytic Preparation of Thorium; 25—Electrolytic Preparation of Lead Dioxide Electrodes and Their Application in Electrolytic Processes; 26—Electrodeposition of Manganese Dioxide from Manganese Sulphate Solutions with Special Reference to Utilisation of Low Grade Manganese Ores; 27—Galvanostatic and Potentiostatic Studies on Zinc; 28—Anodic Passivation of Zinc in Alkaline Solutions; 29—Electropolishing of Copper from Orthophosphoric Acid Bath Using a Hull Cell; 30—Electropolishing of 18-8 Stainless Steel; 31—Studies on Hard Anodizing; 32—Recent Developments in Hard Anodizing; 33—Corrosion and Metal Finishing; 34—Surface Preparation of Steel and Other Metals for Painting; 35—Chromate Treatment of Metals.

There was a good discussion over the papers. Dr. Doss in his concluding remarks stated that the symposium was a great success, and expressed the hope that there will be many such symposia in electrochemistry in the near future. Mr. Balachandra proposed a vote of thanks. The program was rounded off with social functions and two films: Exide Battery by M/S. Chloride and Exide Batteries (Eastern) Ltd., and Electron Microscope by M/S. Philips India Ltd.

As announced earlier in the *Bulletin*, the Section proposes to publish a Special Number covering the proceedings of the symposium.

T. L. Rama Char,
Regional Editor, India

Electronics Division Enlarged Abstracts

The Electronics Division will again publish an "Enlarged Abstracts" booklet for the Spring 1958 convention of the Society in New York City. The booklet will have 1000-word abstracts of the papers to be presented before the Electronics Division in its symposia on

Luminescence
Semiconductors.

The abstracts will contain pertinent information and experimental data given in the papers and will provide these details before publication, thus aiding workers in the field. The abstracts will be "printed but not published."

The abstract booklets should be available by mid-April; the price will be $2.50 per copy.

Checks should be made payable to: Electronics Division, The Electrochemical Society.

Orders and checks should be sent to:

Martin F. Quaely
c/o Westinghouse Electric Corp.
Lamp Div., Research Dept.
Bloomfield, N. J.

Indianapolis Section

The Indianapolis Local Section of the Society held its Winter Technical Meeting on Monday, January 20, at the Student Union and Food Services Building of the Indiana University Medical Center in Indianapolis. Our Society President, Dr. Norman Hackerman, was the guest speaker for the evening.

After a review of the current status of the Society, Dr. Hackerman spoke on "The Passivity of Metals." He covered the dispute concerning the cause of ennoblement of metals like iron and chromium in certain environments and showed that neither the oxide theory nor theories of absorption will serve alone to explain these phenomena. After a presentation of experimental data obtained in his laboratory at the University of Texas and some comparisons to findings reported by other investigators, Dr. Hackerman proposed a sequence model to explain such situations. A spirited question and discussion period then concluded the evening's activities.

T. C. O'Nan,
Secretary-Treasurer

Philadelphia Section

The regular meeting of the Philadelphia Section of The Electrochemical Society was held at the Harrison Lab., University of Pennsylvania, at 8:00 P.M. on January 8.

Attendance was good in spite of below-freezing temperatures and ice-covered sidewalks. Mr. Donald W. Kuester of the Naval Ordnance Lab., Silver Spring, Md., was the speaker of the evening. The subject, "The Solion, Product of a New Elec-

(Continued on page 82C)

Officers of Local Sections of the Society

Boston
L. B. Rogers, Chairman
Charles Levy, Vice-Chairman
G. W. Waring, Sec.-Treas.
C. W. Jerome* (1 yr)
F. C. Benner* (2 yr)

Chicago
Ralph Hovey, Acting Chairman
W. H. Colner, Treasurer
J. Kuderna, Secretary
H. T. Francis*

Cleveland
P. S. Brooks, Chairman
D. E. Kinney, Vice-Chairman
F. A. Shirland, Treasurer
R. A. Powers, Secretary
N. C. Cahoon*
K. S. Willson*

Columbus
C. L. Faust, Chairman
I. E. Campbell, Vice-Chairman
E. F. Stephan, Sec.-Treas.
W. M. Albrecht*
A. C. Tripler, Jr.*

Detroit
Manuel Ben, Chairman
Sam Piken, Vice-Chairman
A. E. Remick, 2nd Vice-Chairman
Manuel Shaw, Sec.-Treas.
Frank Passal*
L. O. Case*

India
M. S. Thacker, Chairman
S. Ramaswamy, Vice-Chairman
S. Srinivas, Vice-Chairman
T. L. Rama Char, Treasurer
J. Balachandra, Secretary

* Representative on Council of Local Sections.

Indianapolis
L. L. Deer, Chairman
A. E. Middleton, Vice-Chairman
T. C. O'Nan, Sec.-Treas.
F. C. Mathers*
A. Herczog*

Midland
H. W. Schmidt, Chairman
P. F. George, Vice-Chairman
R. S. Karpiuk, Sec.-Treas.
R. C. Kirk* (1 yr)

Mohawk-Hudson
H. R. Schmidt, Chairman
J. H. Westbrook, Vice-Chairman
A. L. Jenny, Sec.-Treas.
J. F. Murphy*

New York Metropolitan
K. B. McCain, Chairman
G. D. Stendahl, Vice-Chairman
F. S. Lang, Sec.-Treas.
A. C. Loonam*
M. F. Quaely*

Niagara Falls
L. A. Stoyell, Chairman
W. E. Kuhn, Vice-Chairman
K. E. Kunkel, Sec.-Treas.
Robert Stambaugh*
Joseph Sullivan*

Ontario-Quebec
John Convey, Honorary Chairman
R. R. Rogers, Chairman
H. A. Timm, Vice-Chairman (Program)
L. G. Henry, Vice-Chairman (Membership)
Jack Noy, Sec.-Treas.
L. G. Henry*

Pacific Northwest
G. B. Adams, Jr., Chairman
Cornelius Groot, Vice-Chairman
H. J. Wittrock, Sec.-Treas.
G. H. Kissin*

Philadelphia
G. F. Temple, Chairman
G. W. Bodamer, Vice-Chairman
A. A. Ware, Treasurer
H. C. Mandell, Jr., Secretary
J. F. Hazel*
J. F. Gall*

Pittsburgh
J. J. Stokes, Jr., Chairman
Ling Yang, Vice-Chairman
E. H. Phelps, Sec.-Treas.
A. J. Cornish* (2 yr)
R. A. Woofter* (1 yr)

San Francisco
H. F. Myers, Chairman
Bernard Porter, Vice-Chairman
J. F. Aicher, Treasurer
R. A. Zimmerly, Secretary
S. H. Dreisbach*
C. D. Hunt*

Southern California-Nevada
W. M. Hetherington, Jr., Chairman
Q. H. McKenna, Vice-Chairman
L. J. Droege, Sec.-Treas.
M. E. Carlisle* (2 yr)

Washington-Baltimore
Ralph Roberts, Chairman
G. B. Wood, Vice-Chairman
Jerome Kruger, Treasurer
David Schlain, Secretary
J. C. White*
Fielding Ogburn*

Officers of Divisions of the Society

Battery
U. B. Thomas, Chairman
J. C. White, Vice-Chairman
E. J. Ritchie, Sec.-Treas.

Corrosion
C. V. King, Chairman
M. A. Streicher, Vice-Chairman
R. T. Foley, Sec.-Treas.

Electric Insulation
L. J. Frisco, Chairman
A. J. Sherburne, Vice-Chairman
Emanuel Brancato, Sec.-Treas.

Electrodeposition
Sidney Barnartt, Chairman
Abner Brenner, Vice-Chairman
D. G. Foulke, Sec.-Treas.

Electronics
Herbert Bandes, Chairman
R. J. Ginther, Vice-Chairman (Luminescence)
C. T. Lattimer, Vice-Chairman (General Electronics)
J. W. Faust, Jr., Vice-Chairman (Semiconductors)
M. F. Quaely, Sec.-Treas.

Electro-Organic
Stanley Wawzonek, Chairman
Garrett Thiessen, Vice-Chairman
Milton Allen, Sec.-Treas.

Electrothermics and Metallurgy
A. U. Seybolt, Chairman
G. M. Butler, Vice-Chairman
E. M. Sherwood, Vice-Chairman
J. H. Westbrook, Sec.-Treas.

Industrial Electrolytic
Milton Janes, Chairman
J. C. Cole, Vice-Chairman
W. D. Sherrow, Sec.-Treas.

Theoretical Electrochemistry
Paul Delahay, Chairman
Charles Tobias, Vice-Chairman
Ralph Roberts, Sec.-Treas.

(Continued from page 80C)

tronic Technology," was one of interest to electrochemists representing either the chemical or electronic industries.

Photographs of several embodiments of this new family of devices were shown; a detector, an amplifier, a log detector, and an electrochemical integrator were described.

J. W. Tiley

San Francisco Section

At the January 22 Section meeting, Dr. Douglas Skoog, of Stanford University's Chemistry Dept., presented a talk on "Coulometric Titrations in Analytical Chemistry."

The speaker pointed out that the requirements for coulometric titrations were much the same as for volumetric titrations (e.g., rapid and complete reactions) and that the same type of end-point detection was used in both cases. Only, instead of metering volumes of standard solutions, a quantity of electricity is metered in a coulometric titration. This is most conveniently done by using a constant-current source, a high-grade stop clock, and a switching arrangement; several examples were given.

Normally, in order to stabilize electrode potentials yet obtain reasonable reaction rates, the "indirect method" of titration is used, i.e., the solution is loaded with an excess of an auxiliary oxidizable or reducible ion. Electrode reactions then generate the auxiliary oxidant or reductant *in situ*, and the generated substance reacts with the ion or compound to be determined. Typical examples of oxidants (Ce^{++++}, Br, etc.) and reductants (Fe^{++}, H_2) were discussed.

The main advantages of the coulometric titration method are its versatility (the current can be varied over a considerable range quite readily) and the fact that it is not necessary to prepare any standard solutions. This method lends itself readily to automatic titrations.

Morris Feinleib

New Members

In January 1958 the following were approved for membership in The Electrochemical Society by the Admissions Committee:

Active Members Sponsored by a Sustaining Member

William J. Arner, Libbey-Owens-Ford Glass Co., 1701 E. Broadway, Toledo 5, Ohio (Electrothermics & Metallurgy)

George F. Johnson, Motorola Inc., Plated Circuit Engineering Dept., 1915 Elston Ave., Chicago 22, Ill. (Electric Insulation, Electrodeposition, Electronics, Electrothermics & Metallurgy)

John Mirza, Sumner Chemical Co., Div. of Miles Labs., Inc., 1127 Myrtle St., Elkhart, Ind. (Electro-Organic)

Reinstatement and Transfer from Active to Active Sponsored by Sustaining Member

Harold E. Zahn, Gould-National Batteries Inc., 55 Neoga St., Depew, N. Y. (Battery)

Active Members

Robert H. Aborn, Edgar C. Bain Lab. for Fundamental Research, U. S. Steel Corp., Monroeville, Pa. (Electrothermics & Metallurgy)

William B. Arnold, Great Lakes Carbon Corp., P.O. Box 637, Niagara Falls, N. Y. (Industrial Electrolytic)

Frederick G. Barker, Aluminium Ltd., P.O. Box 6090, Montreal, Que., Canada (Electrothermics & Metallurgy, Industrial Electrolytic)

Wilfred R. Bekebrede, Raytheon Manufacturing Co.; Mail add: 20 Morrison Rd., Watertown 72, Mass. (Electronics)

Morris V. Boley, United States Mint; Mail add: 911 Hacienda Dr., Millbrae, Calif. (Electrodeposition)

James J. Casey, Sprague Electric Co.; Mail add: 108 Cole Ave., Williamstown, Mass. (Electronics)

Peter A. Denes, Allen-Bradley Co.; Mail add: 2934 No. Downer Ave., Milwaukee 11, Wis. (Battery)

Arthur T. Devlin, General Electric Semi-Conductor Products Dept.; Mail add: 137 Lancaster Ave., Buffalo 22, N. Y. (Electronics)

Emory P. Estep, International Minerals & Chemical Corp.; Mail add: 160 Marilyn Dr., Grand Island, N. Y. (Industrial Electrolytic)

Ahmad Geneidy, Cairo University, Chemical Engineering Dept., Cairo, Egypt (Battery, Corrosion, Electrodeposition, Electro-Organic, Electrothermics & Metallurgy, Industrial Electrolytic, Theoretical Electrochemistry)

Claus H. Haake, Westinghouse Electric Corp.; Mail add: 12 Cedar Parkway So., Livingston, N. J. (Electronics)

Walter W. Harvey, Massachusetts Institute of Technology, Lincoln Lab., P.O. Box 73, Lexington 73, Mass. (Electronics, Theoretical Electrochemistry)

Archie Khachadoorian, Raytheon Manufacturing Co.; Mail add: 475 Shawmut Ave., Boston 18, Mass. (Electronics)

Stanley J. Klima, Sperry Gyroscope Co.; Mail add: 40-15 Hampton St., Elmhurst 73, N. Y. (Electrodeposition)

Bernard L. Kravitz, General Transistor Corp.; Mail add: 105-45 63rd Dr., Forest Hills, L. I., N. Y. (Electronics)

Willi Lehmann, Westinghouse Electric Corp.; Mail add: 13 Dickinson Lane, Livingston, N. J. (Electronics)

Mario Mori, Societa Edison, Corso Italia, 13, Milan, Italy

Paul J. Rappaport, U. S. Army Signal Engineering Labs.; Mail add: 287 Westwood Ave., Long Branch, N. J. (Battery)

Marcel Rey, Societe d'Electro Chemie d'Ugine, Laboratoire de Recherches, 82, Rue Arago, Saint Ouen, (Seine) France (Electrothermics & Metallurgy, Theoretical Electrochemistry)

Charles R. Rogers, Hammond Lead Products, Inc., Box 912, Hammond, Ind. (Battery)

Robert F. Rolsten, E. I. du Pont de Nemours & Co.; Mail add: 2019 Oak Lane Rd., Wilmington 3, Del. (Electrothermics & Metallurgy)

Norman W. Rosenberg, Ionics Inc., 152 Sixth St., Cambridge, Mass. (Industrial Electrolytic, Theoretical Electrochemistry)

Robert E. Rummel, Vanderbilt University, Chemistry Dept., Box 1505, Nashville, 5, Tenn. (Electronics)

K. Schwabe, Technische Hochschule; Mail add: Dresden A 27, Bergstr. 66b, DDR, Germany (Corrosion, Theoretical Electrochemistry)

Karl Sollner, National Institutes of Health, Lab. of Physical Biology, Bethesda 14, Md. (Theoretical Electrochemistry)

Richard R. Stead, Texas Instruments, Inc.; Mail add: 628 Northill Dr., Richardson, Tex. (Electronics)

Donald E. Witt, M. W. Freeman Co.; Mail add: 13110 Evanston, Detroit 13, Mich. (Electrodeposition)

Pietr Zuman, Polarographic Institute, Czechoslovak Academy; Mail add: Blanicka 15, Prague XII, Czechoslovakia (Electro-Organic, Theoretical Electrochemistry)

By action of the Board of Directors of the Society, all prospective members must include first year's dues with their applications for membership.

Also, please note that, if sponsors sign the application form itself, processing can be expedited considerably.

Associate Members

Robert L. Bleutge, National Carbon Co.; Mail add: 13801 Clifton Blvd., Lakewood 7, Ohio (Battery)

Harry D. Hays, Micro Switch; Mail add: R. R. #1, Freeport, Ill. (Electrodeposition)

Herbert I. Moss, Indiana University, Chemistry Dept., Bloomington, Ind. (Electrothermics & Metallurgy)

Student Associate Member

Zisis Andrew Foroulis, Massachusetts Institute of Technology; Mail add: 109 Peterborough St., Boston 15, Mass. (Corrosion)

Transfers from Associate to Active Membership

Robert E. DeLaRue, Jr., Stanford Research Institute; Mail add: 622 Enright Ave., Santa Clara, Calif. (Theoretical Electrochemistry)

Richard M. Peekema, General Electric Co.; Mail add: 505 Basswood Ave., Richland, Wash. (Theoretical Electrochemistry)

Reinstatements to Active Membership

William N. Carson, Jr., General Engineering Lab., General Electric Co.; Mail add: 14 Marjon Ave., Scotia 2, N. Y. (Electronics)

David Linden, U. S. Army Signal Engineering Labs.; Mail add: 78 Lovett Ave., Little Silver, N. J. (Battery)

Deceased—Reported in December 1957

R. O. Hull, Rocky River, Ohio

Personals

O. H. Lindberg has been promoted to supervisory engineer in the Solid State Electronics Development Section, Materials Engineering Depts., Westinghouse Electric Corp., East Pittsburgh, Pa. The section, part of the Solid State Electronics Dept., is engaged in development work on semiconductor materials and devices. Prior to his promotion Mr. Lindberg was a senior engineer in the section.

Wilbur L. Meier, formerly with Chatham Electronics Corp. in Livingston, N. J., recently became affiliated with National Radiac, Inc., Newark, N. J.

M. G. Sanchez has transferred to the Washington Research Center of W. R. Grace & Co. in Clarksville, Md. He had been with the Davison Chemical Co., Div. of W. R. Grace & Co., in Baltimore.

Frank Matossi, formerly of Rockville, Md., is now full professor at the University of Freiburg in Freiburg/Baden, West Germany.

Joseph V. Petrocelli has been appointed head of the Electrochemical Section of the International Nickel Co.'s Research Lab. at Bayonne, N. J.

J. V. Petrocelli

Formerly director of research and development for the Patent Button Co., Waterbury, Conn., Dr. Petrocelli joined the Bayonne laboratory staff in August 1957 as a research electrochemist. As head of the International Nickel Electrochemical Section of the Research Lab., Dr. Petrocelli directs activities in the principal fields of study such as improvement of existing processes of nickel plating and plating of nickel alloys, the development of new plating processes, study of the mechanism of corrosion of electrodeposits, study of the microstructure of electrodeposits, and development of new engineering applications for chemically reduced and electrodeposited coatings of nickel and nickel alloys.

Dr. Petrocelli has served as Chairman of the Society's Corrosion Division, and was Corrosion Editor for the JOURNAL for several years.

Joseph L. Wood, former manager of the McIntosh, Ala., plant of Mathieson Alabama Chemical Corp., a subsidiary of Olin Mathieson Chemical Corp., has been named electrochemical engineer in the operations department at Baltimore.

Parker S. Dunn, vice-president, manufacturing, of American Potash & Chemical Corp., Los Angeles, Calif., has been elected to the company's board of directors.

A. H. Roebuck recently became associated with the Western Co., Midland, Texas. Previously he was with the Continental Oil Co., Ponca City, Okla.

Albert E. Hendrickson, formerly of Flushing, N. Y., has taken a position with the Microwave Tube Lab., Sylvania Electric Products Inc., Mountain View, Calif.

Jan Joop Hermans, formerly of Leiden, Netherlands, is now at the Cellulose Research Institute, State University College of Forestry at Syracuse University, Syracuse, N. Y.

News Items

Palladium Medal Award in 1959

The fifth Palladium Medal of The Electrochemical Society will be awarded at the Fall Meeting of the Society in Columbus, Ohio, October 18-22, 1959. The medal was established in 1951 by the Corrosion Division for distinguished contributions to fundamental knowledge of theoretical electrochemistry and of corrosion processes. It is awarded biennially to a candidate selected by a committee appointed by the Society's Board of Directors. This year the committee members are A. L. Ferguson, H. A. Liebhafsky, T. P. May, E. B. Yeager, and H. A. Laitinen, *Chairman.*

The Committee invites Sections, Divisions, and members of the Society to send suggestions for candidates, accompanied by supporting information, to *H. A. Laitinen, Dept. of Chemistry, University of Illinois, Urbana, Ill.* Candidates may be citizens of any country and need not be members of the Society. Previous medalists have been: Carl Wagner, Massachusetts Institute of Technology [now with Max Planck Institut für Physikalische Chemie]; N. H. Furman, Princeton University, U. R. Evans, Cambridge University; and K. F. Bonhoeffer, Max Planck Institut für Physikalische Chemie (posthumous award).

New Sustaining Members

The following recently became Sustaining Members of The Electrochemical Society: Catalyst Research Corp., Baltimore, Md.; Continental Can Co., Inc., Chicago, Ill.; Cooper Metallurgical Associates, Cleveland, Ohio; Eastman Kodak Co., Rochester, N. Y.; Hughes Aircraft Corp., Culver City, Calif.; Keokuk Electro-Metals Co., Keokuk, Iowa.

Charge Transfer Processes

A symposium sponsored by the Physical Chemistry Division of the Chemical Institute of Canada on charge transfer processes at interfaces and in solution will be held at the University of Toronto on September 4 and 5, 1958. The papers to be presented will be preprinted and mailed to all those who will have indicated their intention to attend, thereby allowing opportunity for extended discussion at the meeting. All

communications regarding submission of papers and attendance at the meeting should be addressed to the Chairman of the meeting, Dr. B. E. Conway, Dept. of Chemistry, University of Ottawa, Canada.

A more detailed announcement will be published shortly.

Meetings of Interest to Electrochemists

May 5-7—Association of Battery Manufacturers Convention, Statler Hotel, New York City.

June 4-14—International Conference of Large Electrical Systems, Paris, France.

June 12-14—National Society of Professional Engineers Convention, St. Louis, Mo.

June 16-20—American Society for Engineering Education Meeting, Berkeley, Calif.

June 22-28—American Society for Testing Materials Meeting, Boston, Mass.

July 8-18—International Electrotechnical Committee Meeting, Stockholm, Sweden.

Sept. 22-25—Solar House Symposium, Phoenix, Ariz. Sponsored by the Association for Applied Solar Energy, Arizona State College, and University of Arizona.

Oct. 28—Consulting Chemists and Chemical Engineers Meeting, New York City.

Secretary Weeks Releases Details on Foreign Technical Information Center

Secretary of Commerce Sinclair Weeks has announced new measures to increase scientific knowledge through establishment of a Foreign Technical Information Center within the Dept. of Commerce.

To finance prompt action on the new project, the department is requesting a special appropriation of $300,000 to initiate the program. In addition, the President's budget for 1959 includes $1,250,000 for the department's Foreign Technical Information program.

The new program will set up a central clearinghouse in the Commerce Dept.'s Office of Technical Services, headed by John C. Green. The Center is to collect, evaluate, and distribute valuable foreign scientific and technical literature for the use of American scientists and engineers.

Arrangements have been made to obtain from government and other agencies copies of abstracts and translations of foreign technical articles, monographs, and books. It is estimated that these will be supplied at an annual rate of 50,000 abstracts and 10,000 complete translations.

The items will be catalogued in the library of the Office of Technical Services. It is planned that the abstracts will be published and released to the technical press, and that copies of translations will be made available to the public.

A staff of engineer-translators will be added to review and analyze foreign publications and select those of greatest value. It is planned to appoint a scientific advisory committee to assist in the selection. Arrangements will be made for full translations of important articles and studies. Among the materials the engineer-translators will receive are copies of 200 important Russian scientific journals.

The new Center will operate a coordination service to eliminate duplication of translating among U. S. public and private agencies and by friendly foreign governments. In its own translation work, the Center will concentrate on technology.

Clyde Williams Forms New Company

Clyde Williams, formerly president of Battelle Institute, has announced the formation of a new company to assist boards of directors and top management of industrial corporations with broad technical and business problems. The new firm, to be known as Clyde Williams and Co., will serve a wide range of industries in the United States and abroad, and will have its central operations at 50 West Gay St., Columbus, Ohio.

Dr. Williams states that his company will provide services in research programming and administration, in the application of science and technology to industry, and in problems of business organization and operation. Much of the firm's effort will be directed to the growth and expansion of existing companies and to the formation of wholly new companies through the finding of new products to develop, company acquisitions and mergers, and the utilization of new technologies.

Dr. Williams will serve as president and has named the following officers: Bruce B. Robe, vice-president; Clyde Williams, Jr., secretary-treasurer and general counsel; and Jeanne E. Purnhagen, assistant secretary-treasurer.

Journals Wanted

If any member of the Society wishes to sell his unbound copies of the JOURNAL for 1951 (Vol. 98), please communicate direct with Col. George C. Cox, 3711 Washington Ave., S. E., Charleston 4, W. Va.

Book Reviews

Zirconium—Metallurgy of the Rarer Metals, No. 2—2nd Ed., by G. L. Miller. Published by Academic Press, Inc., New York City, 1957. 547 pages; $12.50.

The major incentive for the development of a zirconium technology derives from the use of the metal in the cores of nuclear reactors. Consequently, at the time of publication of the first edition of this book in 1954, much of the existing information was still classified. Since then, a great deal has been made public and a comprehensive book ("The Metallurgy of Zirconium") has been published under the auspices of the U. S. Atomic Energy Commission. As a result, Dr. Miller has found it necessary to revise his original work and to expand it by more than 40%.

The basic plan of the book remains substantially unchanged. It deals first with the sources, uses, and extraction of zirconium from its ores with particular emphasis upon separation from the hafnium which is undesirable in nuclear applications. The methods of reduction are then described with greatest attention to the Kroll process. A considerable portion of the text is devoted to the properties of zirconium and to its resistance to gases and a variety of corrosive media. This is followed by a consideration of alloying characteristics and a summary of known binary systems. The last section of the book describes melting and fabrication techniques and powder metallurgy methods.

The book contains a wealth of detail drawn from the numerous listed references. There may be some objection to the style, which resembles that of a literature survey, but there can be no doubt of the book's value to all who use or contemplate the use of zirconium.

M. Kolodney

Economics of Atomic Energy, by Mary S. Goldring. Published by Philosophical Library, New York City, 1957. 179 pages; $6.00.

This is an interesting and informative book, clear in outline and well supplied with data. However, atomic research is advancing so rapidly that some of its conclusions are being challenged by current events.

The driving force behind the development of atomic energy as a new source of power is the simple fact that supplies of existing fuels are limited while demand is increasing. While these limits are generous, nevertheless the price of conventional fuels will rise sharply as the costs

of extraction and processing become greater. Power from atomic energy, although not cheap at the outset, will become increasingly competitive.

Any estimate of the minimum investment required to establish the nucleus of an atomic industry would lie close to $300,000,000. However, in the present day setup, a large fraction of this expenditure will be borne by military budgets, the production of atomic weapons being an integral part of our atomic industry. Estimation of the cost of electricity from individual atomic reactors is complicated. While a specific price may be placed on a pound of uranium, the life expectancy of it as a fuel is not known. There are, as yet, no guides to the length of time a uranium fuel rod will continue to give off useful quantities of heat. It is not possible to place a value on the plutonium produced in the reactors. There is no market for the metal at present; it is not a commodity that can be bought and sold.

In spite of these obstacles, Miss Goldring makes a resourceful effort to determine over-all costs for the electricity produced. She is well informed as to currently accepted data, and her methods are logical. She concludes that within the very near future electricity from atomic power can be produced at a cost nearly equivalent to that from ordinary coal- and oil-fired power stations.

In considering the export market for atomic reactors, Miss Goldring claims economic competitivity for the British gas-cooled reactor, fueled with natural uranium, as against the more efficient American type that uses fuel enriched with U 235. She arrives at this claim by attempting to show that a 2% enrichment for a Calder-type installation using natural uranium would cost at present prices nearly $112,000,000. On the other hand, an enriched reactor uses a much smaller tonnage of fuel.

While this book deals primarily with the economics of atomic energy produced by fission, certain sections dealing with atomic power from the fusion process are of interest. There is a reference to the lecture given by the Russian, Kurchatov, at Harwell in 1956, in which he described how temperatures very close to those required for the fusion process had already been attained. Considering that Professor Kurchatov started this work back in 1952, one wonders how far advanced is present Russian research. Miss Goldring states that there is confidence in Britain that power from fusion will be a reality in approximately 20 years. This is in agreement with the latest joint American and British announcement which estimates it will take about 10 years for the "break-even" point to be reached, and 20 years for the actual production of electricity. (The "break-even" point is that at which as much energy is being produced as is consumed in the process.) These estimates may prove too conservative as indicated by a recent article in *Nature* magazine. In this article, scientists affiliated with Associated Electric Industries Ltd. state that they have already attained temperatures of 4 million degrees and hope to reach 30-40 million, the "break-even" point, by the end of the year.

Chester B. Kremer

Galvanotechnik (Electroplating), 2nd Ed., by Jean Billiter. Published by Springer Verlag, Vienna, 1957. 441 pages; price DM66 (about $16.70).

In view of the multiplicity of fine German textbooks on electroplating (including a translation by Dettner of the ECS's "Modern Electroplating"), it is difficult to see much purpose in a new edition of Billiter, except as a book-selling venture. However, if one can read German and desires a text which constantly emphasizes factors affecting the structure of deposits, Billiter may have something to be recommended.

A very substantial effort has been made toward revision and rewriting the first edition. There are 154 figures, compared to 86 in the first edition. More than 100 pages of new material has been added and some of the old material omitted, although the omissions are not always for the best. For example, there is an excellent table of hydrogen overvoltages, the source references being given in the first edition but omitted in the second. The introductory sections have been considerably amplified and extended, especially the discussion of the cathode film composition and the structure of the double layer. Emphasis is placed throughout the text on the effect of colloids and other addition agents in improving the appearance and mechanical properties of deposits.

The book is confined strictly to electrolytic processes with no discussion of procedures for coating or finishing, lacquering, polishing, etc., and with only a few pages devoted to engineering and equipment problems. Although the arrangement or order is completely changed, the treatment of the various metals is essentially similar to that in the first edition. Extensive additions have been made to the chapters on copper, nickel, chromium, and tin, but the only entirely new chapters are on anodic processes, anodizing aluminum, and electropolishing.

As with so many modern German books, one is appalled by the numerous typographical or bibliographical errors. A few samples: page 29, Fuller's work on the diffusion of hydrogen is in the TRANSACTIONS of The Electrochemical Society and not the Faraday Society; page 323, Bruni and Papasogli should be Bartoli and Papasogli; Varverth and Curry should be Garveth and Curry; page 339, Starek should be Stareck, and so on, endlessly. It would seem that an expensive book of some merit could have better proofreading, and that mistakes should not be repeated in editions 23 years apart.

The chapter on chromium plating includes an extensive treatment of the newer self-regulating baths, but the historical development of the subject is somewhat lacking or provincial in its outlook. Reese is incorrectly given credit for electrodepositing chromium in 1899, and Fink is not even mentioned in connection

December 1958 Discussion Section

A Discussion Section, covering papers published in the January-June 1958 JOURNALS, is scheduled for publication in the December 1958 issue. Any discussion which did not reach the Editor in time for inclusion in the June 1958 Discussion Section will be included in the December 1958 issue.

Those who plan to contribute remarks for this Discussion Section should submit their comments or questions in triplicate to the Managing Editor of the JOURNAL, 1860 Broadway, New York 23, N. Y., *not later than September 1, 1958*. All discussions will be forwarded to the author(s) for reply before being printed in the JOURNAL.

with chromium, although he appeared in a footnote in the first edition.

On the whole, however, this is a well-balanced textbook on electrodeposition of metals, with emphasis throughout on the factors which affect the structure and properties of the deposits.

G. Dubpernell

Vacuum Symposium Transactions, 1956, by E. S. Perry and J. H. Durant. Published by Pergamon Press Inc., New York City, 1956. 234 pages; $12.50.

These papers are concerned primarily with apparatus and technique. ECS members might be interested in the papers on: a high-vacuum laboratory for vapor deposition of conductors on dielectrics; a vacuum-arc study chamber; melting and refining molybdenum and columbium by the vacuum-arc cast process; electron optical studies of oxidation processes occurring in high vacuum; vacuum induction melting; thermodynamics of the vacuum induction melting process; high-vacuum extraction of hydrogen from titanium in the solid state.

H. W. Salzberg

Engineering Materials Handbook. Edited by C. L. Mantell. Published by McGraw-Hill Book Co., New York City, 1958. 80 pages; $21.50.

This is actually a one-volume encyclopedia, not a handbook in the standard sense. Instead of data tables, the book is organized into extremely informative discussions of properties and processes, complete with tables and usually with references at the end of the section. I would call it a very valuable reference book not only for the practicing engineer or chemist but also for the undergraduate student who needs to relate the somewhat esoteric discipline he is studying to the actual practice of chemistry.

The emphasis is on the fabricated material with an operational viewpoint. In each case the techniques of fabrication are discussed along with the advantages and disadvantages of each form and comparisons of different materials for the same uses. These uses, by the way, are right up to date. For example, there are sections on the best material to use in rockets and for insulation against various types of radioactivity. The sources also are right up to date, some references being as late as the spring of 1957.

The actual organization is in the form of individual sections devoted to each separate material or process. The introductory sections comprise an alphabetized list of properties, complete with definitions, equations, and explanations, where necessary. There is also a description of the various quantitative tests involved. The introductory material also has a comprehensive discussion of all types of fabrication processes, complete with detailed drawings of the machinery involved. Following the introductory sections is a discussion of the metals. This includes sections on the usual structural materials, of course, but also heat transfer metals for use in reactors, specialty metals for alloying, precious metals, etc. There is also a discussion of special techniques such as powder metallurgy, welding, and electroplating.

The next grouping is that of inorganic materials, such as refractories, glasses, concrete, and stone. The final section, devoted to materials, covers the organic substances, such as tar, asphalt, plastics, waxes, lacquers, and paints. The final section of the book is a detailed discussion of both theory and practices of protection from deterioration, corrosion, brittleness, fatigue, etc.

H. W. Salzberg

Announcements from Publishers

"Development of a Nondestructive Test for Evaluation of Adhesion of Electrodeposits on Steel as in Silver-Plated Aircraft Bearings," A. L. Walters and S. A. Wenk, Battelle Memorial Institute, for Wright Air Development Center, U. S. Air Force, Nov. 1953. Report PB 131226,* 65 pages, $1.75.

Reliable nondestructive test methods used commercially for inspection of silver-plated aircraft bearings are discussed. Selection of the test method depends on whether a copper or nickel strike is applied to the bearing shell before silver plating. The shot peening test, in which the surface of the silver plate is lightly shot peened under controlled conditions, is used principally on bearings having a copper strike. In the bake test, nickel strike bearings are tested by heating the bearing to 950°F, followed by rough boring, or machining to size and then x-raying the bearing surface. A summary of processing operating procedures for silver plating and bond testing at one industrial plant is included, together with plating and testing data for experimental panels processed at Battelle. The report also suggests changes in an Air Force Technical Order to improve the procedure for silver plating and reduce the occurrence of poorly adherent silver plate at USAF depots overhauling aircraft engines.

* Order from Office of Technical Services, U. S. Dept. of Commerce, Washington 25, D. C.

"The Effect of Corrosion Preventives and Initial Barrier Wrappers on Preservation of Anti-Friction Bearings," L. H. Wagner, Rock Island Arsenal Lab., U. S. Army, May 1956. Report PB 131262,* 51 pages, $1.50.

Deterioration of stored antifriction bearings caused by either the corrosion preventive or the initial barrier wrapper or the combination of these materials was investigated. Steel, brass, and copper specimens were used in tests in a climatizer under dynamic conditions employing moisture-laden air. Among the results it was found that polyethylene laminates, aluminum foil, and moldproofed wrappers were most compatible with corrosion preventives. A polyethylene kraft laminated wrapper was superior as initial barrier to a glassine grease-proof wrapper. Initial barrier materials, if corrosive, were shown to aid in causing breakdown of the corrosion preventive with subsequent deterioration of the metal surfaces.

"Investigation of the Applicability of High Frequency Sound Waves (Ultrasonics) for Cleaning of Precision Parts," O. E. Mattiat and P. P. Zapponi, Clevite Research Center, for Wright Air Development Center, June 1957. Report PB 131361,* 76 pages, $2.00.

Accessible soils of all kinds are shown to be easily removed from small precision parts by the ultrasonic systems studied. Inaccessible soils, such as steel particles in bearings and grease in blind holes, require high sonic intensities and a coupling fluid with optimum cavitating and solubility or dispersability properties for the particular soil. Low-frequency systems appeared more effective than high-frequency systems for removing most soils investigated. Those included greases, burnt-on carbon, lapping and buffing compounds, steel particles, and a synthetic soil. It was further observed that bearing damage resulting from ultrasonic treatment is insignificant for the short cleaning times normally required. Processes are recommended for cleaning precision parts and bearings. A coupling fluid—trichloroethylene—is

shown to be best for removal of soils. The steel-removal and probe methods, two new processes for evaluating ultrasonic systems and factors, are described.

"Investigation of Hydrofluoric Acid as a Corrosion Inhibitor for Fuming Nitric Acids," M. J. Keeler and E. F. Knoll, Aerojet-General Corp., for Wright Air Development Center, U. S. Air Force, Nov. 1956. Report PB 121864,* 180 pages, $4.50.

Small amounts of hydrogen fluoride are effective in inhibiting corrosion by fuming nitric acid, the highly corrosive oxidizer for liquid rocket power plants. Tests showed that the corrosion rates of 6061-T6 aluminum and type 347 stainless steel were generally reduced by a factor varying from about 10 to 100. An initial HF content of about 0.75% by weight was most effective. Increase in HF content to 2.0% brought no further reduction in corrosion rate, while 0.5% usually provided less inhibition. Tests conducted with other metals gave similar results of reduced corrosion in the inhibited acids. The final report also describes studies of methods for determining HF content and for identifying other constituents of acids.

Literature from Industry

Semiconductor Power Rectifiers—Bulletin GEA-6375A, 12 pages, discusses both silicon and germanium power rectifiers for use in electrochemical processes, aluminum and copper production, electroplating, anodizing, and steel process lines. Explains how high efficiency conversion can be obtained at relatively low cost with semiconductor rectifiers; describes features and applications of water-cooled and air-cooled designs. *General Electric Co., Schenectady 5, N. Y.*

Employment Situations

Please address replies to box shown, c/o The Electrochemical Society, Inc., 1860 Broadway, New York 23, N. Y.

Position Wanted

Chemist, inorganic, 11 years' experience: Electroplating (copper-acid, alkali; tin-acid, alkali; nickel; chromium), batteries, gelatines, glues, pyrotechny, general physical and chemical commercial testing, seeks position in New Jersey and environs; has held supervisory positions, experienced in analysis, capable of producing new ideas, anxious to forge ahead. *Reply to Box 363.*

Positions Available

Engineers (Aeronautical, Electrical, Electronic, Industrial, General, Mechanical, and Power Plant), **Electronic Scientists, Metallurgists, Physicists, Technologists**—Vacancies exist for professional personnel in the above positions. Starting salaries range from $4480 per annum to $8645 per annum. The Naval Air Material Center is currently engaged in an extensive program of aeronautical research, development, experimentation, and test operations for the advancement of Naval aviation. Personnel are needed for work on projects involving modification, overhauling, and testing of aeronautical equipment, materials, accessories, power plants, launching and arresting devices, and for modification and structural testing of aircraft. Also, for work involving the basic design of catapults, launchers, arresting gear and their component parts; test and development work at shore stations and on board U. S. Navy ships; evaluation of new equipment and establishment of performance parameters, and applied research on the many problems relevant to this field.

Interested persons should file an Application for Federal Employment, Standard Form 57, with the Industrial Relations Dept., Naval Air Material Center, Naval Base, Philadelphia 12, Pa. Applications may be obtained from the above address, or information as to where they are available may be obtained from any first or second class post office.

Required—Chemist with experience in fundamental research on electrode processes to lead battery research in industrial organization. *Reply to Box 999.*

Advertiser's Index

The Electrochemical Society

Patron Members

Aluminum Company of Canada, Ltd., Montreal, Que., Canada
International Nickel Company, Inc., New York, N. Y.
Olin Mathieson Chemical Corporation, Niagara Falls, N. Y.
  Industrial Chemicals Division, Research and Development Department
Union Carbide Corporation
  Divisions:
    Electro Metallurgical Company, New York, N. Y.
    National Carbon Company, New York, N. Y.
Westinghouse Electric Corporation, Pittsburgh, Pa.

Sustaining Members

Air Reduction Company, Inc., New York, N. Y.
Ajax Electro Metallurgical Corporation, Philadelphia, Pa.
Allied Chemical & Dye Corporation
  General Chemical Division, Morristown, N. J.
  Solvay Process Division, Syracuse, N. Y. (3 memberships)
Alloy Steel Products Company, Inc., Linden, N. J.
Aluminum Company of America, New Kensington, Pa.
American Machine & Foundry Company, Raleigh, N. C.
American Metal Company, Ltd., New York, N. Y.
American Platinum Works, Newark, N. J. (2 memberships)
American Potash & Chemical Corporation, Los Angeles, Calif. (2 memberships)
American Zinc Company of Illinois, East St. Louis, Ill.
American Zinc, Lead & Smelting Company, St. Louis, Mo.
American Zinc Oxide Company, Columbus, Ohio
Auto City Plating Company Foundation, Detroit, Mich.
Bart Manufacturing Company, Bellville, N. J.
Basic Incorporated, Cleveland, Ohio
Bell Telephone Laboratories, Inc., New York, N. Y. (2 memberships)
Bethlehem Steel Company, Bethlehem, Pa. (2 memberships)
Boeing Airplane Company, Seattle, Wash.
Burgess Battery Company, Freeport, Ill. (4 memberships)
C & D Batteries, Inc., Conshohocken, Pa.
Canadian Industries Ltd., Montreal, Que., Canada
Carborundum Company, Niagara Falls, N. Y.
Catalyst Research Corporation, Baltimore, Md.
Chrysler Corporation, Detroit, Mich.
Columbian Carbon Company, New York, N. Y.
Columbia-Southern Chemical Corporation, Pittsburgh, Pa.
Consolidated Mining & Smelting Company of Canada, Ltd., Trail, B. C., Canada (2 memberships)
Continental Can Company, Inc., Chicago, Ill.
Cooper Metallurgical Associates, Cleveland, Ohio
Corning Glass Works, Corning, N. Y.
Cramet, Inc., Chattanooga, Tenn.
Crane Company, Chicago, Ill.
Diamond Alkali Company, Painesville, Ohio (2 memberships)
Dow Chemical Company, Midland, Mich.
Wilbur B. Driver Company, Newark, N. J. (2 memberships)
E. I. du Pont de Nemours & Company, Inc., Wilmington, Del.
Eagle-Picher Company, Chemical Division, Joplin, Mo.
Eastman Kodak Company, Rochester, N. Y.
Eaton Manufacturing Company, Stamping Division, Cleveland, Ohio
Electric Auto-Lite Company, Toledo, Ohio
Electric Storage Battery Company, Philadelphia, Pa.
The Eppley Laboratory, Inc., Newport, R. I. (2 memberships)
Federal Telecommunication Laboratories, Nutley, N. J.
Food Machinery & Chemical Corporation
  Becco Chemical Division, Buffalo, N. Y.
  Westvaco Chlor-Alkali Division, South Charleston, W. Va.
Ford Motor Company, Dearborn, Mich.
General Electric Company, Schenectady, N. Y.
  Chemistry & Chemical Engineering Component, General Engineering Laboratory
  Chemistry Research Department

(Sustaining Members cont'd)

General Electric Company (cont'd)
Metallurgy & Ceramics Research Department
General Motors Corporation
Brown-Lipe-Chapin Division, Syracuse, N. Y. (2 memberships)
Guide Lamp Division, Anderson, Ind.
Research Laboratories Division, Detroit, Mich.
Gillette Safety Razor Company, Boston, Mass.
Gould-National Batteries, Inc., Depew, N. Y.
Graham, Crowley & Associates, Inc., Chicago, Ill.
Great Lakes Carbon Corporation, New York, N. Y.
Hanson-Van Winkle-Munning Company, Matawan, N. J. (3 memberships)
Harshaw Chemical Company, Cleveland, Ohio (2 memberships)
Hercules Powder Company, Wilmington, Del.
Hooker Electrochemical Company, Niagara Falls, N. Y. (3 memberships)
Houdaille-Hershey Corporation, Detroit, Mich.
Hughes Aircraft Corporation, Culver City, Calif.
International Business Machines Corporation, Poughkeepsie, N. Y.
International Minerals & Chemical Corporation, Chicago, Ill.
Jones & Laughlin Steel Corporation, Pittsburgh, Pa.
K. W. Battery Company, Skokie, Ind.
Kaiser Aluminum & Chemical Corporation
Chemical Research Department, Permanente, Calif.
Division of Metallurgical Research, Spokane, Wash.
Keokuk Electro-Metals Company, Keokuk, Iowa
Libbey-Owens-Ford Glass Company, Toledo, Ohio
P. R. Mallory & Company, Indianapolis, Ind.
McGean Chemical Company, Cleveland, Ohio
Merck & Company, Inc., Rahway, N. J.
Metal & Thermit Corporation, Detroit, Mich.
Minnesota Mining & Manufacturing Company, St. Paul, Minn.
Monsanto Chemical Company, St. Louis, Mo.
Motorola, Inc., Chicago, Ill.
National Cash Register Company, Dayton, Ohio
National Lead Company, New York, N. Y.
National Research Corporation, Cambridge, Mass.
Norton Company, Worcester, Mass.
Olin Mathieson Chemical Corporation, Niagara Falls, N. Y.
High Energy Fuels Organization (2 memberships)
Pennsalt Chemicals Corporation, Philadelphia, Pa.
Philips Laboratories, Inc., Irvington-on-Hudson, N. Y.
Pittsburgh Metallurgical Company, Inc., Niagara Falls, N. Y.
Poor & Company, Promat Division, Waukegan, Ill.
Potash Company of America, Carlsbad, N. Mex.
Radio Corporation of America, Harrison, N. J.
Ray-O-Vac Company, Madison, Wis.
Raytheon Manufacturing Company, Waltham, Mass.
Reynolds Metals Company, Richmond, Va. (2 memberships)
Shawinigan Chemicals Ltd., Montreal, Que. Canada
Speer Carbon Company
International Graphite & Electrode Division, St. Marys, Pa. (2 memberships)
Sprague Electric Company, North Adams, Mass.
Stackpole Carbon Company, St. Marys, Pa. (2 memberships)
Stauffer Chemical Company, Henderson, Nev., and New York, N. Y. (2 memberships)
Sumner Chemical Company, Division of Miles Laboratories, Inc., Elkhart, Ind.
Superior Tube Company, Norristown, Pa.
Sylvania Electric Products Inc., Bayside, N. Y. (2 memberships)
Sarkes Tarzian, Inc., Bloomington, Ind.
Tennessee Products & Chemical Corporation, Nashville, Tenn.
Texas Instruments, Inc., Dallas, Texas
Titanium Metals Corporation of America, Henderson, Nev.
Udylite Corporation, Detroit, Mich. (4 memberships)
Upjohn Company, Kalamazoo, Mich.
Victor Chemical Works, Chicago, Ill.
Wagner Brothers, Inc., Detroit, Mich.
Weirton Steel Company, Weirton, W. Va.
Western Electric Company, Inc., Chicago, Ill.
Wyandotte Chemicals Corporation, Wyandotte, Mich.
Yardney Electric Corporation, New York, N. Y.

How to make metal stripping an exact science: What metal do you want to strip? There are eight metal strippers in the Enthone "ENSTRIP" series, which, in most cases, will do the specialized job thoroughly, quickly, economically. If one of these standard strippers won't precisely cover your requirements, there are special Enthone research developments available. Write us about your particular needs or problems. Include a sample of your product if possible. We'll be glad to recommend the best methods to follow. Enthone, Inc., 442 Elm Street, New Haven 11, Conn.

ENTHONE

ENTHONE, INC. IS A SUBSIDIARY OF AMERICAN SMELTING AND REFINING COMPANY